

***Rafts and Piled Raft Foundations at Surfers Paradise,
Gold Coast, Australia - Analytical Study Using PLAXIS
Software***

By

MIN HUANG

**A Dissertation submitted in partial fulfilment of the
requirements of the degree of**

THE MASTER OF CIVIL ENGINEERING

from

**GRIFFITH UNIVERSITY
GOLD COAST CAMPUS
SCHOOL OF ENGINEERING**

June 2006

***Rafts and Piled Raft Foundations at Surfers Paradise,
Gold Coast, Australia - Analytical Study Using PLAXIS
Software***

DECLARATION

I certify that the activities and documentation of this Dissertation have been undertaken by myself, and that the content is the direct result of my own effort except where contributed data and external assistance has been acknowledged.

Name :

Student Number :

Date:

Supervisor :

Date:

GRIFFITH UNIVERSITY

GOLD COAST CAMPUS

SCHOOL OF ENGINEERING

7109ENG DISSERTATION

LIMITATIONS OF USE

This topic has been undertaken by a postgraduate student as part of the academic requirements of the Master of Civil Engineering degree.

This report is the end of an educational exercise and the report, and any associated hardware, software, drawings or other appendices, or any part of the report was not intended to be used for any other purpose and if so used are used at the sole risk of the user.

The recommending of a particular grade for the course has been based on the particular academic criteria applicable to the course and does not necessarily imply any industrial or commercial value of the material associated with either the investigation or the report.

Head of School

ACKNOWLEDGEMENTS

The research on which this thesis was undertaken in Infrastructure Engineering and Management and School of Engineering, Griffith University Gold Coast campus, under the supervision of Professor A.S. Balasubramaniam. The author is greatly indebted to Professor Balasubramaniam for having provided this research opportunity and for his guidance, inculcation, enlightening inspiration and invaluable technical suggestion throughout this research. The author also appreciates the guidance in improving his research skill and the support provided for him to attend short course related to his research.

Special thanks would like to extend to Bill Chambers, from Frankipile Australia, for his assistant with providing research data and technical supports; to Dr. Balakumar; Dr.Park Sawon, from Escoeng Consultant Company, South Korea; Dr.Pastsakorn Kitiyodom, from Kanazawa University, Japan, for providing knowledgeable advices, which made this research possible.

The author also thanks all the academic, technical staff in the Infrastructure Engineering and Management and School of Engineering, Griffith University, particularly to Mr. Y.N.Oh and Mr. M. Bolton for providing constructive advices and technical assistance.

Last, but not least, the author is indebted to his family member for their understanding and encouragement. The completion of this research is but a very small reward for their efforts and great expectations.

Project Brief

Student Name: Min Huang
Student Number: s2161988
Course: 7109 ENG Dissertation
Date: 09 / 08 / 2005
Supervisor: Prof. A. S. Balasubramaniam

Title of Project: Rafts and Piled Raft Foundations at Surfers Paradise, Gold Coast, Australia - Analytical Study Using PLAXIS Software

Background:

This study directly relates to the analysis of unpiled and piled raft foundation. First reliable subsoil layer model was established for Surfers Paradise from some 25 or more borehole data at four sites with the boreholes extending to some 50m below the ground surface up to the rock stratum. A seven layer subsoil model was established and the geotechnical parameters for these layers are estimated from SPT tests.

Objectives:

- Study the subsoil profiles at Surfers Paradise using the data gathered from 26 boreholes extending to some 40-50m depth and to make sub-soil profile models at all the four sites.
- Develop models for the geotechnical parameters and other material models as needed in the PLAXIS analysis.
- Analysis of the unpiled raft foundation for typical cases using PLAXIS software.
- Conduct parametric studies of the raft and piled raft foundations for various raft size and thickness, loading conditions, pile spacing, number of piles and pile length. Evaluation of the effects of the raft thickness, the pile spacing, the pile length and the number of piles on the settlements, and bending moment in the raft and the pile loads and their bending moments.

Min Huang (2161988)
(Student)

Prof. A. S. Balasubramaniam
(Supervisor)

Dr.Sanaul Chowdhury
(Course Convenor)

ABSTRACT

This study relates to the analysis of unpiled and piled raft foundations with soil conditions similar to those at the ARTIQUE in Surfers Paradise Gold Coast. Initially the subsoil layer model was established for Surfers Paradise from some 25 or more borehole data at four sites and the boreholes extend to some 50m below the ground and up to the rock stratum. A seven layer subsoil model was established and the geotechnical parameters for these layers are estimated from SPT tests. Based on these geotechnical parameters, a PLAXIS analysis was conducted on unpiled and piled raft foundations.

The conclusions of the study are in three parts. Part one relates to the sub-surface model, while part two is on the geotechnical parameters and part three is on the results of the PLAXIS analysis. Numerical values of the results are tabulated in CHAPTER V under results and discussions.

For the most predominant sand layers, the modulus of elasticity were taken from 55 to 120MPa based on the relative density of the sand; the corresponding angle of internal friction ranged from 37 to 42 degrees. For the sandy clay, a lower angle of friction of 25 degrees was adopted.

For the unpiled raft, the normalised settlement parameter, I_R , for the three raft sizes of 8m×8m, 15m×15m and 30m×30m ranged as 1.02-1.15, 0.64-0.81, and 0.38-0.54 respectively. The intensity of loading is 215 kN/m² for the unpiled raft. For the 8m×8m raft, the normalised maximum bending moment ranged from 0.164 to 1.02. This range changed to 0.035 to 1.225, when the raft size is 15m×15m. For the raft size of 30m×30m the range of normalized bending moment is 0.007 to 1.077.

In the case of the piled raft with raft thicknesses of 0.25, 0.4, 0.8, 1.5 and 3m, pile were adopted as 16m length, 0.7m diameters, the intensity of loading is 645 kN/m². The corresponding maximum settlements are 64, 63.3, 62.6, 62.3 and 62.2 mm, and the bending moment values are 107, 160, 321, 446 and 485 kNm. The pile loads ranged from 1.19 to 1.41 MN for the edge pile and the corresponding values for the centre pile are 0.91 to 1.06MN.

In the study of pile spacing effects, the raft thickness is 0.8m and the dimension of the raft will increase with increased pile spacing. The piles are 0.7m diameter and 16m length. Three values of intensity of loading as 215, 430 and 645kN/m² are studied. The maximum values of the settlements decreased only by a little value as the raft thickness increased. However, the hogging moment in the raft increased greatly when the raft thickness increased from 0.25 to 3m. The pile loads only varied slightly within the range 1.19~1.41MN in the edge piles, and 0.91~1.06MN in the centre piles.

Under three loading conditions (215kN/m², 430kN/m² and 645kN/m²), the effects of the pile spacing varied as 3d to 7d have been investigated. The pile length is 16m and the diameter is 0.7m. The maximum settlements, different settlement and the maximum moment all increase with increasing pile spacing; the proportion of the load carried by the piles reduced.

Increasing the pile length reduced the settlement of the piled raft, whereas large positive bending moments were carried by the raft in the positions beneath piles. Pile lengths beyond 6m, showed little effect on both the settlement and the bending moment of piled raft.

Finally, effects of number of piles have been found that the settlement at the centre decreased when more piles are under the raft; the proportion of the load carried by the piles increased.

Keywords: Sand, Settlement, Piled Raft, PLAXIS, Parametric study

TABLE OF CONTENTS

Title Page	i
Declaration	ii
Limitations of Use	iii
Acknowledgments	iv
Project Brief	v
Abstract	vi
Table of Contents	vii
List of Tables	x
List of Figures	xii
Notations	xv

CHAPTER

1. INTRODUCTION	1
1.1 Background	1
1.2 Objectives of the Study	3
1.3 Layout of The Thesis	3
2. LITERATURE REVIEW	5
2.1 General	5
2.2 Soils Condition in Surfers Paradise, Gold Coast	5
2.3 Static Analysis of Pile Capacity	5
2.3.1 Pile Analysis Based on Results of In-situ Tests	5
2.3.2 Static Analysis of Pile Foundations	6
2.3.3 Pile Group Capacity	6
2.3.4 Load-Deformation Behaviour of Piles Under Axial Loading.....	7
2.4 Analysis of Piled Raft Foundations	7
2.4.1 Simplified Calculation Methods	7
2.4.1.1 Poulos and Davis Method	7
2.4.1.2 Randolph Method	7
2.4.2 Approximate Computer Based Method	8
2.4.2.1 Strip on Spring Approach	8
2.4.2.2 Plate on Spring Approach	8
2.4.3 Rigorous Computer-based Methods	8
2.4.3.1 Boundary Element Methods	8
2.4.3.2 Combined Boundary and Finite Element Method	9

2.4.3.3	Simplified Finite Element Method	9
2.4.3.4	Variational Approach	10
2.4.3.5	Three Dimensional Finite Element Method	10
2.5	A Review of Softwares for the Analysis of Piles and Piled Raft Foundations.....	10
2.5.1	PLAXIS Program	11
2.5.2	Material Models	12
2.5.3	Calculations.....	13
2.6	Conclusion Remarks	14
3.	REARCH METHODOLOGY	16
3.1	General	16
3.2	Project Details and Sub-surface Investigations	16
3.3	Description of Subsoil Conditions.....	16
3.4	Corrected SPT Test Results.....	17
3.4.1	Correlations of Friction angle, $\bar{\phi}$, Undrained Shear Strength, s_u and Young's Modulus E with SPT N Value	18
3.4.1.1	Friction Angle $\bar{\phi}$,	19
3.4.1.2	Undrained Shear Strength, s_u	19
3.4.1.3	Young's Modulus, E	19
3.5	Modelling and Analysis of Piled Raft System.....	19
3.5.1	Selection of Software	19
3.5.2	Model Calibration	20
3.5.3	PLAXIS Analysis Including Details of Parametric Study.....	20
3.6	Conclusion Remarks	21
4.	NUMERICAL MODELLING	22
4.1	General	22
4.2	Finite Element Method Applied to Piled Raft Foundation	22
4.3	Numerical Modelling of Piled Raft Foundation	22
4.3.1	Numerical Model	22
4.3.2	Select of Appropriate Model	22
4.3.3	Type and Size of Finite Element Mesh	23
4.3.4	Boundary Condition	23
4.3.5	Number of Elements	24
4.3.6	Type of Element.....	24
4.4	Constitute Law	24
4.4.1	Modelling of Raft and Pile Materials	24
4.4.2	Soil Model	25
4.4.2.1	General	25
4.4.2.2	The Mohr-Coulomb Model: Elastic Perfectly Plastic behaviour	25
4.4.2.3	Formulation of Mohr-Coulomb Model	26
4.4.2.4	Basic Parameters of the Mohr-Coulomb Model	27
4.4.3	Pile Soil Interface Element Model	29
4.5	Input Parameters	29
4.6	Finite Element Output	29
4.7	Conclusion Remarks	30

5.	RESULTS AND DISCUSSIONS	31
5.1	General	31
5.2	Establishment of Sub-surface Soil Layer Models	31
5.3	Geotechnical Parameters for Subsoil Layers	32
5.4	Presentation of Analysis of Unpiled Raft Foundation	32
5.4.1	Settlement of Unpiled Raft	32
5.4.2	Bending Momenet of Unpiled Raft	33
5.4.3	Effect of Raft Thickness on Performance of Unpiled Raft Foundation	34
5.5	Parametric Study of Piled Rafts	34
5.5.1	Effects of Raft Thickness on Piled Raft Foundation	35
5.5.2	Effects of Pile Spacing	35
5.5.3	Effects of Pile Length	36
5.5.3	Effects of Number of Piles	36
5.6	Conclusion Remarks	36
6.	CONCLUSIONS AND RECOMMENTDATIONS	38
6.1	General	39
6.2	Typical Gold Coast Subsoil at Surfers Paradise	39
6.3	Geotechnical Parameters Used in PLAXIS Analysis Input Parameters	39
6.4	Performance of Unpiled Raft	39
6.4.1	The Settlement of Unpiled Raft	39
6.4.2	Normalized Bending Moment of Unpiled Raft	39
6.4.3	Parameter Study of Unpiled Raft	39
6.5	Parametric Analysis of Piled Raft Foundation	39
6.5.1	The Settlement of Unpiled Raft	39
6.5.2	Effect of Raft Thickness	40
6.5.3	Effect of Pile Spacing	40
6.5.2	Effect of Pile Length	40
6.5.3	Effect of Number of Piles	40
6.6	Recommendations	40
	REFERENCES	41
	TABLES	48
	FIGURES	74
	APPENDIX A-1 FEA RESULTS - UNPILED RAFT (DEFORM MESH)	133
	APPENDIX A-2 FEA RESULTS - UNPILE RAFT (SETTLEMENT PROFILE)	137
	APPENDIX A-3 FEA RESULTS - PILED RAFT VARING THICKNESS	141
	APPENDIX A-4 FEA RESULTS - PILED RAFT VARING PILE SPACING	144
	APPENDIX A-5 FEA RESULTS - PILED RAFT VARING PILE LENGTH	153

APPENDIX A-6 FEA RESULTS - PILED RAFT VARIOUS NUMBER OF PILES	
(LOAD = 645 kN/m²)	159
APPENDIX B-1 BORHOLE RECORDS - ARTIQUE	160
APPENDIX B-2 BORHOLE RECORDS - Q1 TOWER	184
APPENDIX B-3 BORHOLE RECORDS - CIRCLE ON CAVILL	202
APPENDIX B-4 BORHOLE RECORDS - SOLAIRE	222
APPENDIX C FINITE ELEMENT CALCULATION PROCESS BASED ON THE ELASTIC STIFFNESS MATRIX	244

LISTS OF TABLE

Tables	Title	
Table 2.1 (a)	Skin Friction Factor α and β for Driven Piles (after Poulos, 1989)	48
Table 2.1 (b)	Skin Friction Factor α and β for Bored Piles (after Poulos, 1989)	49
Table 2.1 (c)	End bearing capacity of pile tip, f_b (after Poulos, 1989).....	49
Table 2.2	Notable Researches on Pile Groups	50
Table 2.3	Numbers of Research on Piles and Piled Raft Using Computer Program	51
Table 2.4	Numerical Programs Using for Analysis of Piles and Piled Raft	52
Table 3.1	Summarised Project Information Used in Study	53
Table 3.2	ARTIQUE - Summary of Stratigraphy.....	54
Table 3.3	Q1 Tower - Summary of Stratigraphy.....	55
Table 3.4	Circle on Cavill - Summary of Stratigraphy	56
Table 3.5	SOLAIRE - Summary of Stratigraphy	57
Table 3.6	SPT Hammer Efficiencies (Adapted from Clayton, 1990).....	58
Table 3.7	Borehole, Sampler, and Rod Correction Factors (after Skempton, 1986).....	58
Table 3.8(a)	ARTIQUE: Summarised average SPT N, N_{60} , $(N_1)_{60}$	59
Table 3.8(b)	Q1 Tower: Summarised average SPT N, N_{60} , $(N_1)_{60}$	59
Table 3.8(c)	Circle on Cavill: Summarised average SPT N, N_{60} , $(N_1)_{60}$	60
Table 3.8(d)	SOLAIRE: Summarised average SPT N, N_{60} , $(N_1)_{60}$	60
Table 3.9	SPT N vs. ϕ Relationships	61
Table 3.10	Approximate s_u versus N Relationship (after Terzaghi and Peck, 1967)	61
Table 3.11	Typical Ranges of Drained Modulus for Sand (Kulhawy and Mayne, 1990).....	61
Table 3.12	Suggested Average Values of E_s for Driven Piles in Sand	61
Table 3.13	Typical Range of Undrained Modulus for Clay (Kulhawy & Mayne, 1990)	62
Table 3.14	Required Parameters for the Analysis of Piled Rafts for Elastic Analysis	62
Table 4.1	Summarised Material properties of the Raft	63
Table 4.2	Summarised Material properties of the Pile.....	63
Table 4.3	Suggested Cohesion, c Value in PLAXIS (Huybrechts and Whenham, 2004)	63
Table 4.4	Newton-Cotes Integrations	64
Table 4.5	Adopted Soil Properties and the Interfaces Using for Analysis	64
Table 5.1	Range of Normalized Settlement for Each Raft Size	65
Table 5.2	Value of K_R , Raft Relative Stiffness for Each Thickness	65
Table 5.3	Maximum Settlement of Different Size Unpiled Raft. Loads = 215 kN/m ²	65
Table 5.4	Summarised Relative Stiffness Zone for Different Size Raft Foundation.....	65
Table 5.5	Normalized Differential Settlement for Each Raft Size	65
Table 5.6a	Maximum Normalized Bending Moment for Each Thickness. 8m×8m Unpiled Raft	66
Table 5.6b	Maximum Normalized Bending Moment for Each Thickness. 15m×15m Unpiled Raft	66
Table 5.6c	Maximum Normalized Bending Moment for Each Thickness. 30m×30m Unpiled Raft	66
Table 5.7	Effect of Raft Thickness: Maximum Settlement in Piled Raft.....	67
Table 5.8	Effect of Raft Thickness: Maximum Bending Moment in Piled Raft.....	67
Table 5.9(a)	Effect of Raft Thickness: Maximum Axial Force on Pile 1 (at the edge)	67

Table 5.9(b)	Effect of Raft Thickness: Maximum Axial Force Pile 2 (at the centre).....	67
Table 5.10	Effect of Pile Spacing: Piled Raft Maximum Settlement. Load=215kN/m ²	68
Table 5.11	Effect of Pile Spacing: Piled Raft Maximum Bending Moment.	
Load=215kN/m ²	68
Table 5.12(a)	Effect of Pile Spacing: Maximum axial force on Pile 1 (at the edge).	
Load=215kN/m ²	68
Table 5.12(b)	Effect of Pile Spacing: Maximum axial force on Pile 2 (at the centre).	
Load=215kN/m ²	68
Table 5.13(a)	Effect of Pile Spacing: Maximum Bending Moment on Pile 1 (at the edge).	
Load=215kN/m ²	69
Table 5.13(b)	Effect of Pile Spacing: Maximum Bending Moment on Pile 2 (at the	
centre).		
Load=215kN/m ²	69
Table 5.14	Effect of Pile Spacing: Piled Raft Maximum Settlement.	
Load=430kN/m ²	70
Table 5.15	Effect of Pile Spacing: Piled Raft Maximum Bending Moment.	
Load=430kN/m ²	70
Table 5.16(a)	Effect of Pile Spacing: Maximum axial force on Pile 1 (at the edge).	
Load=430kN/m ²	70
Table 5.16(b)	Effect of Pile Spacing: Maximum axial force on Pile 2 (at the centre).	
Load=430kN/m ²	70
Table 5.17(a)	Effect of Pile Spacing: Maximum Bending Moment on Pile 1 (at the edge).	
Load=430kN/m ²	71
Table 5.17(b)	Effect of Pile Spacing: Maximum Bending Moment on Pile 2 (at the	
centre).		
Load=430kN/m ²	71
Table 5.18	Effect of Pile Spacing: Piled Raft Maximum Settlement. Load=645kN/m ²	72
Table 5.19	Effect of Pile Spacing: Piled Raft Maximum Bending Moment.	
Load=645kN/m ²	72
Table 5.20(a)	Effect of Pile Spacing: Maximum axial force on Pile 1 (at the edge).	
Load=645kN/m ²	72
Table 5.20(b)	Effect of Pile Spacing: Maximum axial force on Pile 2 (at the centre).	
Load=645kN/m ²	72
Table 5.21(a)	Effect of Pile Spacing: Maximum Bending Moment on Pile 1 (at the edge).	
Load=645kN/m ²	73
Table 5.21(b)	Effect of Pile Spacing: Maximum Bending Moment on Pile 2 (at the	
centre).		
Load=645kN/m ²	73

LISTS OF FIGURES

Tables	Title	
Figure 2.1	GOLD COAST Subsoil Profile.....	74
Figure 3.1(a)	ARTIQUE - Borehole Location Plan (APPROX.).....	75
Figure 3.1(b)	ARTIQUE - Soil Profile along Section A-A'	75
Figure 3.2	ARTIQUE - General Site Soil Profile	76
Figure 3.3(a)	Q1 - Borehole and Pile Location Plan	77
Figure 3.3(b)	Q1 - Soil Profile along Section B-B'	77
Figure 3.4	Q1 - General Site Soil Profile	78
Figure 3.5(a)	Circle on Cavill - Borehole Location Plan (APPROX-)	79
Figure 3.5(b)	Circle on Cavill - Soil Profile along Section C-C'	79
Figure 3.6	Circle on Cavill - General Site Soil Profile	80
Figure 3.7(a)	SOLAIRE - Borehole Location Plan (APPROX-)	81
Figure 3.7(b)	SOLAIRE - Soil Profile along Section D -D'	81
Figure 3.8	SOLAIRE – General Site Soil Profile	82
Figure 3.9	Correction Factor for influence of effective overburden pressure on SPT “N” value	83
Figure 3.10(a)	ARTIQUE: SPT N value vs. Depth.....	84
Figure 3.10(b)	Q1-Tower: SPT N value vs. Depth.....	84
Figure 3.10(c)	Circle on Cavill: SPT N value vs. Depth	85
Figure 3.10(d)	SOLAIRE: SPT N value vs. Depth	85
Figure 3.11	N versus ϕ (after Peck <i>et al</i> , 1974).....	86
Figure 3.12	N versus ϕ' and Overburden Pressure (after Schmertmann, 1975).....	86
Figure 3.13(a)	Effective of Overburden Stress and Relative Density, Dr on SPT N Value (after Gibbs and Holtz, 1957).....	87
Figure 3.13(b)	Relative Density - N - Stress Relationship (after Holtz and Gibbs, 1979).....	87
Figure 3.13(c)	Variation of ϕ' and $(N1)_{60}$ with ϕ_{cs} and OCR (after Stroud, 1989)	88
Figure 3.13(d)	Variation of ϕ' and Relative Density, Dr with ϕ'_{cs} and OCR (after Stroud, 1989)	89
Figure 3.14	Selected Relationships between N and s_u (Djoenaidi, 1985).....	90
Figure 3.15	Relationships between s_u and SPT N Value (after Hara et al, 1974).....	90
Figure 3.16	Comparative Plots of Drained Modulus Correlations for Sand (Callanna and Kulhawy, 1985).....	91
Figure 3.17	Backfigured soil Modulus Es for Piles in Clay (after Poulos and Davis, 1980)	91
Figure 3.18	Undrained Modulus for Drilled Shafts in Compression and Uplift	

	(Callanand and Kulhawy, 1985).....	92
Figure 3.19(a)	ARTIQUE: Summarized Soil Parameters for Each Soil Layers.....	93
Figure 3.19(b)	Q1 Tower: Summarized Soil Properties for Each Soil Layers	93
Figure 3.19(c)	Circle on Cavill: Summarized Soil Properties for Each Soil Layers.....	94
Figure 3.19(d)	SOLAIRE: Summarized Soil Properties for Each Soil Layers.....	94
Figure 3.20	Generalized Soil Profile Adopted for Analysis.....	95
Figure 4.1	Finite Element Idealisation of the Pile Raft Element	96
Figure 4.2	Diagrammatic View of Boundary Condition Using for Modelling.....	97
Figure 4.3	Schematic View of the Finite Element Mesh	97
Figure 4.4	Positions of Nodes and Stress Points in Soil Elements.....	98
Figure 4.5	Position of Nodes and Stress Points in 3-node and 5-node Beam Element	98
Figure 4.6	Thin Layer Interface Elements.....	99
Figure 4.7	Basic Idea of an Elastic Perfectly Plastic Model.....	99
Figure 4.8	Mohr-Coulomb Yield Surface in Principal Stress Space ($c = 0$)	100
Figure 4.9	Definition of E_0 and E_{50} for Standard Drained Triaxial Test Results	100
Figure 4.10	Illustration of Dilatancy Angle	101
Figure 4.11	Distribution of Nodes and Stress Point in Interface Elements and Their Connection to Soil Elements.....	102
Figure 5.1	Typical Rafts and Piled Raft Configurations for Analysis	103
Figure 5.2(a)	Normalised Vertical Displacement of 8m×8m Squared Unpiled Raft	104
Figure 5.2(b)	Normalised Vertical Displacement of 15m×15m Square Unpiled Raft.....	104
Figure 5.2(c)	Normalised Vertical Displacement of 30m×30m Square Unpiled Raft.....	105
Figure 5.3(a)	Settlement Influence Factors of 8m×8m Square Unpiled Raft	106
Figure 5.3(b)	Settlement Influence Factors of 15m×15m Square Unpiled Raft	106
Figure 5.3(c)	Settlement Influence Factors of 30m×30m Square Unpiled Raft	107
Figure 5.4	Variation of Normalized Differential Settlement with Stiffness.....	108
Figure 5.5(a)	Normalised Bending Moment in 8m×8m Unpiled Raft.....	109
Figure 5.5(b)	Normalised Bending Moment in 15m×15m Unpiled Raft.....	109
Figure 5.5(c)	Normalised Bending Moment in 30m×30m Unpiled Raft.....	110
Figure 5.6	Effect of Thickness on Unpiled Raft Performance. Square Raft = 8m×8m	111
Figure 5.7	Effect of raft thickness on Computed Settlement of Piled Raft	112
Figure 5.8	Effect of raft thickness on Bending Moment of Piled Raft	112
Figure 5.9	Effect of Raft Thickness on Pile Axial Load.....	113
Figure 5.10	Effect of raft Thickness on Pile Bending Moment	114
Figure 5.11	Summarized Effect of Raft Thickness on Piled Raft Performance. Raft with 16 Piles, 16m long. Load = 645 kN/m ²	115
Figure 5.12	Comparison of Piled Raft Settlement Response for Different Spacing of Piles. Q = 215 kN/m ²	116
Figure 5.13	Comparison of Piled Raft Bending Moment Response for Different Spacing of Piles. q = 215 kN/m ²	116
Figure 5.14	Effect of Pile Spacing on Pile Bending Moment. q = 215kN/m ²	117
Figure 5.15	Effect of Raft thickness on Pile Bending Moment. q = 215 kN/m ²	118
Figure 5.16	Comparison of Piled Raft Settlement Response for Different Spacing of Piles. Q = 430 kN/m ²	119

Figure 5.17	Comparison of Piled Raft Bending Moment Response for Different Spacing of Piles. $q = 430 \text{ kN/m}^2$	119
Figure 5.18	Effect of Pile Spacing on Pile Axial Load. $q = 430 \text{ kN/m}^2$	120
Figure 5.19	Effect of Pile Spacing on Pile Bending Moment. $q = 430 \text{ kN/m}^2$	121
Figure 5.20	Comparison of Piled Raft Settlement Response for Different Spacing of Piles. $Q = 645 \text{ kN/m}^2$	122
Figure 5.21	Comparison of Piled Raft Bending Moment Response for Different Spacing of Piles. $q = 645 \text{ kN/m}^2$	122
Figure 5.22	Effect of Raft Thickness on Pile Axial Load. $q = 645 \text{ kN/m}^2$	123
Figure 5.23	Effect of Raft Thickness on Pile Bending Moment. $q = 645 \text{ kN/m}^2$	124
Figure 5.24(a)	Summarized Effect of Pile Spacing on Piled Raft Performance. Raft with 16 Piles, 16m long. Load = 215 kN/m^2	125
Figure 5.24(b)	Summarized Effect of Pile Spacing on Piled Raft Performance. Raft with 16 Piles, 16m long. Load = 430 kN/m^2	126
Figure 5.24(c)	Summarized Effect of Pile Spacing on Piled Raft Performance. Raft with 16 Piles, 16m long. Load = 645 kN/m^2	127
Figure 5.25	Comparison of the Piled Raft Response on Settlement Profile for Different Length of Piles. Raft Thickness = 0.25 m . $q = 215 \text{ kN/m}^2$	128
Figure 5.26	Comparison of the Piled Raft Response on Bending Moment Profile for Different Length of Piles. Raft Thickness = 0.25 m . $q = 215 \text{ kN/m}^2$	128
Figure 5.27	Comparison of the Piled Raft Response on Settlement Profile for Different Length of Piles. Raft Thickness = 0.25 m . $q = 430 \text{ kN/m}^2$	129
Figure 5.28	Comparison of the Piled Raft Response on Bending Moment Profile for Different Length of Piles. Raft Thickness = 0.25 m . $q = 430 \text{ kN/m}^2$	129
Figure 5.29(a)	Summarized Effect of Pile Length on Piled Raft Performance. Load = 215 kN/m^2	130
Figure 5.29(b)	Summarized Effect of Pile Length on Piled Raft Performance. Load = 430 kN/m^2	131
Figure 5.30	Effect of Number of piles on Piled Raft Performance. Load = 645 kN/m^2	132

NOTATIONS

2-D	Two-dimensional
3-D	Three-dimensional
A_p	Area of pile cross section
B_R	Width of raft
C_N	Correction factor for overburden pressure
C_B	Borehole diameter correction
C_R	Rod length correction (from Table 3.7)
C_S	Sample correction (from Table 3.7)
\bar{c}	Cohesion of soil
CPT	Cone Penetration Test
d	Diameter of Pile
E	Young's Modulus
E_{eq}	Equivalent plane strain pile Young's modulus
E_u	Undrained Young's modulus
E_m	Hammer efficiency
E_R	Young's modulus of raft
E_s	Young's modulus of soil
FEM	Finite element method
G	Shear modulus of Soil
GPa	Giga pascal

I_r	Rigidity index
I_R	Settlement influence factor for unpiled raft = $\frac{w_i E_s}{q B_R (1 - \nu_s^2)}$
K_o	Earth pressure coefficient at rest
K_R	Relative raft stiffness = $\frac{4 E_R (1 - \nu_s^2) t_R^3}{3 E_s (1 - \nu_R^2)}$
k_x	Permeability in hor. direction
k_y	Permeability in ver. direction
L	Length of Pile
m	the general harmonic term
M	bending moment
M_{xx}	transverse bending moment
MPa	Mega pascal
$n_{p-row i}$	Number of piles in row i
N	Measured SPT N value
N_{60}	SPT N value corrected for field procedures
$(N_1)_{60}$	Corrected N value for overburden pressure
n	Number of piles in the pile group
q	Vertical load intensity per unit area
Q_u	Ultimate capacity of the individual pile in the pile group
Q_{ug}	Ultimate capacity of the pile group
R_{inter}	Strength reduction factor inter
SPT	Standard penetration test
SF	Safety Factor
s_u	Undrained Shear Strength
t_R	Thickness of raft
ΣM_{sf}	Total multiplier
τ	Shear Stress
$\bar{\phi}$	Internal Friction Angle
ψ	Dilatancy angle
η_g	Pile group efficiency
γ_{unsat}	Soil unit weight above phreatic level
γ_{sat}	Soil unit weight below phreatic level
ν	Poisson's ration
ν_i	Poisson's ration of i^{th} layer
ν_R	Poisson's ration of raft
ν_s	Poisson's ration of soil

CHAPTER I

INTRODUCTION

1.1 Background

Many tall buildings at Surfers Paradise along the coastal strip of Gold Coast involve piles as well as raft and piled raft foundations. As such this thesis is devoted to the analysis of rafts and piled raft foundations for typical sub-surface soil profiles at

Surfers Paradise using the PLAXIS computer software. Four major projects are selected for the study and these are named as ARTIQUE, Q1, Circle on Cavill and SOLAIRE throughout this thesis. The subsoil conditions at Surfers Paradise is an estuarine deposit and typically consist of an upper layer of medium dense sand (Layer 1), followed by very dense sand (Layer 2). Below this layer of very dense sand, there is a layer of peat (Layer 3). At some locations the Layer 3 is missing. Below the peat layer is a very dense sand layer (Layer 4) followed by sandy clay (Layer 5). This in turn is underlain by clayey sand (Layer 6) which overlies a layer of gravelly sand (Layer 7). In some locations, the gravelly sand layer is missing and the clayey sand rest on rock formation. At the ARTIQUE site, rock is encountered around 30 to 35 m below the ground surface, while at the Q1 site this depth to the rock surface is about 40m. For the Circle on Cavill site the rock surface is encountered at depths of 33 to 46m. Similarly at the SOLAIRE site the depth to rock surface ranged from 30 to 36 m.

The Q1 Tower is 78 stories and some 323 m high founded on piles bearing in the rock layer. Similarly, the Circle on Cavil has two towers each 50 and 70 storey and the corresponding heights are 158m and 219m respectively. The towers at Circle on Cavill are also founded on pile groups which extend to the underlying rock stratum. The SOLAIRE and ARQIQUE towers are only 20 and 30 storey and with height of 72 and 95m. These two towers are founded on piled raft foundations. This is the first time, deep foundation studies at the Surfers Paradise were carried out by the Griffith University researchers. Taking this opportunity a detail study of the subsoil conditions were made from some 25 or more borehole extending at some locations to as deep as 5m from the ground surface. Using these borehole data soil profile models are established which can be helpful in future foundation engineering projects in this rapidly growing stretch along the coastline of Gold coast.

In all four sites only standard penetration test (SPT) test data are available. Now cone penetration tests (CPT) are common in Gold Coast and as such future research will enable correlations to be established between the SPT and CPT measurements. The work of Clayton (1990), Skempton (1986), Liao and Whitman (1985), Kulhawy and Mayne (1990) were used to carry out the various corrections for the measured SPT. Well established correlations of SPT with the engineering properties of soils are now available as Peck *et al.* (1974), Schmertmann (1975), Gibbs and Holt (1957), Holtz and Gibbs (1979), Stroud (1989), Djoenaidi (1985), Hara *et al* (1974), Callanan and Kulhawy (1985) and Poulos and Davis (1980) among others. These correlations are also reviewed in this thesis.

Outstanding contributions on piled foundations and piled raft foundations were also made by pioneering workers such as Berezantzev *et al* (1961), Vesic (1972), Burland (1973), Meyerhof (1976), API (1984), Semple and Rigden (1984), Poulos (1989), Fleming *et al.* (1992) among a very large number of researchers. Currently, Guo and Randolph (1997) have done some excellent analytical work on piles and pile groups subjected to vertical and lateral loadings. Equally impressive works on pile group behaviour is there from Poulos (1968), Butterfield and Banerjee (1971), Ottaviani (1975), Randolph and Wroth (1979), Kuwabara (1989), El Sharnouby and Novak (1990), Fleming *et al* (1992), Lee (1993), Guo and Randolph (1996), Shen *et al.* (2000), and Chow *et al.* (2001).

Various computer softwares are now available for the study of piles and piled raft foundations PILEGRP (Chow, 1989), UNIPILE (Fellenius, 2004), CAPWAP (Lee *et al.*, 1996), GASP (Poulos, 1991), GARP (Poulos, 1994), GROUP (Reese, 1994), FLAC (Hewitt and Gue, 1994), NAPRA (Russo, 1998), FLAC (Small and Zhang, 2000), PLAXIS (Prakoso and Kulhawy, 2001), ANSYS (Liang *et al.*, 2003), PRAB (Kitiyodom and Matsumoto, 2003) and ABAQUS (Reul and Randolph, 2003) among others.

In this study, PLAXIS version 8 software is used and a two dimensional plane strain analysis is carried out. Ideally speaking a 3-D analysis is the best for rafts and piled raft foundations, but as iterated before, this is the first attempt to study the deep foundation conditions in sand at Surfers Paradise and it is important that a step by step cautious approach is followed. Additionally, the work of Prakoso and Kulhawy (2001) has demonstrated that a 2-D plane strain analysis can yield good results for piled raft analysis without excessive computing and modelling time. Also, among the four projects mentioned above, complete data is available on the ARTIQUE site and as such concentration will only be made in the analysis of raft and piled raft foundations at this site using PLAXIS software.

Generally, raft foundations are used in stiff soils where the settlement is of less concern. While piles as an important element placed beneath the raft area use for not only transmitting the superstructure load to soils, but also as settlement reducer to control the settlement or differential settlement. In the conventional design of the piled foundation the load contribution by the raft is ignored. But the recent studies have demonstrated that rafts can carry up to 30% of the total load. In addition, most of the researches had been treating raft either as a perfectly flexible or as perfectly rigid structure element. However, the effects of raft flexibility on bending moments and differential settlement of the raft as well as axial forces and bending moments on the piles has been emphasised by recent studies of Clancy and Randolph (1993), Poulos *et al.* (1997) and Ta and Small (1997) in clay soil. Moreover, both Horikoshi and Randolph (1998) and Cunha *et al.* (2001) carried out numerous of parametric analysis on performance of piled raft in non homogenous clay soil. In order to carry out the study on this complex performance, a numerical program PLAXIS version 8 were employed. PLAXIS package provide varieties of constitutive models for simulation of the non-linear, time-dependent and anisotropic behaviour of soils, and capable to deal with various aspects of complex geotechnical structure.

1.2 Objectives of Study

In line with the background information provided above, the objectives of the study are to:

- Study the subsoil profiles at Surfers Paradise using the data gathered from the 26 boreholes extending to some 40-50m and to make sub-soil profile models at all the four sites.
- Develop models for the geotechnical parameters and other material models as needed in the PLAXIS analysis.

- Analysis of unpiled raft foundation for typical cases. These include three unpiled rafts varying in size from 8m×8m, 15m×15m and 30m×30m and also in each case the raft thickness is varied as 0.25m, 0.4m, 0.8m 1.5m and 3m. The vertical loading was 215 kN/m².
- Then 8m×8m piled rafts are considered with raft thicknesses of 0.25m, 0.4m, 0.8m 1.5m and 3m. The vertical loading was 645 kN/m².
- A parametric study was made with piled raft 0.8m thick and piles (16 in numbers) spaced at 3d, 4d, 5d, 6d and 7d. For each case three vertical loadings of 215, 430 and 645 kN/m² were considered. All piles were 16m long.
- A parametric study on 0.25m thick raft with piles (16 in number) spaced at 3d and pile lengths 0m (unpiled), 6m, 10m, 16m and 25m. For each case the vertical loadings were 215 and 430 kN/m².
- Piled raft with raft thickness 0.8m and number of piles varied as 4, 8, 12 and 16. All piles were 16m long. The vertical loading was 645 kN/m².

1.3 Layout of the Thesis

Chapter I of the thesis gives the background information which included brief summary of the four tall buildings considered in the thesis and the site conditions. The availability of only the SPT data was used for the evaluation of geotechnical parameters other than unit weight. Various computer softwares are available for the analysis of rafts and piled raft foundations. The details of the study conducted using PLAXIS software.

Following Chapter I, the next chapter is devoted to literature review. The initial part of the review is on static analytical methods available for capacity estimation of single piles and pile groups. Also discussed in this chapter is the use of in-situ tests such as SPT and CPT in estimation of pile capacity. Then a review is presented as related to piled raft foundations under the headings: simplified calculation methods, approximate computer based methods and more rigorous computer based methods. Rigorous numerical analyses were also introduced. Rigorous computer based methods included the boundary element methods, combined boundary element and finite element methods, simplified finite element method, variational method and the 3-D finite element methods. The PLAXIS analysis conducted here falls under the simplified finite element method. A breakdown of the description of PLAXIS deals with the elements type, pore pressure distributions in the soils, mesh generation, automatic loading steps, the calculation and the presentation of results. Also described under the PLAXIS program are the available soil and rock models: linear elastic, Mohr-Coulomb (MC), jointed rock (JR), hardening soil models (HIS), soft soil models (SS), soft soil creep model (SSC) and user defined soil model. The PLAXIS calculations incorporate the nonlinear behaviour of the soils, estimation of elastoplastic deformations, consolidation analysis, and safety analysis by phi-c reduction.

Under Chapter III in research methodology, details are given on the estimation of the subsoil profile models at all four sites, the SPT data and its corrections and correlations with engineering properties and the program of numerical analysis using PLAXIS.

Chapter IV is fully devoted to numerical modelling. Aspects such as selection of soil models, type and size of element mesh, boundary conditions, modelling pile and raft, and basic parameters needed in the Mohr-Coulomb model used in this thesis are some but not all of the topics described in this chapter.

Finally, the results and discussions are presented in Chapter V. A detail discussion is presented on the parametric study conducted. Finally, conclusions and the recommendations for future works are presented in Chapter VI.

CHAPTER II

LITERATURE REVIEW

2.1 General

In this chapter, a brief presentation is made on the subsoil conditions at Surfers Paradise. This is then followed by the static methods of estimating pile capacity using in-situ tests and mainly SPT and CPT. A brief section on pile group analysis is also included. Much of the work presented in this chapter relates to piled raft foundations. Under the simplified calculation methods Poulos and Davis Method (1980), Randolph Method (1994), Approximate computer based methods including strip and spring approach, plate on spring approach are also discussed. Under the rigorous computer based methods, boundary element methods, combined boundary element and finite element method, simplified finite element method, variation method and three dimensional finite element methods are discussed. Since the thesis used the PLAXIS software. Aspects of the PLAXIS program are discussed in detail.

2.2 Soils Condition in Surfers Paradise, Gold Coast

The subsoil conditions in Surfers Paradise, Gold Coast is characterised mainly by sand and rock (Figure 2.1). The upper subsurface profile consists of loose to medium dense sand. Then the dense to very dense sand continued until a compressible organic peat layer was encountered. The depth, thickness and strength of the peat layer vary across the site, with the thickness of the layer increasing from around 1m to around 4m to 5m at the ocean end. Beneath the peat layer, dense to very dense alluvial sand followed by stiff to very stiff residual clays. Weathered bedrock was encountered beneath the dense sand layer and the stiff clay layer. Since the sites are closer to the Pacific Ocean, and the estuarine deposit is mainly sand with high permeability, the ground water level is affected by tidal heights; it generally fluctuates between RL +1m to RL -1.5m. .

2.3 Static Analysis of Pile Capacity

Analysis and design procedures can be divided into three broad categories (Poulos, 1989), depending on the level of sophistication and rigour. For preliminary design purpose, static analysis can meet the requirements by directly or indirectly using in-situ test data. More rigorously, based on theory and using site-specific analysis, or numerical techniques such as finite element, boundary element and finite difference method, the performance of pile foundation can be predicted with better accuracy.

2.3.1 Pile Analysis Based on Results of In-situ Tests

With this method, the analysis and design of foundations can be made with the measured data from in-situ tests without the evaluation of any characteristic soil parameters. The application of direct methods to the analysis and design of foundations are, however, usually based on empirical or semi-empirical relationships. The direct methods are based mainly on SPT and CPT. In the SPT methods, most expressions relate the pile bearing capacity to the SPT blow count N and other correlation factors. These methods include the work of Meyerhof (1956, 1976, 1983), Aoki and Velloso (1975), Reese and O'Neil (1989), and Neely (1990, 1991); while Briaud and Tucker (1984) presented a hyperbolic formula for the base and shaft resistance as a function of pile settlement with SPT N value.

Meanwhile, the cone penetration test is regarded as a better alternative to the SPT because it reflects well the vertical pile loading mechanism. The widely used CPT methods include Nottingham and Schmertmann method (Nottingham, 1975, Schmertmann, 1978), Dutch method (DeRuiter and Beringen, 1979), LCPC method (Bustamante and Gianselli, 1982), Meyerhof method (1956, 1976, 1983), Tumay and Fakhroo method (Tumay and Fakhroo, 1981) and Eslami and Fellenius method (Eslami and Fellenius, 1997). Recently, Clausen *et al* (2005) proposed a new empirical calculation method called NGI-99; based on NGI-99 a best fit correlation between SPT and CPT is established. Lehane *et al* (2005) described a new method for the evaluation of the axial capacity of driven piles in siliceous sand using CPT, q_c data. This method is shown to provide better predictions than three other published CPT based methods (Fugro-04, ICP-05 and NGI-04) for a new extended data base of static load tests.

2.3.2 Static Analysis of Pile Foundations

Static analysis requires the estimation of soil parameters, such as the angle of internal friction $\bar{\phi}$ and the undrained shear strength s_u , from in-situ tests. These parameters are then used to evaluate the end bearing capacity of the pile and the skin friction using formulae based on semi-empirical or theoretical methods.

There are three methods to design piles in cohesive soils: the total stress (α) method, the effective stress (β) method and the pseudo-effective stress (λ) method. Tables 2.1(a) to (c) has been summarise the work done in relation to the evaluation of the soil parameters from in situ and laboratory tests for the static analysis of pile foundations.

2.3.3 Pile Group Capacity

Generally, for a group of end-bearing piles, the capacity can be evaluated by summing up the capacity of each individual pile in the group. For floating piles the capacity is lesser of the sum of the individual pile capacities, or the capacity of the block containing the piles and the soil. Moreover, for the capped pile group the capacity is taken as the lesser of the capacity of the block plus a portion of the cap outside the block perimeter, or the sum of the capacity of individual piles plus net area of the cap. When a pile group is founded in dense cohesionless soil of limited thickness underlain

by a week deposit, the capacity is taken as the less of the sum of the individual pile capacities, or the capacity of the equivalent block.

Pile group capacity is calculated using the group efficiency factor η_g (Eq. 2.1). Group efficiency can be varied with different soil conditions and construction methods and the ratio of the pile diameter to the pile spacing. For a group of driven piles in cohesive soil or in dense cohesionless material underlain by a layer of compressible soil, the efficiency is usually less than one. The recommended values of the pile group efficiency for cohesive soils are illustrated in NAVFC DM-7.2 (1986). However, the efficiency of a group of driven piles in sand is usually greater than one due to the densification of the sand during driving. An efficiency factor $\eta_g = 0.67$ was suggested by Meyerhof (1976) for bored piles in sand not underlain by a weaker layer.

$$\eta_g = \frac{Q_{ug}}{nQ_u} \quad (\text{Eq. 2.1})$$

Where: η_g = Pile group efficiency
 Q_{ug} = Ultimate capacity of the pile group
 n = Number of piles in the pile group
 Q_u = Ultimate capacity of the individual pile in the pile group

A summary of notable research on pile groups is given in Table 2.2

2.3.4 Load-Deformation Behaviour of Piles under Axial Loading

A numbers of approaches may be considered for predicting the settlement of piles under axial load. These are:

- The elastic methods based on Mindlin's equations for the effects of subsurface loading in a semi-infinite elastic medium (Poulos and Davis, 1980; Randolph and Worth, 1978; Banerjee and Davies, 1978)
- The t-z method (Coyle and Reese, 1966; Focht and Kraft, 1981)
- Finite element methods (Desai, 1974; Ottaviani, 1975)

2.4 Analysis of Piled Raft Foundations

The methods for the analysis and design of piled raft foundations were reviewed by Poulos *et al* (1997). They fall into three categories:

- a) Simplified calculation methods
- b) Approximate computer-based methods
- c) More rigorous computer-based methods.

2.4.1 Simplified Calculation Methods

The simplified methods include those of Poulos and Davis (1980), Randolph (1994). These methods involve a number of simplifications in relation to the modelling of the soil profile and the loading conditions on the raft.

2.4.1.1 Poulos-Davis Method (1980)

The method yields the overall load settlement curve up to failure for piled raft with perfectly rigid or perfectly flexible raft. It is based on elastic solutions and uses the stiffness of the piled raft, the stiffness of the raft and the ultimate capacities of the piles and the raft. A tri-linear load settlement relation is obtained from the analysis.

2.4.1.2 Randolph Method (1994)

This method considers the linear behaviour of the piled raft system and provides convenient approximate equations for the stiffness of the piled raft system and the load sharing among the piles and the raft. It can be modified to provide a tri-linear load settlement curve following the same approach as of Poulos and Davis (1980)

2.4.2 Approximate Computer Based Method

In this category, the piled raft system is modelled as strip on spring and plate on spring system under approximate computer-based methods.

2.4.2.1 Strip on Spring Approach

This method presented by Poulos (1991) considers the raft as strips and the piles as springs. The raft was divided into a series of three strips in each direction. In the long direction, the nonlinear effects were considered for the springs running in the long direction, while purely linear behaviour was assumed for the strips in the shorter direction. The stiffness of the individual piles was analysed using the equations of Randolph and Wroth (1978), and simplified expressions were used to obtain the pile-pile interaction factors. For the analysis of each strip, the effects of the other strips in that direction were considered by computing the free-field settlement due to those strips, and imposing those settlements on to the strip being analysed.

2.4.2.2 Plate on Spring Approach

In this approach, the raft is modelled as an elastic plate, the soil is represented by an elastic continuum and the piles are modelled as interacting springs. A finite different method for the plate has been employed by Poulos (1994), and has allowed various interactions via elastic solutions. Meanwhile, allowance has been made for the layering of the soil profile, the effects of piles reaching their ultimate capacity, the development of bearing capacity failure below the raft, and the presence of free-field soil settlements acting on the foundation system.

Clancy and Randolph (1993) modelled piles as series of rod finite elements and raft as two-dimensional thin plate finite elements considering with four components of interactions with elastic analysis.

Russo (1998) has described a similar approach to the above methods. The geometry of the raft and the stiffness are modelled as those of a thin plate and solved via FEM (Finite Element Method). The piles and the soil are represented as linear or non-linear interaction springs using the superposition factors. An allowance was made for a complete but simple description of a non-linear load-settlement relationship for the piles.

2.4.3 Rigorous Computer-based Methods

Generally, the following analytical methods are classified as rigorous methods by Poulos *et al* (1997):

- Boundary Element Methods
- Combined boundary element and finite element method
- Simplified finite element method
- Variational Method
- Three dimensional finite element method

2.4.3.1 Boundary Element Methods

In this type of approach, the raft and each pile within the foundation system are discretised. In the early example of this approach, Butterfield and Banerjee (1971) analysed pile groups in an elastic soil mass with a rigid cap resting on the surface. However, Kuwabara (1989) presented an analysis based on an elastic theory for a piled raft foundation subjected to vertical load in homogeneous isotropic elastic half-space. The raft was assumed to be rigid and the compressibility of the piles was taken into account. It was found that the reduction of the settlement caused by the presence of the raft is very small, but the raft transmits 20-40% of the applied load direct to the soil. Poulos (1993) extended the work of Kuwabara (1989) to allow for the effects of free-field soil movements and for limiting contact pressures between the raft and the soil, as well as for the development of ultimate compression or tensile loads in the piles.

2.4.3.2 Combined Boundary Element and Finite Element Method

This method considered the raft as a series of thin-plate finite elements, while the characteristics of the piles were computed from boundary element analyses. Hain and Lee (1978) were the first to use this method with an interaction factor suggested by Poulos (1968) to reduce the computational effort. This method considers the complete interaction between the raft, the pile group, and the supporting soil, thus providing a procedure to predict the effectiveness of a pile group in reducing the settlement. Several factors for piled raft analysis were introduced. However, the limitation of this analysis was that the supporting soil was represented by a homogeneous semi-infinite elastic mass.

Frank *et al.* (1994) describe a technique involving the use of boundary element analysis for the piles and finite element analysis for the raft. Ta and Small (1997) presents a solution to use this combined boundary element and the finite element technique to obtain differential settlements and moments in the raft, loads in the piles and the overall deflections in the raft. This method can also be used for layered soils and the soil can be homogeneous, non-homogeneous or have cross-anisotropic properties.

Small and Zhang (2000) analysed the piled raft system subjected to general loadings using combined boundary element and finite element technique. While Zhang and Small (2000) implemented this technique via a program APPRAF (Analysis of Piles and Piled Raft foundation) to predict the behaviour of capped pile groups under horizontal and vertical loadings.

Mendoca and Paiva (2003) analysed a flexible piled raft in smooth and continuous contact with the supporting soil. The bending plate was modelled by FEM and the soil is considered as an elastic half-space in the BEM. The plate-soil interface is divided into triangular boundary elements.

2.4.3.3 Simplified Finite Element Method

Generally, the simplified finite element method of analysis usually involves the represented models of pile group and the piled raft as either a plane strain problem (e.g. Desai, 1974; Prakoso and Kulhawy, 2001) or as an axi-symmetric problem. In each case, finite elements are used to discretise both the raft and the soil, and it is therefore a relatively simple matter to take account of nonlinear soil and raft behaviour. Also, using the FEM technique, the two-phase behaviour of the soil can be incorporated, so that time-dependency of settlement and pile load distribution due to consolidation of the soil can be allowed.

Desai (1974) modelled the soil and the pile using quadrilateral iso-parametric elements. Sets of pile and soil properties had been chosen to evaluate the load-carrying capacity for different lengths of embedment and sizes of piles. Desai *et al* (1974) idealized the three dimensional lock-pile foundation system as a two dimensional problem; using plane strain model can provide good results.

Prakoso and Kulhawy (2001) illustrated a method in which the piled raft is simulated using a simplified linear elastic and a nonlinear plane strain finite element model in the PLAXIS software. The effects of raft and pile group system geometries and pile group compression capacity were evaluated on the settlement and differential settlements, raft bending moments and pile butt load ratio of the piled rafts.

2.4.3.4 Variational Approach

Using the variational Approach, the raft and piles are both analysed by the use of the principle of minimum potential energy. Finite series have been used to present the deformation of the piles and the raft foundation. This method is based on the research of the variational solutions for the bending analysis of rafts by Shen *et al.* (1999) and the analysis of pile group-pile cap interaction by Shen *et al.* (2000). Within this approach, the discretisation of the pile shafts and raft itself is no longer required, and

it is very highly efficient to analysis large pile groups. A surface stiffness that relates the load-settlement relationship at the pile head-raft-soil interface is incorporated in the raft analysis, making available an efficient and complete solution of a piled raft.

2.4.3.5 Three Dimensional Finite Element Method

In term of our ability to model a real problem, three-dimensional finite element analyses are usually providing much more details and the results are realistic. Ottaviani (1975) was the first to use a three-dimensional finite element approximation to analyse a very rigid raft resting on compressible piles embedded in an elastic layer. Lee (1993) performed parametric studies for settlement and load distribution within the piled raft. Ta and Small (1996) also applied thin plate finite elements for the raft and a finite layer method for layered linear elastic soil. Smith and Wang (1998) analysed a differentially loaded raft with full three-dimensional FEM and presented the benefits of using the statistics of preconditioned conjugate gradient (PCG) computation, which can solve a large problems (around 1 million degrees of freedom) in a matter of minutes. Reul (2004) investigated t the interaction between piles and a raft is a major influence in over consolidated clay. Reul and Randolph (2003) study 259 different piled raft configurations for piled raft behaviour considering the pile positions, the pile number, the pile length, the raft-soil stiffness ratio as well as the load distribution on the raft by means of three-dimensional elasto-plastic FEM technique.

2.5 A Review of Softwares for the Analysis of Piles and Piled Raft Foundations

Extensive research has been carried on piles and piled raft using computer techniques (Table 2.3). Choosing proper software depends on the significance and scale of the problem, the method of analysis, the nature of the problem, and the availability of the software. Currently, there are several computers program available and are being used for analysing piles and piled rafts. Each program has its own characteristics. A summary of some of the widely used programs is provided in Table 2.4

In the present study, the wide applicability, the operating simplicity, the speed and the availability of software and the computer are considered as the governing factors for the analysis. Desai *et al* (1974) proved that plane strain model can provide good results for piled rafts. In addition, this model can be used to analyse a relatively large pile raft without excessive modelling and computation time (Prakoso and Kulhawy, 2001). Therefore, PLAXIS version 8 is chosen in this study for the analysis of pile groups and piled rafts.

2.5.1 PLAXIS Program

PLAXIS version 8 is a 2-D finite element package intended for the two-dimensional analysis of deformation and stability in geotechnical engineering. Geotechnical applications require advanced constitutive models for the simulation of the non-linear and time dependent behaviour of soils. Since soil is a multi-phase material, special procedures are required to deal with hydrostatic and non-hydrostatic pore pressures in the soil. Although the modelling of the soil itself is an important issue, many geotechnical engineering projects, like piles and piled raft foundation, involve the

modelling of structures and the interaction between the structures and the soil. PLAXIS is equipped with special features to deal with the numerous aspects of complex geotechnical structures. Some of features are listed as follows:

a) Elements

Either quadratic 6-node or 4th order 15-node triangular elements can be chosen for modelling the deformations and stresses in the soil. Plate elements can be using to model retaining wall, shells or other slender structures. The behaviour of these elements is defined using a flexural rigidity, a normal stiffness and an ultimate bending moment. Interface element is an important element to model soil structure interaction which can be used to simulate the thin zone of intensely shearing material at the contact between structural element and the surrounding soil. Plates with interface may be used to perform many realistic analyses of geotechnical structures, like retaining walls, pile groups and piled rafts (Prakoso and Kulhawy, 2001).

b) Pore Pressures

Complex pore pressure distributions may be generated on the basis of a combination of phreatic level or direct input of water pressures. As an alternative, a steady-state groundwater flow calculation can be performed to calculate the pore pressure distribution in problems that involve steady flow or seepage. In addition, PLAXIS distinguishes between drained and undrained soils to model permeable sands as well as nearly impermeable clays. Excess pore pressures are computed during plastic calculation when undrained soil layers are subjected to loads. Undrained loading situations are often decisive for the stability of geotechnical structures.

c) Mesh Generation

PLAXIS allows for the full automatic generation of finite element meshes. The mesh generator is a special version of the Triangle mesh generator developed by Sepra. The generation of the mesh is based on a robust triangulation procedure, but the numerical performance of such meshes is usually better than regular (structured) meshes.

d) Automatic Load Stepping

The PLAXIS program can be run in an automatic step size and automatic time step selection mode. This avoids the need for users to select suitable load increments for plastic calculations and it guarantees an efficient and robust calculation process.

e) Calculation Facilities

The staged construction facility has been extended to allow for the activation and change of external loadings. This system improves the possibilities of varying external loads and combining individual loads with excavation or construction stages. In addition, a new and more robust calculation kernel has been implemented for steady-state groundwater flow calculations. Consolidation calculations have been extended to allow for staged construction in time and also for large deformation effects. Structural elements have been improved by the inclusion of an enhanced plasticity formulation for plates and anchors

f) Presentation of Results

The PLAXIS postprocessor has enhanced graphical features for displacing computational results. Values of displacement, stress, strains and structure behaviour can be obtained from the output tables. Plots and tables can also presented by MS

EXCELTM by using the provided data. In addition, animations are now available with this latest package; the animations include displacements and forces in structural elements. A report Generator has been implemented to provide a report of input data and output results that can be further edited in MS WordTM.

2.5.2 Material Models

The mechanical behaviour of soils may be modelled at various degrees of accuracy. In PLAXIS, a number of models are available which are briefly introduced as follows:

a) Linear Elastic Model

This model represents Hook's law of isotropic linear elasticity. The model involves two elastic stiffness parameters, namely Young's modulus (E), and Poisson's ratio (ν). While linear elastic model is very limited for the simulation of soil behaviour, it is primarily used for modelling structural elements in the soil.

b) Mohr-Coulomb Model (MC)

This model is used as a first approximation of the soil behaviour. The model involves five parameters, namely Young's modulus (E), Poisson's ratio (ν), the cohesion (\bar{c}), the friction angle ($\bar{\phi}$), and the dilatancy angle (ψ). Beside this five model parameters, initial soil conditions play an essential role in most soil deformation problems. Initial horizontal soil stresses have to be generated by selecting proper K_0 -values.

c) Jointed Rock Model (JR)

This is an anisotropic elastic-plastic model where plastic shearing can only occur in a limited number of shearing directions. This model can be used to simulate the behaviour of stratified or jointed rock.

d) Hardening-Soil Model (HS)

This is an elasto-plastic type of hyperbolic model, formulated in the framework of friction hardening plasticity. Moreover, the model involves compression hardening to simulate irreversible compaction of soil under primary compression. This second-order model can be used to simulate the behaviour of sands and gravel as well as softer types of soil such as clays and silts.

e) Soft Soil Model (SS)

This is a Cam Clay type model that can be used to simulate the behaviour of soft soils like normally consolidated clays and peat. The model performs best in situations of primary compression.

f) Soft-Soil-Creep model (SSC)

This is a second order model formulated in the framework of visco-plasticity. The model can be used to simulate the time-dependent behaviour of soft soils like normally consolidated clays and peat. The model includes logarithmic compression.

g) User-defined Soil Model

This facility allows user to implement a wide range of constitutive soil models to simulate the problem of soil-structure interaction. Such models must be programmed in FORTRAN, then compiled as a Dynamic Link Library (DLL) and then added to the PLAXIS program directory.

From the available material models, the MC model and HS model are often used to simulate the hard soils such as compacted soils and overconsolidated clays while the SS model is usually used to simulate the soft soils such as normally consolidated clay and lightly overconsolidated soils.

2.5.3 Calculations

In the real geotechnical engineering practice, a project of calculation phase is the activation of a particular loading at a certain time, the simulation of a construction stage, the introduction of a consolidation period, the calculation of a safety factor, etc. Each calculation phase is generally divided into a number of calculation steps because the non-linear behaviour of the soil requires loadings to be applied in load steps.

PLAXIS allows for a different type of finite element calculations, including a plastic calculation, a consolidation analysis, phi-c reduction (safety analysis), and dynamic calculations. The first three types of calculations (plastic, consolidation, phi-c reduction) optionally allow for the effects of large displacements being taken into account. This is termed *updated mesh*. The different types of calculations are explained as follows:

a) Plastic Calculation

A plastic calculation should be selected in order to carry out an elastic-plastic deformation. The stiffness matrix in the plastic calculation is based on the original undeformed geometry. This type of calculation is used in many practical geotechnical applications. In general, a plastic calculation does not take time effects into account, except when the Soft Soil Creep model is used. Considering the quick loading of water-saturated clay-type soils, a plastic calculation may be used for the limiting cases of fully undrained behaviour using the undrained option I in the material data sets. On the other hand, the settlements at the end of consolidation can be assessed by performing a fully drained analysis. This will give a reasonably accurate prediction of the final situation, although the precise loading history is not followed and the process of consolidation is not dealt with explicitly.

b) Consolidation Analysis

A consolidation analysis should be selected when it is necessary to analyse the development and dissipation of excess pore pressures in water-saturated clay-type soils as a function of time. PLAXIS allows for true elastic consolidation analyses. In general, a consolidation analysis without adding loading is performed after an undrained plastic calculation. It is also possible to apply loads during a consolidation analysis, but there are some limitations in PLAXIS on the types of loading that can be considered in a consolidation analysis. The first limitation is that it is not possible to perform a staged construction calculation with simultaneous consolidation. Activation or deactivation of clusters and structures must therefore be applied in a proceeding undrained plastic calculation. Another limitation is that the iteration process will not converge as the structure approaches failure. This means that a consolidation analysis

cannot be used to analyse failure conditions. Finally, a consolidation analysis in PLAXIS cannot be performed in the framework of large deformation theory (updated mesh analysis) and can therefore not be used after an updated mesh calculation.

c) Updated Mesh Analysis

An updated mesh analysis is a plastic calculation where effects of large deformations are taken into account. This type of calculation should be considered when deformations are to be expected that significantly influence the shape of the geometry. This stiffness matrix in an updated mesh analysis is asked on the deformed geometry. In addition, a special definition of stress rates is adopted that include rotation terms. These calculation procedures are based on an approach known as an Updated Lagrange formulation. For most applications the effects of large deformations are negligible so that a normal plastic calculation is sufficiently adequate, but there are circumstances under which it may be necessary to take these effects into accounts. Typical applications are the analysis of reinforced soil structures, the analysis the collapse load of large offshore footing sand the study of projects involving soft soils where large deformations can occur.

d) A Safety Analysis (Phi-c Reduction)

Phi-c reduction is an option available in PLAXIS to compute safety factors. This option is only available for plastic calculations. In the Phi-c reduction approach the strength parameter $\tan \bar{\phi}$ and \bar{c} of the soil are successively reduced until failure of the structure occurs. The total multiplier $\sum Msf$ is used to define the value of the soil strength parameters at the given stage in the analysis:

$$\sum Msf = \frac{\tan \phi_{input}}{\tan \phi_{reduced}} = \frac{c_{input}}{c_{reduced}} \quad \text{Eq. 2.2}$$

Where the strength parameters with the subscript input refer to the properties entered in the material sets and parameters with the subscript reduced refer to the reduced values used in the analysis. In contrast to other total multipliers, $\sum Msf$ is set to 1.0 at the start of a calculation to set all material strengths to their unreduced values. The strength parameters are successively reduced automatically until failure of the structure occurs. At this point the factor of safety is given by:

$$SF = \frac{\text{available strength}}{\text{strength at failure}} = \text{value of } \sum Msf \text{ at failure} \quad \text{Eq. 2.3}$$

2.6 Conclusion Remarks

Extensive research on pile foundation has been done in the last four decades. Early research work was on experimental works, based on SPT test or CPT test data, or as based on simple theoretical considerations. Based on these works, improved design procedures were developed due to the availability of powerful numerical techniques. Approximate computers-based method and more rigorous methods had been suitable to deal with complex soil-structure interaction problems. Simplified finite element method, using PLAXIS code was chosen as the numerical technique to simulate piled

raft performance. PLAXIS version 8 provided varieties of soil models and types of calculation to deal with most geotechnical problems.

CHAPTER III

RESEARCH METHODOLOGY

3.1 General

This chapter summarises the methodology adopted in this study. As stated before, this is the first time foundation conditions are researched at the Surfers Paradise. Thus lot of efforts are spent in acquiring case histories which involve deep foundations. Four case histories were identified. Each project will briefly summarise with pertinent information as related to the site investigation adopted. The Surfers Paradise Geotechnical Practice rely heavily on standard penetrations tests (SPT) and as such substantial time is spent in re-visiting the early research on the numerous somewhat confusing corrections to be adopted to the measured SPT N values and also the variety of correlations available which make this test a unique one in obtaining geotechnical parameters for foundation design. Nowadays, the cone penetration tests (CPT) have also entered into the market for site investigation works at Surfers Paradise. Recently, another interesting Griffith Project is completed in this interesting utility of CPT. Also, currently the prospect of using dilatometer test is in progress. Thus, future research at Griffith in Geotechnics has enormous scope.

CHAPTER IV is fully devoted to numerical modelling and as such this aspect will not be dealt with in this chapter. However, the various cases considered in the PLAXIS analysis is summarised in this chapter.

3.2 Project Details and Sub-surface Investigations

The four projects studied in this thesis are; ARTIQUE, Q1, Circle on Cavill and SOLAIRE. In future reference to these projects, they will be called with names as mentioned here. The laboratory test data mainly concerned with the clay layer and in particular the natural water content and index properties. For the Artique tower and SOLAIRE, piled raft foundation is used and the piles extend to the dense sand layer. The Q1 tower and the two towers of Circle on Cavill are founded in the rock stratum. The rock stratum typically varies from 35 to 50 m from site to site. Table 3.1 contains further information related to the foundations.

3.3 Description of Subsoil Conditions

a) ARTIQUE

Six boreholes were drilled at this site (see Figure 3.1). There is thin layer of fill material at the surface, less than a meter thickness. Below this is the Layer 1 of medium dense sand about 9.4m thick. The layer 2 is very dense sand and varied in thickness at the site from 1.8m to 4.6m. Below these two layers a third layer of peat is encountered and this varied from 1.2m to 1.5m thick. Then the fourth layer is again very dense sand. This is some time called the lower layer of sand. This layer ranged in thickness from 10 to 10.5m. Below this fourth layer is the fifth layer and it is sandy clay, ranging in thickness from 7.9m to 9.5m. Rock stratum is encountered at depths

of 30 to 35m. Table 3.2 gives additional details. An idealized soil profile is shown in Figure. 3.2.

b) Q1 Tower

At the Q1 tower three borehole data was available (see also Figure 3.3). Detailed Borehole information is in Appendix B. Here the boreholes were taken down to about 50 m deep. At this site, the First Layer of medium dense. The second layer of very dense sand ranged in thickness from 20 to 23m. The layer three is stiff clay and it ranged in thickness from 3.7 to 4.3 m. The peat layer labeled Layer 4 was missing at this site as per the borehole records. The fifth layer is clayey sand and its thickness is 4.3 to 6.1m. Below this clayey sand layer is the seventh layer and it is gravel of 2 to 4.7m thick. At this site the rock stratum is encountered at a depth of about 40m. Table 3.3 gives further details. Figure 3.4 is an idealized model for the sub-soil profile at the Q1 site.

c) Circle on Cavill

A total of 16 boreholes data is available at this site (Figure 3.5). The layer one which is medium dense ranged in thickness from 3.8 to 5.3m. The second layer which is very dense sand ranged in thickness from 8.7 to 13.5m. The third layer of peat is about 3m thick. This peat layer is followed by the fourth layer of very dense sand which ranged in thickness from 6.4 to 11.1m. Layer 5 is sandy clay and its thickness varied from 10.7 to 11.5m. Rock stratum is encountered at this site at a depth of 40m or so. Additional details are given in Table 3.4 and the idealized section is presented in Figure. 3.6

d) SOLAIRE

Six bore holes were done at this site (see Figure 3.7). Layer one which is medium dense sand ranged in thickness from 4.2 to 5.6m. This is followed by very dense sand which varied in thickness from 8.7 to 9.3m. The peat layer is 3.2 to 3.8m thick. The fourth layer which is very dense sand ranged in thickness from 4.4 to 5.5m. The stiff clay layer which is the fifth one ranged in thickness from 5.4m to 6.9m. Below this is also a very dense sand layer 1.2 to 2.3m thick. Rock is encountered at this site at a depth of about 33 m. Table 3.5 contains further details. Finally, Fig. 3.8 is an idealized plot of the sub-surface model at this site.

3.4 Corrected SPT Test Results

(N_{60}) is defined as the corrected SPT number at 60 percent hammer energy. Normalized N_{60} values provide better design parameters when correlated with soil strength, bearing capacity, unit weight, liquefaction susceptibility and other properties. The variations in testing procedures may be at least compensated by converting the measured N to N_{60} as follows (Skempton, 1986):

$$N_{60} = \frac{E_m C_B C_S C_R N}{0.60} \quad \text{Eq. 3.1}$$

Where:

N_{60} = SPT N value corrected for field procedures
 E_m = hammer efficiency (from Table 3.6)

C_B = Borehole diameter correction (from Table 3.7)
 C_S = sample correction (from Table 3.7)
 C_R = rod length correction (from Table 3.7)
 N = measured SPT N value

The SPT data also may be adjusted using an overburden correction that compensates for the effects of the effective stress. Deep test in a uniform soil deposit will have higher N values than the shallow tests in the same soil. So the overburden correction adjusts the measured N value to the corrected value given by

$$(N_1)_{60} = C_N N_{60} \quad \text{Eq. 3.2}$$

Where, C_N = correction factor for overburden pressure.

The overburden corrections were given by Peck and Bazara (1969), Tomlinson (1969), Peck et al., (1974) and Liao and Whitman (1985). A simple correction chart is given in Figure 3.9. Basically, most of the methods give similar corrections for $\sigma' > 50$ kPa within the range of expected accuracy for the SPT except Tomlinson (1969) which should be applied with caution. Most of the methods have been derived from field data.

The corrected SPT data vs. depth for the four projects are presented in Figures 3.10a to 3.10d. Also the summarised values are given in Tables 3.8 (a) to (d).

3.4.1 Correlations of Friction Angle $\bar{\phi}$, Undrained Shear Strength s_u and Young's Modulus E with SPT N Value

3.4.1.1 General

The standard penetration test (SPT) N values have been used extensively to estimate soil parameters in-situ (see Meyerhof, 1956; Terzaghi and Peck, 1967). In the following sections the estimation of geotechnical parameters from SPT measurements and their corrected values will be presented.

3.4.1.2 Friction Angle, $\bar{\phi}$

SPT test can be one of the methods to estimate the friction angle of cohesionless soils. Table 3.9 summarise the early research on the correlation of the friction angle $\bar{\phi}$, with SPT N value. Peck *et al* (1974) provided an approach which is more conservative in design. Their work is presented in Figure 3.11. The N values actually depend on the stress level. Figure 3.12 presents the correlation between N and $\bar{\phi}$ as a function of the stress level. The relative density estimation is given in Figures 3.13a and b. Meanwhile, Stroud (1989) replotted all the available data to obtain the variation of $\bar{\phi}$ with $(N_1)_{60}$ and $(N_1)_{60}$ versus relative density D_r for different OCR and different $\bar{\phi}_{cs}$ (see Figures 3.13 c and d).

3.4.1.3 Undrained Shear Strength, s_u

The correlation of SPT N with s_u is given in Table 3.10. Other such relationships are contained in -. These relationships represent a wide variety of interpretations of soil types and testing conditions as there is no indication of the reference strength used to determine s_u . For clays within a given geology, a reasonable correlation might be expected between s_u and N and Figure 3.15 indicate this behaviour over a wide range of N value), the same drilling equipment, SPT procedure, and consistent reference strength were employed. From this figure, the reported regression equation is given by:

$$s_u = 29 N^{0.72} \quad \text{Eq. 3.3}$$

The above correlation would be used to evaluate the shear strength s_u of clay in this thesis work.

3.4.1.4 Young's Modulus, E

Callahan and Kulhawy (1985) established correlations of SPT N values with the drained modulus of elasticity (see Table 3.11 and Figure. 3.16). Poulos and Davis (1980) have suggested that for the prediction of the load-settlement behaviour of piles in sand, the values of the average soil modulus E_s , along the shaft, can be estimated from Table 3.12. In addition, for clays, Kulhawy and Mayne (1990) have given typical ranges for the undrained modulus, and these ranges are summarised in Table 3.13. More commonly, the undrained modulus (E_u) is normalized directly with the undrained shear strength (s_u), to give E_u/s_u . This ratio is assumed to be independent of the type of test. Also commonly used is the rigidity index (I_r), which is defined as the ratio of the shear modulus (G) to the strength. For undrained case ($\phi_u=0$), I_r is given as:

$$I_r = G/s_u \quad \text{Eq. 3.4}$$

For undrained loading, E_u is equal to $3G$ and therefore:

$$E_u/s_u = 3 I_r = 3G/s_u \quad \text{Eq. 3.5}$$

More rigorously, the moduli values back-figured from analysis of full-scale field load tests have proved to be more useful in estimating the modulus of cohesion soils as used in pile design. Figure 3.17 shows an interpretation based on limited data for driven piles and drilled shafts. Figure 3.18 includes more data for drilled shaft as a function of depth (D) to diameter (B) ratio. It has been shown that E_{us}/s_u is normally greater than 200. Lastly, from analysis of the axial deformation of piles at working load levels, Randolph (1983) suggested the following range for rigidity index ($I_r = G/s_u$)

$$150 \leq I_r \leq 200 \quad \text{Eq. 3.6}$$

In many of the test, it is not possible to determine whether the value of E_s is the undrained or the drained value. It is possibly reasonable to consider the values of E_s in these figures provided in this section as drained Young's modulus, E'_s and in the

absence of other information, the undrained modulus E_u may be estimated from the following relationship suggested by Poulos and Davis (1980) for an ideal isotropic elastic two-phase soil:

$$E_u = \frac{3E'_s}{2(1 + \nu'_s)} \quad \text{Eq. 3.7}$$

Finally, based on the SPT data combined with laboratory results, the adopted geotechnical parameters for all four projects are given in Figures 3.19 (a) to (d).

3.5 Modelling and Analysis of Piled System

3.5.1 Selection of Software

Detail features of the available softwares as used in Geotechnical Engineering is presented in CHAPTER II. The latest version of PLAXIS has been chosen as the software for numerical analysis. This is a two dimensional plane strain finite element program, which can accommodate various constitutive soil models. This explicit finite element code is especially developed for the geotechnical analysis and covers a wide range of soil-structure interaction problems. Prakoso and Kulhawy (2001) showed that this type of model can provide good results in simulating piled raft behaviour. In addition, this model can be used to analyse a relatively large piled raft without excessive modelling and computing time.

3.5.2 Model Calibration

For the purpose of simplicity in the analysis, a generalised three layer subsoil profile for Surfers Paradise area consisting of medium dense sand, very dense sand and stiff clay have been adopted for the FEM analysis (see Figure 3.20). In particular, the ARTIQUE site has been chosen for detailed analysis.

Generally, the PLAXIS software requires a number of geotechnical parameters for the analysis of the piles and the piled raft using the elastic analysis (Table 3.14). The various parameters used in the numerical analysis are as follows:

E_1, E_2, E_3	Moduli for the three layers as obtained from SPT data
ν_1, ν_2, ν_3	Poisson's ratio for the three layers obtained from existing literature
E_p, E_R	Pile material properties
$I_R, I_p, \pi d, A$	Geometrical properties of composite raft, pile section
$\bar{c}, \bar{\phi}$	Estimated from SPT data
R_{inter}	From PLAXIS design manual (Huybrechts <i>et al</i> , 2004)

The three layers generalised for simplified computation have distinct stiffness properties. Young's modulus of each of the layer was determined through study on correlated to SPT test results, which had been considered with effects of overburden burden pressure. In analysing the piled raft system, pile is considered as linear

material of E_p and ν_p , and modelled soil is modelled as isotropic elastic materials with E_s and ν_s .

3.5.3 PLAXIS Analysis Including Details of Parametric Study

In the plane strain analysis using PLAXIS, the raft was modelled as a plate element, while the piles are modelled as series of beam elements with the appropriate geometrical parameters and geometrical boundaries as suggested by Prakoso and Kulhawy (2001).

Seven different types of simulations were carried out. For each of this simulation four cases are considered. The details are listed below:

- Case - 1: Unpiled raft 8m×8m with thicknesses of 0.25m, 0.4m, 0.8m, 1.5m and 3m. Vertical loading intensity 215 kN/m².
- Case - 2: Unpiled raft 15m×15m with thicknesses of 0.25m, 0.4m, 0.8m, 1.5m and 3m. Vertical loading intensity of 215 kN/m².
- Case - 3: Unpiled raft 30m×30m with thicknesses of 0.25m, 0.4m, 0.8m, 1.5m and 3m. Vertical loading intensity of 215 kN/m².
- Case - 4: Piled Raft, 8m×8m with raft thicknesses of 0.25m, 0.4m, 0.8m, 1.5m and 3m. The pile spacing is 3d. The length of piles is 16m.
- Case - 5: Piled raft with raft thickness of 0.8m. Pile spacing varied as 3d, 4d, 5d, 6d and 7d and for each pile spacing with vertical loading intensity of 215 kN/m², 430 kN/m², 645 kN/m². The pile length is 16m.
- Case - 6: Unpiled raft and piled raft (8m x 8m) with raft thickness of 0.25m. The pile spacing is 3d. The pile lengths varied as 0m (unpiled), 6m, 10m, 16m and 25m under vertical loading of 215 kN/m² and 430 kN/m².
- Case - 7: Piled raft 8mx 8m and thickness 0.8m with 4, 8, 12 and 16 piles. The pile length is 16m. The vertical loading intensity is 645 kN/m².

The serviceability load is 215kN/m², twice of serviceability load is 430kN/m² and three times of the serviceability load is 645kN/m². The thickness of the raft was varied to investigate the effect of the relative stiffness of raft on settlements differential settlements, bending moments and the proportion of the loads shared by the piles. Similarly, the effects of pile spacing, pile length and number of piles were also investigated.

3.6 Concluding Remarks

The sub-soil profile at four sites in Surfers Paradise is evaluated for the analysis of raft and piled raft foundations. A soil model is prepared for each site. The rock stratum was encountered from 30 to 50 m depth and this depth varied from site to site.

A detail analysis of the SPT data is made at each site. These SPT data are subjected to the corrections established by various authors for hammer energy, and overburden pressure effects. From well known and established correlations, the geotechnical parameters as needed for the analysis is then determined and presented in the form of Tables and figures. Seven cases of PLAXIS analysis were conducted. Three of them were for unpiled raft. In this parametric study the width of the unpiled raft and also the thicknesses were changed. The other four cases refer to the piled raft and the parameters varies are the raft thickness, the pile spacing and length and the intensity of loading.

CHAPTER IV

NUMERICAL MODELLING

4.1 General

Numerical analyses using finite element techniques are popular in recent years in the field of foundation engineering. To date, a variety of finite element computer programs have been developed with a number of useful facilities and to suit different needs. The behaviour of soil is also incorporated with appropriate stress-strain laws as applied to discrete elements. The finite element method provides a valuable analytical tool for the analysis and design of foundations. The analyses of piles and piled raft using finite element method is done in an excellent manner by many authors including Ottaviani (1975), Chen and Poulos (1993), Reul and Randolph (2003). Also the analysis of axially loaded piles in sand have been reported by Desai (1974), and Randolph and Wroth (1978) among others.

4.2 Finite Element Method Applied to Piled Raft Foundation

In reality the analysis of axially loaded piled raft represents a three dimensional problem. Since the loading and geometry are symmetrical, symmetric approaches permit to reduce it to two dimensions. Figure 4.1 illustrates the symmetric idealization of the piled raft problem. Since the piled raft is a typical example of soil-structure interaction, a special type of element at pile-soil interface, simulating the displacement discontinuity between the pile and the soil mass is needed. This element should be capable of simulating different models of interface behaviour. For the piles under static vertical loading conditions, the relative slip between the pile and the soil mass becomes very important.

4.3 Numerical Modelling of Piled Raft Foundation

4.3.1 Numerical Model

The numerical analysis in the present investigation was carried out using the finite element code PLAXIS. The numerical models include the following feature:

- Undrained, drained and coupled consolidation analysis either for two dimensional plane strain or axisymmetric loading conditions.
- The mechanical behaviour of soil may be modeled at various degrees of accuracy using Hooke's law of linear, isotropic elasticity, elastoplastic, elastic perfectly plastic behaviour for soils and jointed rock behaviour, Mohr-Coulomb yield criterion, and hardening-soil models.

4.3.2 Selection of Appropriate Soil Model

Based on the materials and for mainly sand soil, it is preferable to use the Mohr-Coulomb model for relatively quick and simple and first analysis of any problem considered. When good soil data is lacking, there is no use in adopting more advanced analyses. In many cases, if good data can be collected on dominant soil layers, it is perhaps appropriate to use the hardening-soil model as a refinement in the analysis. The above idea of analyzing geotechnical problems with different soil models should be considered in view of the different subsoils encountered. Undoubtedly, one seldom has test results from both triaxial and Oedometer tests, but good quality data from one type of test can be supplemented with data from correlations and/or in situ testing. It should be known that Mohr-Coulomb analysis is relatively quick and a simple way to model the soil behaviour in sand.

4.3.3 Type and Size of Finite Element Mesh

The mesh used in the present study was determined according to the size of the raft and pile, and the amount of deformation expected during the analysis. The region of interest is mainly limited to that below the raft and a few diameters beyond the edge of the raft and piles. Obviously, a symmetrical analysis for a mesh is the most

efficient solution for the symmetrical problems, whereas full scale analysis can provide a more accurate and reliable result in a realistic situation. The choice of the number of elements and mesh design reflects a compromise between an acceptable degree of accuracy and computing time. It is recommended that the size of the mesh near the interested area should be refined, i.e. the areas under the raft foundation and the cluster area surrounding the piled raft foundation. In PLAXIS, only triangular elements are used, which will generate unsymmetrical mesh when full scale analysis is involved. With the use of a very coarse mesh, unsymmetrical behaviour of the foundation can be experienced. Based on this phenomenon, it is strongly recommended that the mesh size should be adapted to a very fine level to achieve symmetrical results when full scale analyses are carried out. Wehnert and Vermeer (2004) had studied the effects of mesh on load-settlement of drilled shafts based on PLAXIS code.

4.3.4 Boundary Conditions

The following boundary condition should be considered as a proper restrain on the mesh. The nodes belonging to the periphery of the symmetrical mesh are fixed against displacement in both horizontal directions, yet remain free to have the displacement vertically, and the nodes constituting the bottom of the mesh are fixed against displacement in both horizontal and vertical directions. In addition, the boundary should be placed far enough from the region of interest in order not to affect the deformations within the region. The mesh is designed to be denser in the vicinity of the pile shaft and area under the raft, where the deformations and stresses are expected to have major variations.

Randolph and Wroth (1978) recommended boundary conditions for the finite element mesh to be 50 times the pile radius in the lateral direction, and to be 1.5 times the pile length below the tip in the vertical direction. Meanwhile, for piled raft foundation, Prakoso and Kulhawy (2001) recommended that the boundary condition in lateral direction should be 5 times of the piled raft cluster area, and twice of the pile length in vertical direction. However, the boundary condition in the vertical direction at times has been limited by the realistic problem concerned i.e. very hard bearing layer is relatively low or not. The boundary conditions used in this study are as follows:

- (1) The horizontal boundary was placed at least 5 times the piled raft cluster radius measured from piled raft symmetrical axis. Figure 4.2
- (2) The vertical boundary was placed until the bottom of the stiff clay, where the weathered rock starts. It is 35m under the ground surface.

These conditions will vary depending on piled raft geometry and the observed zone of failure around the pile shaft. Figure 4.3 shows schematic views of the adopted finite element meshes and the distribution of elements. These boundary conditions were imposed to minimize the boundary effect on the zone of interest (around the shaft), and to provide sufficient accuracy in the analyses.

4.3.5 Number of Elements

The number of elements required in the analysis to achieve sufficient accuracy is considered to be between 100 and 200 elements as suggested by Duncan (1972). Obviously, more elements will produce more accurate results at the expense of more computation time. In this study, it was found that a minimum of 500 elements for unpiled raft and 900 elements for piled raft foundation are adequate to achieve the desired accuracy in using the PLAXIS program.

4.3.6 Types of Elements

The soil was modelled using 15-node or 6-node triangular elements (Figure 4.4). The 15-node element is a very accurate element that has produced high quality stress distributions for difficult problems. Smaller sized 15-node soil elements were selected beneath the unpiled raft area, where variations in stresses and strains were expected to be more significant. Whereas, 6-node triangular elements were chosen for modelling the soil layer in piled raft analysis due to the increased computational effort needed in the analysis of piled raft systems.

In addition to the soil element, compatible plate (beam) elements are used to simulate the behaviour the raft and the pile with a significant flexural rigidity and a normal stiffness. Plates in the 2-D finite element model are composed of beam elements (line elements) with three degrees of freedom per node: two translational degrees of freedom (u_x , u_y) and one rotational degree of freedom (rotation in the x-y plane: ϕ_z). When 6-node soil elements are employed then each beam element is de then the 15-node soil elements are adopted (Figure 4.5). The beam elements are based on Mindlin's beam theory. This theory allows for beam deflections due to shearing as well as bending. In addition, the element can change length when an axial force is applied. Beam elements can become plastic if a prescribed maximum value is specified for the elastic range; however the raft and the pile in these studies always lie in the elastic range.

Desai *et al* (1984) developed a thin layer interface element, which can simulate the various interface deformation modes. It has proven successful in various soil-structure interaction problems. This thin layer element (Figure 4.6) is treated essentially like a small finite thickness of solid element, with elastic-perfectly plastic constitutive behaviour. The normal stiffness of the interface elements is assumed to be the same as the joining soil elements. The shearing stiffness in the plane of the interface is defined based on the consolidated drained direct shear simulation of the interface.

4.4 Constitutive Laws

4.4.1 Modelling of Raft and Pile Materials

The elements constituting both the pile and the raft were assumed to behave elastically at all times. The maximum stresses attained during this study did not exceed the yield limit of the chosen material (reinforced concrete). Table 4.1 shows the typical elastic parameters required by the program to model the raft. For modelling the pile, the piles are simplified as strips (see Prakoso and Kulhawy, 2001). These authors suggested that an in-plane row of piles has to be simplified into an equivalent plane strain pile having the following Young's modulus:

$$E_{eq} = \frac{n_{p-row i} A_p E_p}{L_r B} \quad \text{Eq. 4.1}$$

Where $n_{p-row i}$ = number of piles in row i ; A_p = area of pile cross section; E_p = pile Young's modulus; L_r = raft length (in-plane); and B = pile diameter.

4.4.2 Soil Model

4.4.2.1 General

The soil is assumed to be homogenous. The deformation of the soil is considered as linear elastic and modelled by the classical theory of elasticity. During non-linear behaviour the constitutive model used for the soil is the Mohr-Coulomb plasticity model. This model was selected among the several soil models available in the library of PLAXIS because it can be implemented easily. Its parameters can be related to the physical properties of the soil, and furthermore it is widely used in practice.

4.4.2.2 The Mohr-Coulomb Model: Elastic Perfectly Plastic Behaviour

The basic principle of elastoplasticity (Figure 4.7) is that strain rates are decomposed into an elastic part and a plastic part:

$$\underline{\underline{\dot{\epsilon}}} = \underline{\underline{\dot{\epsilon}}}^e + \underline{\underline{\dot{\epsilon}}}^p \quad \text{Eq. 4.2}$$

Hooke's law is used to relate the stress rates to the elastic strain rates. Substitution of Eq. 4.2 into Hooke's Law leads to:

$$\underline{\underline{\dot{\sigma}}} = \underline{\underline{D}}^e \underline{\underline{\dot{\epsilon}}}^e = \underline{\underline{D}}^e (\underline{\underline{\dot{\epsilon}}} - \underline{\underline{\dot{\epsilon}}}^p) \quad \text{Eq. 4.3}$$

According to the classical theory of plasticity, plastic strain rates are proportional to the derivative of the yield function with respect to the stresses. This means that the plastic strain rates can be represented as vectors perpendicular to the yield surface. This classical form of the theory is referred to as associated plasticity. However, for Mohr-Coulomb type yield functions, the theory of associated plasticity leads to an overprediction of dilatancy. Therefore, in addition to the yield function, a plastic potential function g is introduced. The case $g \neq f$ is denoted as non-associated plasticity. In general, the plastic strain rates are written as:

$$\underline{\underline{\dot{\epsilon}}}^p = \lambda \frac{\partial g}{\partial \underline{\underline{\sigma}}} \quad \text{Eq. 4.4}$$

In which λ is the plastic multiplier. For purely elastic behaviour λ is zero, whereas in the case of plastic behaviour λ is positive:

$$\lambda = 0 \quad \text{for:} \quad f < 0 \quad \text{or} \quad \frac{\partial f^T}{\partial \underline{\underline{\sigma}}} \underline{\underline{D}}^e \underline{\underline{\dot{\epsilon}}} < 0 \quad (\text{Elasticity}) \quad \text{Eq. 4.5a}$$

$$\lambda > 0 \quad \text{for:} \quad f = 0 \quad \text{or} \quad \frac{\partial f^T}{\partial \underline{\sigma}'} \underline{D}^e \underline{\dot{\epsilon}} > 0 \quad (\text{Plasticity}) \quad \text{Eq. 4.5b}$$

These equations may be used to obtain the following relationship between the effective stress rates and strain rates for elastoplasticity (Smith and Griffith, 1982):

$$\underline{\dot{\sigma}'} = \left(\underline{D}^e - \frac{\alpha}{d} \underline{D}^e \frac{\partial g}{\partial \underline{\sigma}'} \frac{\partial f}{\partial \underline{\sigma}'} \underline{D}^e \right) \underline{\dot{\epsilon}} \quad \text{Eq. 4.6a}$$

Where:

$$d = \frac{\partial f^T}{\partial \underline{\sigma}'} \underline{D}^e \frac{\partial g}{\partial \underline{\sigma}'} \quad \text{Eq. 4.6b}$$

The parameter α is used as a switch. If the material behaviour is elastic, as defined by Eq. (4.5a), the value of α is equal to zero, whilst for plasticity, as defined by Eq. (4.5b), the value of α is equal to unity.

The above theory of plasticity is restricted to smooth yield surfaces and does not cover a multi surface yield contour as present in the Mohr-Coulomb model. For such a yield surface the theory of plasticity has been extended by Koiter (1960) and others to account for flow vertices involving two or more plastic potential functions:

$$\underline{\dot{\epsilon}}^p = \lambda_1 \frac{\partial g_1}{\partial \underline{\sigma}'} + \lambda_2 \frac{\partial g_2}{\partial \underline{\sigma}'} + \dots \quad \text{Eq. 4.7}$$

Similarly, several quasi independent yield functions ($f_1, f_2 \dots$) are used to determine the magnitude of the multipliers ($\lambda_1, \lambda_2 \dots$).

4.4.2.3 Formulation of Mohr-Coulomb Model

The Mohr-Coulomb yield condition is an extension of Coulomb's friction law to general states of stress. In fact, this condition ensures that Coulomb's friction law is obeyed in any plane within a material element. The full Mohr-Coulomb yield condition consists of six yield functions when formulated in terms of principal stresses (Smith and Griffith, 1982):

$$f_{1a} = \frac{1}{2}(\sigma'_2 - \sigma'_3) + \frac{1}{2}(\sigma'_2 + \sigma'_3) \sin \varphi - c \cos \varphi \leq 0 \quad \text{Eq. 4.8a}$$

$$f_{1b} = \frac{1}{2}(\sigma'_3 - \sigma'_2) + \frac{1}{2}(\sigma'_3 + \sigma'_2) \sin \varphi - c \cos \varphi \leq 0 \quad \text{Eq. 4.8b}$$

$$f_{2a} = \frac{1}{2}(\sigma'_3 - \sigma'_1) + \frac{1}{2}(\sigma'_3 + \sigma'_1) \sin \varphi - c \cos \varphi \leq 0 \quad \text{Eq. 4.8c}$$

$$f_{2b} = \frac{1}{2}(\sigma'_1 - \sigma'_3) + \frac{1}{2}(\sigma'_1 + \sigma'_3) \sin \varphi - c \cos \varphi \leq 0 \quad \text{Eq. 4.8d}$$

$$f_{3a} = \frac{1}{2}(\sigma'_1 - \sigma'_2) + \frac{1}{2}(\sigma'_1 + \sigma'_2) \sin \varphi - c \cos \varphi \leq 0 \quad \text{Eq. 4.8e}$$

$$f_{3b} = \frac{1}{2}(\sigma'_2 - \sigma'_1) + \frac{1}{2}(\sigma'_2 + \sigma'_1) \sin \varphi - c \cos \varphi \leq 0 \quad \text{Eq. 4.8f}$$

The two plastic model parameters appearing in the yield functions are the well-known friction angle $\bar{\phi}$ and the cohesion \bar{c} . These yield functions together represent a hexagonal cone in principal stress space as shown in Figure 4.8. In addition to the yield functions, six plastic potential functions are defined for the Mohr-Coulomb model:

$$g_{1a} = \frac{1}{2}(\sigma'_2 - \sigma'_3) + \frac{1}{2}(\sigma'_2 + \sigma'_3) \sin \psi \quad \text{Eq. 4.9a}$$

$$g_{1b} = \frac{1}{2}(\sigma'_3 - \sigma'_2) + \frac{1}{2}(\sigma'_3 + \sigma'_2) \sin \psi \quad \text{Eq. 4.9b}$$

$$g_{2a} = \frac{1}{2}(\sigma'_3 - \sigma'_1) + \frac{1}{2}(\sigma'_3 + \sigma'_1) \sin \psi \quad \text{Eq. 4.9c}$$

$$g_{2b} = \frac{1}{2}(\sigma'_1 - \sigma'_3) + \frac{1}{2}(\sigma'_1 + \sigma'_3) \sin \psi \quad \text{Eq. 4.9d}$$

$$g_{3a} = \frac{1}{2}(\sigma'_1 - \sigma'_2) + \frac{1}{2}(\sigma'_1 + \sigma'_2) \sin \psi \quad \text{Eq. 4.9e}$$

$$g_{3b} = \frac{1}{2}(\sigma'_2 - \sigma'_1) + \frac{1}{2}(\sigma'_2 + \sigma'_1) \sin \psi \quad \text{Eq. 4.9f}$$

As shown the formulas above, the plastic potential functions contain a third plasticity parameter, the dilatancy angle ψ . This parameter is required to model positive plastic volumetric strain increments (dilatancy) as actually observed for dense soils.

4.4.2.4 Basic Parameters of the Mohr-Coulomb Model

(a) General

The Mohr-Coulomb model requires a total of five parameters, which are generally familiar to most geotechnical engineers and which can be obtained from basic tests on soil samples. These parameters with their standard units are listed below:

E	:	Young's modulus	[kN/m ²]
ν	:	Poisson's ratio	[dimensionless]
$\bar{\phi}$:	Friction angle	[°]
\bar{c}	:	Cohesion	[kN/m ²]
ψ	:	Dilatancy angle	[°]

(b) Young's Modulus, E

PLAXIS uses the Young's modulus as the basic stiffness modulus in the elastic model and the Mohr-Coulomb model, but some alternative stiffness moduli are displayed as well. A stiffness modulus has the dimension of stress. The values of the stiffness parameter adopted in a calculation require special attention as many geo-materials show a nonlinear behaviour from the very beginning of loading. In soil mechanics the initial slope is usually indicated as E_0 and the secant modulus at 50% strength is denoted as E_{50} (see Figure 4.9). For materials with a large linear elastic range it is

realistic to use E_0 , but for loading of soils one generally uses E_{50} . E_{ur} is needed instead of E_{50} when unloading problems involved.

For soils, both the unloading modulus, E_{ur} , and the first loading modulus, E_{50} , tend to increase with the confining pressure. Hence, deep soil layers tend to have greater stiffness than shallow layers. Moreover, the observed stiffness depends on the stress path that is followed. The stiffness is much higher for unloading and reloading than for primary loading. Also, the observed soil stiffness in terms of a Young's modulus may be lower for (drained) compression than for shearing. Hence, when using a constant stiffness modulus to represent soil behaviour one should choose a value that is consistent with the stress level and the stress path development. In particularly PLAXIS offers a special option for the input of a stiffness increasing with depth.

(c) Poisson's ratio, ν

Standard drained triaxial tests may yield a significant rate of volume decrease at the very beginning of axial loading and, consequently, a low initial value of Poisson's ratio (ν_0). For some cases, such as particular unloading problems, it may be realistic to use such a low initial value, but in general when using the Mohr-Coulomb model the use of a higher value is recommended.

In many cases one will obtain ν values in the range between 0.3 and 0.4. In general, such values can also be used for loading conditions other than one-dimensional compression. For unloading conditions, however, it is more common to use values in the range between 0.15 and 0.25.

While for clay soil, Poulos and Davis (1980) suggested that the following typical ranges of values of ν_s :

Stiff overconsolidated clays:	0.1~0.2 (average: 0.15)
Medium clays:	0.2~0.35 (average: 0.3)
Soft normally consolidated clays:	0.35~0.45 (average: 0.4)

And for cohesionless soil, vales of Poisson's ration, ν_s , obtained from triaxial tests generally lie between 0.25 and 0.35 at relatively low stress levels. An average value of 0.3 is reasonable when no test data are available (Poulos and Davis, 1980)

(d) Cohesion, \bar{c}

The cohesive strength has the dimension of stress. PLAXIS can handle cohesionless sands ($\bar{c} = 0$), but some options will not perform well. To avoid complications, it is often recommended to enter a low value of cohesion (use $\bar{c} > 0.2$ kPa) (Brinkgreve, 2002). Meanwhile, Huybrechts and Whenham (2004) suggested a range of values of cohesion for cohesive and cohesionless soils which is tabulated in Table 4.3.

(e) Friction Angle, $\bar{\phi}$ and Dilatancy Angle, ψ

The effective angle of internal friction relates to the frictional properties of the soil particles. The relative density or void ratio of sand is critical to its shear behaviour.

Detailed information has been provided in CHAPTER III for how to evaluate friction angle of sand using SPT test data.

Nevertheless, another parameter, which is named as the dilatancy angle, ψ , should be included in the analysis. The dilatancy angle, ψ , is expressed as $\psi = \text{Arctg} (dy/dx)$ where dy and dx are incremental dilation and shear movements respectively (Figure 4.10). The dilation and contraction behaviour of the soil during shear is directly associated with the influence of the relative density on friction angle. For an assumed basic friction angle of the sand ϕ_b the following expression is approximately correct: $\tau \approx \sigma_n \text{Arctg} (\bar{\phi}_b + \psi)$. Bolton (1986) suggested that $\bar{\phi}_p \approx \bar{\phi}_{cs} + 0.8 \psi_p$ by carrying out plane strain tests

Apart from heavily overconsolidated layers, clay soils tend to show little dilatancy ($\psi \approx 0$). The dilatancy of sand depends on both the density and on the friction angle. For quartz sands the order of magnitude is $\psi \approx \bar{\phi} - 30^\circ$. For ϕ -values of less than 30° , however, the angle of dilatancy is mostly zero. A small negative value for ψ is only realistic for extremely loose sands.

(f) Advanced Parameters of the Mohr-Coulomb Model

In PLAXIS, Mohr-Coulomb model provided an advanced feature which allow user to input the increase of stiffness and cohesive strength with depth. In some practical problems, the soil may fail in tension instead of in shear. Such behaviour can be included in PLAXIS analysis by selecting the function of tension cut-off.

4.4.3 The Pile-Soil Interface Element Model

For modelling the pile-soil interaction, interface is required between the pile shaft and the soil. A relative slippage should be permitted when the shear stress mobilized on the shat exceeds the limiting value. Interfaces are composed of interface elements. Figure 4.11 shows how interface elements are connected to soil elements. It had been introduced that 15-node soil elements have been used which the corresponding interface elements are defined by five parrs of nodes. Whereas for 6-node soil elements the corresponding interfaces elements are defined by three pair of nodes.

The numerical integration for interface element is obtained by means of Newton Cotes integration:

$$\text{For Line Elements} \quad \int_{\xi=-1}^1 F(\xi) d\xi \approx \sum_{i=1}^k F(\xi_i) w_i \quad \text{Eq. 4.10a}$$

$$\text{For triangular elements} \quad \iint F(\xi, \eta) d\xi d\eta \approx \sum_{i=1}^k F(\xi_i, \eta_i) w_i \quad \text{Eq. 4.10b}$$

Where $F(\xi_i)$ is the value of the function F at position ξ_i and w_i the weight factor for point i . A total of k sampling point is used. The position and weight factors of the two types of integration are given in Table 4.4. The position of the Newton-Cotes stress points coincides with the node pairs. Hence, five stress points are used for a

10-node interface element whereas three stress points are used for a 6-node interface element

Moreover, finite element calculation processes based on the elastic stiffness matrix have been presented in APPENDIX C.

4.5 Input Parameters

Detailed soil and interface properties such as Young's modulus, cohesion and even strength reduction factor, etc. are summarised in Table 4.5

4.6 Finite Element Output

The results of the present numerical investigation are introduced in graphical forms. The following information for some typical cases is provided in APPENDIX A:

- Deformed/undeformed mesh
- Displacement Contours
- Vertical displacement (Shadings)
- Bending Moment
- Shear Force

4.7 Concluding Remarks

The numerical modelling of the raft and piled raft foundation is presented in this section. The selection of the appropriated models for simulation of soil and structural behaviour, the selection of the boundary conditions, and the selection and generation of the mesh and its are some of the aspects described in this chapter. Moreover, theoretical considerations such as the constitutive law for the structural element and the soil elements were also involved. More importantly, the method of selecting appropriate input parameters is also discussed in the latter part of this chapter.

CHAPTER V

RESULTS AND DISCUSSIONS

5.1 General

The sub-soil conditions at four sites in Surfers Paradise are studied in details. These sites are named as the project title and are called here as ARTIQUE, Q1, Circle on Cavill and SOLAIRE. For the ARTIQUE and SOLAIRE, piled raft foundation is used and the piles extend to the dense sand layer. The Q1 Tower and the two towers of Circle on Cavill are founded in the rock stratum. The rock stratum typically varies from 35 to 50 m from site to site. The Q1 Tower is 78 stories and some 323 m high founded on piles bearing in the rock layer. Similarly, the Circle on Cavill has two towers each 50 and 70 storey and the corresponding heights are 158m and 219m respectively. The towers at Circle on Cavill are also founded on pile groups which extend to the underlying rock stratum. The SOLAIRE and ARTIQUE towers are only 20 and 30 storey and with heights of 72 and 95m. These two towers are founded on piled raft foundations.

In this study, unpiled and piled rafts are analysed for the subsoil conditions encountered at the Surfers Paradise using the PLAXIS Software. First the subsoil profile is modelled and then appropriate geotechnical models are established for the properties of each layer as needed in the PLAXIS analysis. These geotechnical parameters are established from the SPT tests data and its correlation.

5.2 Establishment of Sub-surface Soil Layer Models

The subsoil conditions at Surfers Paradise are an estuarine deposit. A detail study of these soils were made from some 25 or more borehole extending at some locations to as deep as 50 m from the ground surface. The subsoil from this study is established as an upper layer of medium dense sand (Layer 1), followed by very dense sand (Layer 2). Below this layer of very dense sand, there is a layer of peat (Layer 3). At some locations the Layer 3 is missing. Below the peat layer is a very dense sand layer (Layer 4) followed by sandy clay (Layer 5). This in turn is underlain by clayey sand (Layer 6) which overlies a layer of gravely sand (Layer 7). In some locations, the gravely sand layer is missing and the clayey sand rest on rock formation. At the ARTIQUE site, rock is encountered around 30 to 35 m below the ground surface, while at the Q1 site this depth to the rock surface is about 40m. For the Circle on Cavill site the rock surface is encountered at depths of 33 to 46m. Similarly at the SOLAIRE site the depth to rock surface ranged from 30 to 36 m.

From the six boreholes drilled at the ARTIQUE site (see Figure 3.1) it is established that there is a thin layer of fill material at the surface, less than a meter thickness. Below this is the Layer 1 of medium dense sand about 9.4m thick. The layer 2 is very dense sand and varied in thickness at the site from 1.8m to 4.6m. Below these two layers a third layer of peat is encountered and this varied from 1.2m to 1.5m thick. Then the fourth layer is again very dense sand. This is some time called the lower layer of sand. This layer ranged in thickness from 10 to 10.5m. Below this fourth layer is the fifth layer and it is sandy clay, ranging in thickness from 7.9m to 9.5m. Rock stratum is encountered at depths of 30 to 35m. Table 3.2 gives additional details. An idealized soil profile is shown in Fig. 3.2. Similar models were established at the other three sites as well (see chapter 3). Tables 3.3 to 3.5 contain the details of the subsoil layers of these sites and the actual sub-soil layering and the proposed models are included in Figure 3.3 to 3.8. In these figures, the details of the building plans in the sites are also included

5.3 Geotechnical Parameters for Sub-soil Layers

Geotechnical parameters needed in the PLAXIS analysis, as estimated from the SPT correlations are also presented in Figure 3.19 (a) to (d). These properties included the bulk density, strength parameters, and modulus of elasticity and Poisson's ratio. The bulk density of the layers ranged from 17 to 20 kN/m³. The angle of internal friction for the sand was 37 degrees for the medium dense sand and 42 degrees very dense sand. The undrained shear strength for the peat and the stiff clay layers are 15 and 100 kN/m². The modulus of elasticity for the medium dense and dense sand is 55 MPa. For very dense sand this value is 120 MPa. The Poisson's ratio for loose to medium dense sand is 0.35. and for the very dense sand it is 0.3. For the peat layer and the stiff clay layer the Poisson's ratio is taken as 0.45 and 0.4 respectively.

5.4 Presentation of Analysis of Unpiled Raft Foundations

5.4.1 Settlement of Unpiled Raft

The Settlement of the unpiled raft (Figure 5.1) was investigated for different sizes (8m, 15m and 30m) of raft and for different raft thickness (0.25m, 0.4m, 0.8m, 1.5m and

3m), under a uniform intensity of vertical loading. The settlement was normalized and can be described by the influence factor I_R :

$$I_R = \frac{w_i E_s}{q B_R (1 - \nu_s^2)} \quad \text{Eq. 5.1}$$

Where q is the uniform distribution loads acting on the raft, and w_i is the settlement of raft, B_R is the width of raft. E_s and ν_s represent the young's modulus and Poisson's ratio of the soil below the raft.

The distance from edge of the raft was normalized as x/B_R to plot the results. The results of the settlement analysis of the unpiled rafts of widths 8m, 15m and 30m are show in Figure 5.2(a) to (c) respectively. The I_R values were found to decrease as the raft width is increased. Also, the I_R values reduced with increase in thickness of the raft. The influence factor I_R is found to vary in a parabolic type of manner with the maximum value at the centre of the raft. The range of the I_R values for each raft size is tabulated in Table 5.1. The values for I_R were in the range 1.02 to 1.15 when the raft size is 8m×8m. This value reduced to the range 0.64 to 0.81 when the raft size is increased to 15m×15m. Further reduction in I_R is noted as the raft size became 30m×30m and the corresponding I_R value is in the range 0.38 to 0.54.

The effect of the raft flexibility is presented in Figures 5.3(a) to (c) with relative raft stiffness (Eq. 5.2) suggested by Fraser and Wardle (1976), as an abscissa and settlement influence factor, I_R (Eq. 5.1) as an ordinate as suggested by Ta and Small (1997).

$$K_R = \frac{4E_R(1 - \nu_s^2)t_R^3}{3E_s(1 - \nu_R^2)} \quad \text{Eq. 5.2}$$

Where E_R , ν_R , t_R and B_R is the Young's modulus, Poisson's ration, thickness and width of the raft respectively while E_s and ν_s represent the Young's modulus and Poisson's ratio of the soil below the raft.

Relative stiffness for different thickness has been shown in Table 5.2. The K_R values increased from 2.1×10^{-2} to 36.4 when the raft dimension is 8m×8m. This range of K_R increased to 3.2×10^{-3} to 5.52 for the 15m×15m raft and further changed to 4×10^{-4} to 0.69 for the 30m×30m raft.

It can be concluded that the general settlement profile of the raft foundation, which the base was in full contact with the underlying soil under uniform distribution showed in bowl shaped, with the maximum settlement (Table 5.3) at the centre of the raft. For the 8m×8m raft, the variation in the settlement is in a narrow range from 31.5 mm to 32.8 mm. This range increased to 40.1 to 43 mm when the raft size increased to 15m×15m and to 53.2 to 57.4mm when the raft size is 30m×30m. The raft thickness did not have substantial effect on the maximum settlement.

The degree of curvature of the raft increases with decreasing raft thickness. In another word, the differential settlement decrease with the increase of raft stiffness, and also, increasing the distribution loads acting on the raft will increase the differential

settlement with a constant raft thickness under distribution loading condition. Within this analysis, the Young's modulus of the raft was taken as 30 GPa and its Poisson's ratio was taken as 0.2, the later value of thickness (0.8m) turns the raft from fully flexible raft to a raft of intermediate flexibility, and raft with 3m thickness can be treated as vary rigid according to the definition of relative stiffness given by Fraser and Wardle (1976).

According to Table 5.4, it can be concluded that relative stiffness zone will be increased with the increasing size of raft.

Normalized Differential Settlement with Relative stiffness had also been studied (Figure 5.4). 30m×30m raft shows higher normalized different settlement than others, but settlement of 8m×8m raft becomes nearly constant when the relative stiffness reached 4.5 ($t_R = 1.5\text{m}$), where the differential settlement is still large in 15m×15m and 30m×30m rafts. It should be noted that the analysis for varying thickness stops at $t_R = 3\text{m}$, and the differential settlement is still large for 30m×30m raft. Table 5.5 summarise the maximum normalized differential settlement for different raft thicknesses. For the 8m×8m raft the normalized differential settlement reduced from 0.12 to 0.0004 as the raft thickness increased from 0.25m to 3.0m. The corresponding range for the raft size of 15m×15m is 0.23 to 0.005 and for the raft 30m×30m this range is 0.32 to 0.05.

5.4.2 Bending Moment of Unpiled Raft Foundation

Bending moment of the square raft with different sizes (8m, 15m and 30m) was also investigated. With raft thicknesses of 0.25m, 0.4m, 0.8m, 1.5m and 3.0m and under a uniformed distribution load of 215kN/m^2 the variation of the bending moment is also studied. Figures 5.5(a) to (c) present the relationship of the normalised bending moment ($= M_{xx} \times 100 / qB_R^2$) against the normalised distance, x/B_R . The bending moment increases with increase in relative raft stiffness (thickness). Thinner rafts developed small bending moments. Obviously, the maximum bending moment occurred at the center of the raft and minimum (zero) bending moment is at the edge of the raft. Table 5.6(a) to 5.5(c) show values of maximum bending moment where occurred in the raft centre. For the 8m×8m raft, the normalized maximum bending moment ranged from 0.164 to 1.02. This range changed to 0.035 to 1.335, when the raft size is 15m x 15m. When the raft size is 30m×30m the range is 0.007 to 1.07.

5.4.3 Effect of Raft Thickness on Performance of Unpiled Raft Foundation

Figure 5.6 shows the maximum settlements for the unpiled rafts (8m×8m, 15m×15m, 30m×30m). The maximum settlements are 33mm, 44mm, and 57mm in 8m×8m, 15m×15m and 30m×30m rafts respectively. Increasing the raft thickness reduced this maximum value to 1mm, 4mm and 4mm respectively.

From Figure 5.6 it can also be observed that the increase in the maximum bending moment as a result of increasing the raft thickness is 0.12, 0.58 and 1.98 MNm for the three raft sizes

The corresponding bending moments are 0.12, 0.58 and 1.98MNm for raft sizes of 8m×8m, 15m×15m, 30m×30m respectively.

5.5 Parametric Study of Piled Rafts

An extensive parametric study of the piled raft was performed by Horkoshi and Randolph (1996). Normally, for practical applications, it will be generally necessary to model a larger number of piles. However, in this study, a group of only sixteen piles were modelled beneath a relative flexible raft. The parametric analyses which intend to examine the effect of raft thickness, the pile spacing, the pile length and the number of piles on the performance of the piled raft foundation mainly adopted the following variations:

- Raft Thickness: the original thickness used in the project is 0.8m, while thicknesses of 0.25m, 0.4m, 1.5m and 3m were also involved in the analysis to investigate the effect of raft thickness on the performance of the piled raft foundation.
- Pile Spacing: the reference value was 3d (2m). As indicated before, 5 distinct configurations were used, including 4d, 5d, 6d and 7d as well. Under three loading case (215kN/m^2 , 430kN/m^2 and 645kN/m^2 of uniformly distributed load), the effect of pile spacing on maximum settlement, differential settlement, maximum bending moment and the percentage of the load carried by each pile were also studied. It should be noted that the raft thickness adopted is only 0.8m. The pile diameter is 0.7m.
- Pile Length: the reference case involved 16m which is extending to the dense sand layer, while shorter 6m and 10m lengths were also analysed. The longest length analysed was 22m. An unpiled raft was also analysed. Aspects such as the settlement, the differential settlement and the bending moment were studied in detail. It should be known that this parametric study was carried out with the pile diameter taken as 0.7m for the two cases of the intensity of loading (215kN/m^2 and 430kN/m^2)
- Number of Piles: the reference number of piles was 16. Other cases considered were those with 12 piles, 8, 4 piles and no-pile case (unpiled raft). The loading intensity is 645 kN/m^2 . The piles are 0.7m diameter and 16m long. The pile spacing is 3d.

Therefore, 20 distinct parametric alternatives were compared and analysed with the value of the reference design solution used in the project.

5.5.1 Effects of Raft Thickness on Piled Raft Foundation

The results of the analysis of the piled raft with different raft thicknesses are shown in Figures 5.7 to 5.11.

Except for the thinner rafts (0.25m, 0.4m), the piled raft show bowl shaped settlement pattern within the pile area and the edge strips indicated downward curvature (Figure 5.7). Thin rafts (0.25m, 0.4m) show more prominent settlement pattern. Maximum

settlements for different thickness are tabulated in Table 5.7. These values ranged from 62mm to 64 mm in a narrow range.

Increasing the raft thickness, had a greater effect on the maximum bending moment (Figure 5.8) and these values increased from 107 kNm to 485 kNm. The bending moment within the pile group area was affected significantly by increasing the raft stiffness (thickness). For the case considered here, there is little effect on the maximum bending moment when the raft thickness is increased beyond 1.5m. Table 5.8 shows the hogging bending moment in the raft.

From the results presented in Figures 5.9 and 5.10, it is observed that the raft thickness do not have much influence on the axial load of the pile and it's bending moment when raft thickness exceeds 1.5m. Table 5.9 (a) and Table 5.9(b) present the maximum pile head axial force for the edge and centre piles. The pile load ranged from 1.19 to 1.41 MN for the edge pile and the corresponding values for the centre pile is 0.91 to 1.06 MN.

It can be concluded that increasing the raft thickness of 0.25m do not influence the bending moment in the pile (Figure 5.11). However it may be beneficial in resisting the punching shear resulting from the piles and the column loadings.

5.5.2 Effects of Pile Spacing

The effect of the pile spacing (3d to 7d) on the piled raft behaviour is studied for the bending moment and the settlement of the raft, and the axial force and bending moment of the piles for three values of intensity of loading as 215, 430 and 645kN/m². In this analysis, the raft thickness is 0.8m and the dimension of the raft will increase with increased pile spacing. The piles are 0.7m diameter and 16m length.

When the intensity of loading is 215 kN/m², the reduction in pile spacing has the effect of reducing the raft settlement (Figure 5.12). However the differential settlement is not affected much as the loading is very light. Figure 5.13 indicates that the bending moment in the raft increased significantly especially at the pile location, as the pile spacing becomes large. When the pile spacing is increased from 3 to 7D, the bending moment in the pile increased threefold (Figure 5.15). Also, the pile load increased significantly for the piles at the edge. But the pile loads for the centre piles changed regularly from 0.47 to 0.64 as the pile spacing increased (Figure 5.14). Table 5.10 to 5.11 presents the maximum settlement of the piled raft and the maximum bending moment. The pile loads and the bending moments are also presented in Tables 5.12 and Table 5.13.

When the intensity of loading is 430kN/m² there is no significant difference in the settlement below the raft and its bending moment (see Figure 5.16 and Figure 5.17). The centre piles are found to be sensitive for their axial load as the pile spacing is increased (Figure 5.18). Figure 5.19 illustrates that the increased pile spacing contributes to a larger effect on the bending moment at the pile head and hardly any effect at the pile toe. In addition the results are tabulated in Table 5.14 to 5.17.

When the loading intensity increases to 645kN/m², the settlements and the differential settlements were found to increase (Figure 5.20, Figure 5.21). Also the axial force in the central pile increased to a greater extent. Also the bending moment in all piles

increased (Figure 5.22, Figure 5.23). Analysis results were tabulated in Table 5.18 to 5.21

Figures 5.24 (a) to (c) summarize the effect of piles spacing for the three intensity of loadings: 215, 430 and 645kN/m² respectively. As would be expected, the settlements, differential settlement and the maximum moment all increase with increasing pile spacing; the proportion of the load carried by the piles reduced.

5.5.3 Effect of Pile Lengths

For a 0.25m thick raft with 16 piles and a load intensity of 215 kN/m², Figure 5.25 shows how the maximum settlement varied with the pile lengths. Figure 5.26 shows the bending moment variation along the raft for this case. Increasing pile length will reduce the settlement of piled raft, whereas large positive bending moments were carried by the raft in the positions beneath piles. Pile lengths beyond 6m, showed little effect on both the settlement and the bending moment of piled raft. Figures 5.27 and 5.28 show similar trend when the loading intensity increased from 215 kN/m² to 430 kN/m². Finally, Figure 5.29 summarize these two cases, settlements and differential settlements reduced with increasing pile length, while the maximum bending moment in the raft and the proportion of the load carried by the piles decreased.

5.5.4 Effect of Number of Piles

One of the important uses of a piled raft analysis is to assess how many piles are required to achieve the desired performance. Therefore, the effect of the number of piles is studied on the settlement bending moment and other similar quantities. In this case, thickness of 0.8m raft incorporated with 0.7m diameter, 16m length pile had been studied. Figure 5.30 summarise the relationship between the settlement at the centre and the number of piles, and the proportion of the load carried by piles with varying number of piles. It should be noted that the 2-D plane strain simulation can only model the case shown in Figure 5.30 (i) by considering the input Young's modulus of piles (Prakoso and Kuhalwy, 2001). Clearly in Figure 5.30 (ii), the settlement at the centre decreased when more piles are under the raft; the proportion of the load carried by the piles increased.

5.6 Concluding Remarks

From the results presented in Figure 5.11, Figure 5.28, Figure 5.33 and Figure 5.34, it can be concluded that the foregoing simple example demonstrates the following important points for practical design:

- a. The raft thickness affects differential settlement and bending moments, but has little effect on load sharing or maximum settlement.
- b. Piles spacing plays an important role on the performance of piled raft foundation. It affects greatly the maximum settlement, the differential settlement, the bending moment in the raft, and the load shared by the piles.

- c. To reduce the maximum settlement of piled raft foundation, optimum performance is likely to be achieved by increasing the length of the piles involved. While the differential settlement, the maximum bending moment and the load sharing are not affected much by increasing the pile lengths.
- d. Increasing the number of piles, generally have beneficial effects. More piles will increase the load sharing by the piles. However, there is an upper limit to the number of piles, beyond which very little additional benefit can be obtained (Poulos, 2001).

CHAPTER VI

CONCLUSIONS AND RECOMMENDATIONS

6.1 General

This study directly relates to the analysis of unpiled and piled raft foundations similar to the subsoil conditions at the ARTIQUE tower in Surfers Paradise gold coast. Initially the subsoil layer model was established for surfers Paradise from some 25 or more borehole data at four sites in Surfers Paradise and the boreholes extend to some 50m below the ground surface up to the rock stratum. A seven layer subsoil model was established and the geotechnical parameters for these layers were estimated from SPT tests.

Based on these geotechnical parameters a PLAXIS analysis was conducted on unpiled and piled raft foundations. The conclusions are in three parts. Part one relates to the sub-surface model, while part two is on the geotechnical parameters and part three is on the results of the PLAXIS analysis.

6.2 Typical Gold Coast Subsoils at Surfers Paradise

The subsoil conditions at Surfers Paradise is an estuarine deposit and typically consist of an upper layer of medium dense sand (Layer 1), followed by very dense sand (Layer 2). Below this layer of very dense sand, there is a layer of peat (Layer 3). At some locations the Layer 3 is missing. Below the peat layer is a very dense sand layer (Layer 4) followed by sandy clay (Layer 5). This in turn is underlain by clayey sand (Layer 6) which overlies a layer of gravely sand (Layer 7). Finally, Rock layer is encountered after gravely sand Layer.

6.3 Geotechnical Parameters Used in PLAXIS Analysis Input Parameters

Based on SPT results and its correlations with engineering properties, the following soil parameters are adopted in the analysis.

- **Soil Young's Modulus:**

(a) Layer 1	Medium Dense Sand	$E_1 = 55 \text{ MPa}$
(b) Layer 2	Dense to Very Dense Sand	$E_2 = 120 \text{ MPa}$
(c) Layer 3	Sandy Clay	$E_3 = 65 \text{ MPa}$

- **Friction Angle:**

(a) Layer 1	Medium Dense Sand	$\phi_1 = 37$ (deg)
(b) Layer 2	Dense to Very Dense Sand	$\phi_2 = 42$ (deg)
(c) Layer 3	Sandy Clay	$\phi_3 = 25$ (deg)

▪ **Effective Cohesion (very small value as recommended by Plaxis manual)**

(a) Layer 1	Medium Dense Sand	$c = 1$ kN/m ²
(b) Layer 2	Dense to Very Dense Sand	$c = 1$ kN/m ²
(c) Layer 3	Sandy Clay	$c = 25$ kN/m ²

▪ **Poisson Ratio (value as adopted from existing literature)**

(a) Layer 1	Medium Dense Sand	$\nu_1 = 0.3$
(b) Layer 2	Dense to Very Dense Sand	$\nu_2 = 0.3$
(c) Layer 3	Sandy Clay	$\nu_3 = 0.35$

6.4 Performance of Unpiled Raft

6.4.1 The Settlement of Unpiled Raft

- The normalized settlement parameter I_R for the unpiled square raft 8m×8m, 15m×15m and 30m×30m ranged as 1.02~1.15, 0.64~0.81 and 0.38~0.54 respectively.
- According to the settlement response of the unpiled raft with different thicknesses, they can be classified as:

(a) $t_R = 0.25\text{m}, 0.4\text{m}$	Flexible
(b) $t_R = 0.8\text{m}$	Relative rigid
(c) $t_R = 1.5\text{m}, 3\text{m}$	Rigid

6.4.2 Normalized Bending Moment of Unpiled Raft

For the 8m×8m raft, the normalized maximum bending moment ranged from 0.164 to 1.02. This range changed from 0.035 to 1.335, when the raft size is 15m×15m. For the raft size of 30m×30m the range is 0.007 to 1.07.

6.4.3 Parametric Study of Unpiled Raft

- Under the working load intensity of 215 kN/m², maximum settlements for 0.25m thickness raft are 33mm, 44mm, and 57mm for the 8m×8m, 15m×15m and 30m×30m rafts respectively. Increasing the raft thickness to 3m reduced these maximum values to 31mm, 40mm and 52mm respectively.
- The corresponding bending moments are 0.026, 0.017 and 0.013 MNm for raft sizes of 8m×8m, 15m×15m, 30m×30m respectively. Increasing the raft thickness to 3m increased these maximum values to 0.14, 0.59 and 2.083 MNm respectively.

6.5 Parametric Analysis of Piled Raft Foundation

6.5.1 Effect of Raft Thickness

For the 8m×8m raft piled raft with 16 piles of 0.7m diameter and for 16m long with intensity of loading 645kN/m^2 , the maximum settlement, the bending moment and the pile head load were studied. Detailed results are given below:

- When the raft thickness of the piled raft varied as 0.25, 0.4, 0.8, 1.5 and 3m, the corresponding maximum settlements were 64, 63.3, 62.6, 62.3 and 62.2mm
- The corresponding hogging moments for the piled rafts with raft thicknesses of 0.25, 0.4, 0.8, 1.5 and 3m are 107, 160, 321, 446 and 485 kNm.
- The pile loads ranged from 1.19 to 1.41 MN for the edge pile and the corresponding values for the centre pile are 0.91 to 1.06MN.

In conclusion, the maximum values of the settlements decreased only by a little value as the raft thickness increased. However, the hogging moment in the raft increased greatly when the raft thickness increased from 0.25 to 3m. The pile loads only varied slightly within the range 1.19~1.41MN in the edge piles, and 0.91~1.06MN in the centre piles.

6.5.2 Effect of Pile Spacing

Under three loading conditions (215kN/m^2 , 430kN/m^2 and 645kN/m^2), the effects of the pile spacing have been investigated. The pile length is 16m and the diameter is 0.7m.

- Under an intensity of loading of 215kN/m^2 , when the pile spacing is varied as 3d, 4d, 5d, 6d and 7d, the corresponding maximum settlements were 22, 26, 29, 34 and 36mm. The hogging moment in the raft centre developed as 0.197, 0.329, 0.369MNm, 0.42 and 0.44MNm. Similarly, the pile loads increased from 0.265MN to 0.835MN in the edge pile, and 0.475MN to 0.639MN in the centre piles as the pile spacing increased. The pile head bending moment increased greatly in both the edge piles and the centre piles and these ranges are 91.37kNm to 246.17kNm, and 28.91kNm to 69.44kNm respectively

As would be expected, under intensity of loading of 215kN/m^2 , 430kN/m^2 and 645kN/m^2 , the maximum settlements, different settlement and the maximum moment all increase with increasing pile spacing; the proportion of the load carried by the piles reduced.

6.5.3 Effect of Pile Lengths

Increasing the pile length reduced the settlement of the piled raft, whereas large positive bending moments were carried by the raft in the positions beneath piles. Pile lengths beyond 6m, showed little effect on both the settlement and the bending moment of piled raft.

6.5.4 Effect of Number of Piles

One of the important uses of a piled raft analysis is to assess how many piles are required to achieve the desired performance. The settlement at the centre decreased when more piles are under the raft; the proportion of the load carried by the piles increased.

6.6 Recommendations

- The geotechnical parameters in this study were obtained from SPT tests and its correlation with engineering parameters. CPT tests are now being carried out at the surfers Paradise. It is recommended that the data from continuous CPT tests be used in future analysis
- This study was carried out with a 2-D plane strain analysis. A 3-D analysis is better when the raft sizes are small. Thus a proper 3-D analysis is carried out and calibration charts be established to modify the 2-D results to suit 3-D conditions.

REFERENCE

Aoki, N., and Velloso, D. A., 1975. An Approximate Method to Estimate the Bearing Capacity of Piles. *Proceeding of 5th Pan-American Conference of Soil Mechanics and Foundation Engineering, Buenos Aires*, 1, 367-376.

American Petroleum Institute (API), 1984. *Recommended Practice of Planning, Designing and Construction of Fixed Offshore Platforms*. Dallas, Texas: API, (API-RF-2A)

Banerjee, P. K. and Davies, T. G., 1978. The Behaviour of Axially and Laterally Loaded single piles embedded in Non-homogeneous Soils. *Géotechnique*, 28(3), 309-326

Berezantzev, V. G., Khristoforov, V. and Golubkov, V., 1961. Load bearing capacity and deformation of piled foundations. *Proc. 5th Int. Conf. Soil Mech. Fdn Engng, Paris*. 2, 11-15.

Bolton, M. D., 1986. The strength and dilatancy of sands. *Géotechnique*, 36(1), 65-78.

Brinkgreve, R. B. J., 2002. *PLAXIS, Finite element code for soil and rock analyses, users manual*. Rotterdam: Balkema

Briaud, J. L. and Tucker, L., 1984. Piles in Sand: A Method including Residual Stresses. *Journal of Geotechnical Engineering, ASCE*, 110(11), 1666-1680.

Burland, J. B., 1973. Shaft friction of piles in clay: a simple fundamental approach. *Ground Engng*, 6(3), 30 - 42.

- Bustamante, M. and GIANESSELLI., 1982. Pile Bearing Capacity Prediction by Means of Static Penetration CPT. *Proceedings of 2nd European Symposium on Penetration Testing, Amsterdam*, 2, 493-500.
- Butterfield, R. and Banerjee, P. K. 1971. The Elastic Analysis of Compressible Piles and Pile Groups. *Géotechnique*, 21(1), 43-60.
- Callanan, J. F. and Kulhawy, F. H., 1985. Evaluation of Procedures for predicting Foundation Uplift Movements. *Electric Power Research Institute, Palo Alto*, Report EL-4107.
- Chen, L. and Poulos, H. G., 1993. Analysis of Pile-Soil Interaction Under Lateral Loading Using Infinite and Finite Elements. *Computers and Geotechnics*, 15, 189-220
- Clancy, P. and Randolph, M. F., 1993. Analysis and Design of Piled Raft Foundations. *Int. Jnl. Num. Methods in Geomechs.*, 17, 849-869.
- Clausen, C. J. F., Aas, P. M. and Karlsrud, K., 2005. Bearing Capacity of Driven Piles in Sand, The NGI Approach. *Frontiers in Offshore Geotechnics: ISFOG 2005 – Gourvenec & Cassidy (eds) © 2005 Taylor & Francis Group, London*, 677-681.
- Clayton, C.R.I., 1990. SPT Energy Transmission: Theory, Measurement, and Significance. *Ground Engineering*, 23(10), 35-43.
- Chow, Y. K., 1989. Axially Loaded Piles and Pile Groups embedded in a cross-anisotropic Soil. *Géotechnique*, 39(2), 203-211.
- Chow, Y. K., Yong, K.Y. and Shen, W. Y., 2001. Analysis of Piled Raft Foundations Using a Variational Approach. *The International Journal of Geomechanics*, 1(2), 129-147.
- Coyle, H. M. and Reese, L. C., 1966. Load Transfer for Axially Loaded Piles in Clay. *Journal of the Soil Mechanics and Foundations Division, ASCE*, 92(SM2), 1-26.
- Cunha, R. P. Poulos, H. G. and Small, J. C., 2001. Investigation of Design Alternatives for A Piled Raft Case History. *Journal of Geotechnical and Geoenvironmental Engineering, ASCE*, 127(8), 635-641
- Desai, C. S., 1974. Numerical Design - Analysis for Pile in Sand. *Journal of the Soil Mechanics and Foundations Division, ASCE*, 100(GT6), 613-635.
- Desai, C.S., Johnson, L. D. and Hargett, C. M., 1974. Analysis of Pile-supported Gravity Lock. *J. Geotech. Engrg., ASCE*, 100(9), 1009-1029.
- DeRuiter, J. and Beringen, F. L., 1979. Pile Foundation for Large North Sea Structures. *Marine Geotechnology*, 3(3), 267-314.

Desai, C. S., Zamman, M. M., Lightner, J.G. and Siriwardane, H.J., 1984. Thin-layer Element for Interfaces and Joints. *International Journal for Numerical and Analytical Methods in Geomechanics*, 4(8), 19-43.

Djoenaidi, W. J., 1985. *A compendium of Soil Properties and Correlations*. Thesis (M. Eng. Sc.). University of Sydney.

Duncan, J. M., 1972. Finite Element Analysis of Stresses and Movements in Dams, Excavations and Slopes: State - of - the art. *Applications of the Finite Element Method in Geotechnical Engineering*, 267-326.

EI Sharnouby, B. and Novak, M., 1990. Stiffness Constants and Interaction Factors for Vertical Response of Pile Groups. *Canadian Geotechnical Journal*, 27, 813-822.

Eslami, A. and Fellenius, B. H., 1997. Pile capacity estimated from CPT data. *Proceeding of 14th International Conference on Soil Mechanics and Foundation Engineering, A.A.Balkema*, 1, 91-94.

Fellenius, B. H., 2004. UNIPILE Design on Piled Foundations with Emphasis on Settlement Analysis. *Journal of the Soil Mechanics and Foundations Division, ASCE*, 125(GSP), 1-23.

Fleming, W.G.K., Weltman, A.J., Randolph, M.F. and Elson, W.K., (1992). *Piling Engineering*. 2nd Ed., Surrey Univ. Press

Franke, E., Lutz, B. and EI-Mossallamy, Y., 1994. Measurements and Numerical Modelling of High-rise Building Foundations on Frankfurt Clay. *Vert. And Horizl. Deformns. Of Foundns. And Embanks., ASCE Geot. Spec*, 42(2), 1325-1336

Fraser, R. A. and Wardle, L. J. 1976. Numerical analysis of rectangular rafts on layered foundations. *Géotechnique*. 26(4), 613—630.

Focht, J. A. and Kraft, L.M., Prediction of Capacity of Long Piles in Clay: A Status Report. *Presented at the Symposium on Geotechnical Aspects of Offshore and Nearshore Structures, December 1981Bangkok*.

Gibbs, H. J. and Holtz, W. G., 1957. Re-search on determining the density of sand by spoon penetration test, *Proc. 4th International Conference on Soil Mechanics and Foundation Engineering*, 1, 35-39.

Guo, W. D. and Randolph, M. F., 1996. Settlement of Pile Groups in Non-homogeneous soil. *Proc. 7th ANZ Conf. Geomech.* 1, 631- 636.

Guo, W. D. and Randolph, M. F., 1997. Vertically loaded piles in non-homogeneous media. *Int. J. Numer. Anal. Methods Geomech.* 21, 507-532.

Hain, S. J. and Lee, I. K., 1978. The Analysis of Flexible Raft-Pile Systems. *Géotechnique*, 28(1), 65-83.

- Hara, A., Ohta, T., Niwa, M. Tanaka, S. and Banno, T., 1974. Shear Modulus and Shear Strength of Cohesive Soils. *Soils and Foundations*, 14(3), 1-12.
- Hewitt, P. B. and Gue, S. S., 1994. Piled Raft Foundation in a weathered sedimentary formation. *Kualaumpur, Malaysia. Proc.Geotropica*, 1-11
- Holtz, W. G. and Gibbs, H. J., 1979. Discussion of "SPT and relative density in coarse sand". *J. Geotech. Eng. Div., ASCE*. 105(GT3), 439-441.
- Horikoshi, K. and Randolph, M. F., 1996. Centrifuge Modelling of Piled Raft Foundations on Clay, *Géotechnique*, 46(4), 741-752.
- Horikoshi, K. and Randolph, M. F., 1998. A Contribution to Optimum Design of Piled Rafts. *Géotechnique*, 48(3), 301-317.
- Huybrechts, N., Vos, M. D., Whenham, V. and BBRI., 2004. WP3: Design Tools Part 1: Use of Finite Element Method in Geotechnical Design.
- Kitiyodom, P. and Matsumoto, T., 2003. A Simplified Analysis Method for Piled Raft Foundations in Non-homogeneous Soils. *Int. J. Numer. Anal. Meth. Geomech.*, 27, 85-109.
- Koiter, W. T., 1960. General Theorems for Elastic-Plastic Solids. In: I.N. Sneddon, R. Hill, ed. *Progress in Solid Mechanics*. North-Holland, Amsterdam: 1, 165-221.
- Kulhawy, F. H., 1985. Uplift behaviour of shallow soil anchors - an overview. Uplift Behaviour of Anchor Foundations in Soil, Special Publication. Clemence(editor), *ASCE*, 1-25.
- Kulhawy, F. H. and Mayne, P. W., 1990. *Manual on estimating soil properties for foundation design*, Palo Alto, Calif., U.S.A: Electric Power Research Institute (EL-6800/1493-6)
- Kuwabara, F., 1989. An Elastic Analysis for Piled Raft Foundations in a Homogeneous Soil. *Soils and Foundations*, 28(1), 82-92
- Lee, w. j., Lee, I. M., Yoon, S.J., Choi, Y. J. and Kwon, J.H. 1996. Bearing Capacity Evaluation of the Soil-Cement Injected Pile Using CAPWAP. *Proc. of the 5th Int. Conf. on the Application of StresswaY Theory to Piles*. University of Florida, Orlando Florida USA.
- Lee, I. K., 1993. Analysis and Performance of Raft and Raft-pile System. *Keynote Lect., 3rd Int.Conf. Case Hist. In Geot.Eng.*, St.Louis.
- Lehane, B.M., Schneider, J. A. and Xu, X., 2005. The UWA - 05 Method for Prediction of Axial Capacity of Driven Piles in Sand. *Frontiers in Offshore Geotechnics: ISFOG 2005 - Gourvenec & Cassidy (eds) © 2005 Taylor & Francis Group, London*, 683-689.

- Liang, F. Y., Chen, L. Zh. and Shi, X. G. 2003. Numerical Analysis of Composite Piled Raft with Cushion Subjected to Vertical Load. *Computers and Geotechnics*, 30, 443-453.
- Liao, S. S. C. and Whitman, R. V., 1985. Overburden Correction Factors for SPT in Sand. *Journal of Geotechnical Engineering, ASCE*, 112(3), 373-377.
- Mendonca, A. V. and Paiva, J. B., 2003. An Elastostatic FEM/BEM analysis of Vertically Loaded Raft and Piled Raft Foundation. *Engineering Analysis with Boundary Elements*, 27, 919-933
- Meyerhof, G. G., 1956. Penetration Test and Bearing Capacity of Cohesionless Soils. *Journal of the Soil Mechanics and Foundations Division, ASCE*, 82(SM1), 1-19.
- Meyerhof, G.G., 1976. Bearing Capacity and Settlement of Pile Foundation. *Journal of the Soil Mechanics and Foundations Division, ASCE*, 102(GT3), 197-228.
- Meyerhof, G.G., 1983. Scale Effects of Ultimate Pile Capacity. *Journal of the Soil Mechanics and Foundations Division, ASCE*, 109(6), 797-806.
- NAVFAC., 1986. *Foundations and Earth Structures (DM-7.02)*. Washington, D.C: Department of the US Navy.
- Neely, W., 1990. Bearing Capacity of Expanded-Base Piles in Sand. *Journal of Geotechnical Engineering, ASCE*, 116(1), 73-87.
- Neely, W., 1991. Bearing Capacity of Auger-Cast Piles in Sand. *Journal of Geotechnical Engineering, ASCE*, 117(2), 331-345.
- Nottingham, L.C., 1975. *Use of Quasi-static Friction Cone Penetrometer data to Estimate Capacity of Displacement Piles*. Thesis (PhD). University of Florida.
- Ottaviani, M., 1975. Three-dimensional Finite Element Analysis of Vertically Loaded Piles Groups. *Géotechnique*, 25(2), 159-174.
- Peck, R. B. and Bazaraa, A. R. S. S., 1969. Discussion. *Proc. ASCE J. Soil Mech. and Fdn Engng*, 95(SM3), 305-309.
- Peck, R. B., Hanson, W. E. and Thornburn, T. H., 1974. *Foundation Engineering*. New York: John Wiley and Sons, Inc.
- Poulos, H. G., 1968. Analysis of the Settlement of Pile Groups. *Géotechnique*, 18, 449-471.
- Poulos, H.G. and Davies, E.H., 1980. *Pile Foundation Analysis and Design*. New York: Wiley.
- Poulos, H. G., 1989. Pile Behaviour – Theory and Application. *Géotechnique*, 39(3), 365-415.

Poulos, H. G., 1991. Analysis of Piled Strip Foundations. *Comp. Methods and Advances in Geomechs.*, Ed. Beer, G., Booker, J. R., and Carter, J. P., Balkeema, A. A. Rotterdam, 1, 183-191

Poulos, H. G., 1993. Piled rafts in Swelling or Consolidating Soils. *Journal of the Soil Mechanics and Foundations Division, ASCE*, 119(2), 374-380.

Poulos, H. G., 1994. An Approximate Numerical Analysis of Pile Raft Interaction. *Int. Jnl. Num. Anal. Meths. In Geomechs.*, 18, 73-92.

Poulos, H. G., Small, J. C., Ta, L. D., Sinha, J. and Chen, L., 1997. Comparison of some methods for analysis of piled rafts. *Proceedings of the 30th year symposium of the Southeast Asian Geotechnical Society*, 5, 1-6.

Poulos, H. G., 2001. Piled raft foundation: design and application. *Géotechnique*, 51(2), 95-113.

Prakoso, W. A. and Kulhawy, F. H., 2001. Contribution To Piled Raft Foundation Design. *Journal of Geotechnical and Geoenvironmental Engineering, ASCE*, 127(1), 17-24.

Randolph, M. F., 1978. Analysis of Deformation of Vertically Loaded Piles. *Journal of the Soil Mechanics and Foundations Division, ASCE*, 104(GT12), 1465-1488.

Randolph, M.F. and Wroth, C.P., 1978. Analysis of deformation of vertically loaded piles. *Journal of the Geotechnical Engineering Division, ASCE*, 104 (GT12), 1465-1488

Randolph, M.F. and Wroth, P., 1979. An analysis of the vertical deformation of pile groups. *Géotechnique*. 29(4), 423-439.

Randolph, M. F., 1983. PIGLET – A Computer Program for the Analysis and Design of Pile Groups Under General Loading Conditions. *Engineering Department Report, University of Cambridge*.

Randolph, M. F., 1994. Design Methods for Pile groups and Piled Raft. *Proceeding of the Foundation International Conference on Soil Mechanics and Foundation Engineering, New Delhi*, 5, 61-82.

Reese, L. C. AND O'Neill, M. W. 1989. New Desing Method for Drilled Shaft from Common Soil and Rock Test. *Proceedings of Congress Foundation Engineering: Current Principles and Practices, ASCE*, 2, 1026-1039.

Reul, O., 2004. Numerical Study of the Bearing Behaviour of Piled Rafts. *International Journal of Geomechanics*, 4(2), 59-68.

Reul, O. and Randolph, M. F., 2003. Piled Rafts in Overconsolidated Clay: Comparison of *in situ* Measurements and Numerical Analysis. *Géotechnique*, 53(3), 301-315.

- Russo, G., 1998. Numerical Analysis of Piled Rafts. *Int. J. Numer. Anal. Meth. Geomech*, 22, 477-493.
- Schmertmann, J. H., 1975. Measurement of In-situ Strength. *Proceedings of the Conference on In-Situ Measurement of Soil Properties, American Society of Civil Engineers*, 55-138.
- Schmertmann, J. H., 1978. *Guidelines for Cone Test, Performance and Design*. Report FHWA-TS-78209. Washington.
- Semple, R. M. and Rigden, W. J., 1984. Shaft capacity of driven piles in clay, *Proceedings of the symposium on analysis and design of pile foundations, San Francisco*, 59-79.
- Shen, W. Y., Chow, Y. K. and Yong, K. Y., 1999. A variational Approach for The Analysis of Rectangular Rafts on an Elastic Half-space. *Soils and Foundations*, 39(6), 25-32.
- Shen, W. Y., Chow, Y. K. and Yong, K. Y., 2000. A variational Approach for The Analysis of Pile Group-pile Cap Interaction. *Géotechnique*, 50(4), 349-357.
- Skepmton, A. W., 1986. Standard Penetration Test Procedures and the Effects in Sands of Overburden Pressure, Relative Density, Particle Size, Aging and Overconsolidation. *Géotechnique*, 36(3), 425-447.
- Small, J. C. and Zhang, H. H. 2000. Piled Raft Foundation Subjected to General Loading. *Developments in Theoretical Geomechanics*. Smith and Carter (eds), Balkema, Rotterdam.
- Smith, I. M. and Griffith, D. V., 1982. *Programming the Finite Element Method*, 2nd ed. Chisester: John Wiley & Sons.
- Smith, I. M. and Wang, A., 1998. Analysis of Piled Rafts. *Int. J. Numer. Anal. Meth. Geomech*, 22, 777-790
- Stroud, M. A., 1989. The Standard Penetration test - its application and interpretations. *Penetration testing in the UK, Thomas Telford, London*, 29-49.
- Ta, D. L. and Small, J. C., 1996. Analysis of Piled Raft Systems in Layered Soils. *International Journal for Numerical and Analytical Methods in Geomechanics*, 20, 57-72.
- Ta, D. L. and Small, J. C., 1997. An Approximation for Analysis of Raft and Piled Raft Foundations. *Computers and Geotechnics*, 20(2), 105-123.
- Terzaghi, K. and Peck, R. B., 1967. *Soil Mechanics in Engineering Practice*. 2nd ed. New York: John Wiley.
- Tomlinson, M. J., *Foundation Design and Construction*. 2nd ed. New York: Pitman Publishing.

Tumay, M. T. and Fakhroo, M., 1981. Pile capacity in soft clays using electric QCPT data. *ASCE, Cone Penetration Testing and Experience*, 434-455.

Vesic, A. S., 1972. Expansion of Cavities in Infinite Soil Mass. *J. Soil Mech. And Foundations Div. ASCE*. 98, 265-290.

Wehnert, M. and Vermeer, P. A. 2004. Numerical Analysis of Load Test on Bored Piles. *NUMOG 9th – 25 – 27 August 2004, Ottawa Canada*, 1-6.

Zhang, H. H. and Small, J. C., 2000. Analysis of Capped Piled Groups Subjected to Horizontal and Vertical Loads. *Computers and Geotechnics*, 26, 1-21.

Table 2.1(a) Skin Friction Factor α and β for Driven Piles (after Poulos, 1989)

Soil type	Equation	Skin friction factors	Reference
Clay	$f_s = \alpha S_u$	$\alpha = 1.0$ ($S_u \leq 25$ kPa) $\alpha = 0.5$ ($S_u \geq 70$ kPa) $\alpha = 1 - \left(\frac{S_u - 25}{90} \right)$ for $25 \text{ kPa} < S_u < 70 \text{ kPa}$	API (1984)
		$\alpha = 1.0$ ($S_u \leq 35$ kPa) $\alpha = 0.5$ ($S_u \geq 80$ kPa) $\alpha = 1 - \left(\frac{S_u - 35}{90} \right)$ for $35 \text{ kPa} < S_u < 80 \text{ kPa}$	Semple and Rigden (1984)
		$\alpha = \left(\frac{S_u}{\sigma'_{z_{nc}}} \right)^{0.5} \left(\frac{S_u}{\sigma'_{z_{nc}}} \right)^{-0.5}$ for $(S_u / \sigma'_{z_{nc}}) \leq 1$ $\alpha = \left(\frac{S_u}{\sigma'_{z_{nc}}} \right)^{0.5} \left(\frac{S_u}{\sigma'_{z_{nc}}} \right)^{-0.25}$ for $(S_u / \sigma'_{z_{nc}}) \geq 1$	Fleming <i>et al</i> (1992)
	$f_s = \beta \sigma'_z$	$\beta = (1 - \sin \phi')(\tan \phi') \text{OCR}^{0.5}$	Burland (1973)
Sand	$f_s = \beta \sigma'_z$	$\beta = 0.15-0.35$ (compression) $0.10-0.24$ (tension)	McClelland (1974)
		$\beta = 0.44$ for $\Phi = 28^\circ$ 0.75 for $\Phi = 35^\circ$ 1.20 for $\Phi = 37^\circ$	Meyerhof (1976)
		$\beta = (K/K_o)K_o \tan (\Phi' \Phi_i' / \Phi')$ $\Phi' \Phi_i'$ depends on installation method (0.5-1.0) K/K_o depends on installation method (0.5-2.0) K_o = coefficient of earth pressure at rest and is a function of OCR	Stars and Kulhawy (1984)
Uncemented Calcareous Sand	$f_s = \beta \sigma'_z$	$\beta = 0.05-0.1$	Poulos (1988)

Table 2.1 (b) Skin Friction Factor α and β for Bored Piles (after Poulos, 1989)

Soil type	Equation	Skin friction factors	Reference
Clay	$f_s = \alpha S_u$	$\alpha = 0.45$ (London clay)	Skempton (1959)
		$\alpha = 0.7$ times value for driven displacement pile	Fleming et al (1992)
	$f_s = K \tan \delta \sigma'_z$	K is lesser of K_o or $0.5(1+K_o)$	Fleming et al (1992)
		$K/K_o = 2/3$ to 1 ; K_o is a fuction of OCR; δ depends on interface materials	Stas and Kulhawy (1984)
Sand	$f_s = \beta \sigma'_z$	$\beta = 0.1$ for $\Phi = 33^\circ$ 0.2 for $\Phi = 35^\circ$ 0.35 for $\Phi = 37^\circ$	Meyerhof (1976)
		$\beta = F \tan(\Phi' - 5^\circ)$ where $F = 0.7$ (compression) $= 0.5$ (tension)	Kraft and Lyons (1974)
Uncemented Calcareous Sand	$f_s = \beta \sigma'_z$ ($f_s \leq f_{s \text{ lim}}$)	$\beta = 0.5-0.8$ $f_{s \text{ lim}} = 60$ to 100 kN/m^2	Poulos (1988)

Table 2.1(c) End Bearing Capacity of Pile Tip, f_b (after Poulos, 1989)

Soil type	Equation	Skin friction factors	Reference
Clay	$f_b = N_c c_{ub}$	$N_c = 9$ for $L/d \geq 3$ C_{ub} = value of c_u in vicinity of pile tip	Skempton (1959)
Silica sand*	$f_b = N_q \sigma'_v \leq f_{b \text{ lim}}$	$N_q = 40$	API (1984)
		N_q plotted against Φ'	Berezantzev et al (1961)
		N_q related to Φ' , relative density and mean effective stress	Fleming <i>et al.</i> (1992)
		N_q from cavity expansion theory, as a function of Φ' and volumn compressibility	Vesic (1972)

Uncemented Calcareous Sand	$f_b = N_q \sigma_v' \leq f_{b \text{ lim}}$	$N_q = 20$	Datta <i>et al.</i> (1980)
		Typical range of $N_q = 8 - 20$	Poulos(1988)
		N_q determined fro reduced value of Φ' (e.g. 18°)	Dutt and Ingram (1984)

Table 2.2 Notable Research on Pile Groups

Research	Remarks
Poulos, 1968	Boundary Integral Method. Firstly introduced interaction factor to analysis of single pile within a pile group. No slip had been considered between piles and the adjacent soil. Both flexible and rigid pile cap have been analysed.
Butterfied and Banerjee, 1971	Boundary Integral Method. Analysed group settlement response using extended Mindlin's solutions for axially loaded pile groups with floating caps.
Ottaviani, 1975	3D FEM Method. Pile group embedded in a homogeneous linearly elastic medium have been analysed. Settlement against ratio of pile to soil elastic modulus, stress distribution in various piles and in the soil mass are also be analysed for capped piles and without cap.
Randolph and Worth, 1979	Theoretical load-transfer approach. Extended work from Randolph and worth (1978) to analysis of pile group, using the principle of superposition. Rigid and flexible pile group in elastic soil have been studied.
Kuwabara, 1989	Boundary Element Method. Applied boundary element method to study settlement and load transfer in axially loaded free-standing pile group
EI Sharnouby and Novak, 1990	Boundary Element Method. Applied stiffness and flexibility approaches for single pile analysis and group interaction factor for group with rigid and flexible pile caps
Fleming et al, 1992	Theoretical load-transfer approach. Presented a practical method for estimating the overall stiffness of pile groups. Method developed based on pile groups in soil modelled using load-transfer curve
Lee, 1993	Hybrid load transfer approach. Interaction factor are considered separately in individual piles in a group. Both linear and nonlinear pile responses are considered embedded

	in layered soil.
Shen <i>et al</i> , 2000	Practical Approach .This method used simple formulas obtained based on load-transfer curves, together with design charts obtained based on variational solution (Shen <i>et al</i> , 1997) for pile groups
Chow et al, 2001	Variational solution. Both displacement and shear stress of group piles are each represented by a finite series. The principle of minimum potential energy is used to determine the response of pile group.
Lee and Chung, 2005	Applied a experimental study of the interaction of vertically loading pile group in sand, load test have been carried out on: an isolated single pile, single-loaded centre pile in pile group, a unpiled footing, free standing pile group and piled footing.

Table 2.3 Computer Analysis on Pile and Piled Raft Foundation

Research	Remarks	Software
Chow, 1989	Pile group analysis in cross-anisotropic soil	PILEGRP
Fellenius, 1992	Single pile analysis and design	UNPILE
Lee <i>et al</i> , 1996	Design and analysis of pile	CAPWAP
Poulos, 1991	Strip on spring Approach on analysis of piled raft	GASP
Poulos, 1994	Plate on spring Approach on analysis of piled raft	GARP
Reese, 1994	Pile group analysis for axial lateral loading	GROUP
Hewitt and Gue, 1994	Installation effects of bored piles and diaphragm walls	FLAC
Russo, 1998	Non-linear Analysis of Pied raft system	NAPRA
Small and Zhang, 2000	Analysis of Piled raft foundation under general loading	FLAC
Prakoso and Kulhawy (2001)	Plain strain model piled raft system	PLAXIS
Liang <i>et al</i> , 2003	study of axial loading piled raft foundation with cushion	ANSYS
Kitiyodom and Matsumoto (2003)	Piled raft foundation in non-homogeneous soils	PRAB
Reul and Randolph (2003)	3D FEM analysis of Piled raft in overconsolidated clay	ABAQUS

Table 2.4 Numerical Programs using for Analysis of Piles and Piled Raft

Software GROUP	Salient features	Constitutive Models	Capability
	<ul style="list-style-type: none"> Vertical and oblique piles Automatic or user p-y data Laterally loaded case 	<ul style="list-style-type: none"> Linear elastic Non-linear elastic P-y criterion 	<ul style="list-style-type: none"> Load settlement Load transfer ultimate pile capacity
CRISP	<ul style="list-style-type: none"> 2D, 3D FEM program Plane strain, axisymmetric Triangular, quadrilateral and isoparametric elements Undrained, drained and fully coupled analysis 	<ul style="list-style-type: none"> Anisotropic elasticity Inhomogeneous elasticity Critical state Models Elastic-perfectly plastic models 	<ul style="list-style-type: none"> Load settlement Bending moment Shear force Stress and strain plot Plot pressure Stress and Strain path
FLAC 2D	<ul style="list-style-type: none"> 2D finite different Modelling geoengineering project consisted of several staged. Accurate plastic collapse and flow modelling No matrices are formed Simulation of highly nonlinear Dynamic analysis capability 	<ul style="list-style-type: none"> Linear elastic Mohr-Coulomb plasticity Ubiquitous joint Double yield Viscous and strain softening Creep models User defined models 	<ul style="list-style-type: none"> Stress contours Displacement contours Bending moment Shear force Deformed shape Pore pressure contour Stress and strain path
FLAC 3D	<ul style="list-style-type: none"> Lagrangian type finite difference method 3 dimensional modelling Supports mixed discretisation scheme Capable to analyse plastic flow and collapse Plane stress, plane strain, axisymmetric cases Undrained, drained and fully coupled cases Structural element models thermal and Vis-plastic models 	<ul style="list-style-type: none"> Null Linear elastic Elastic-plastic Drucker-Prager Mohr-Coulomb Ubiquitous joint Strain softening Strain Hardening Liquefaction model Creep models User defined 	<ul style="list-style-type: none"> 3D modelling Stress contours Displacement contours Bending moment Shear force Stress and strain path Pore pressure contour Deform shape Dynamic analysis

		model	<ul style="list-style-type: none"> Thermal analysis
PLAXIS 2D	<ul style="list-style-type: none"> Plane strain, axisymmetric Interface element Automatic load stepping Construction staged Realistic simulation of the building process Tunnel Model 2D dynamic module Defined by a phreatic surface 	<ul style="list-style-type: none"> Linear elastic Mohr-Coulomb Cam clay Elastoplastic hyperbolic Jointed Rock model Hardening soil model Soft soil creep model Soft soil model Advanced soil model User defined model 	<ul style="list-style-type: none"> Stress contours Displacement contours Axial loading Bending moment Shear force Deformed shape Pore pressure contour Stress and strain path Dynamic analysis
PLAXIS 3D	<ul style="list-style-type: none"> Design for piled raft analysis Soil layer defined using borehole Work plane Modelled pile using pile designer tool Automatic mesh generation Volume element Automatic load stepping Construction staged Arc-length control 	<ul style="list-style-type: none"> Linear elastic Mohr-Coulomb Hardening soil model 	<ul style="list-style-type: none"> 3D modelling Displacement Stress and strain in interface and structure Shear force Stress and strain path Pore pressure contour

Table 3.1 Summarised Project information used in Study

Project	Story	Height (m)	Foundation	Bearing Stratum
ARTIQUE	30	95	Piled Raft	Sand
Q1 Tower	78	323	Pile	Rock
Circle on Cavill Tower A	50	158	Pile Group	Rock
Circle on Cavill Tower B	70	219	Pile Group	Rock
SOLAIRE	20	72	Piled Raft	Sand

Table 3.2 ARTIQUE - Summary of Stratigraphy

Borehole	Surface Level		Medium Dense Sand Layer		Very Dense Sand Layer		Peat Layer		Very Dense Sand Layer		Stiff Clay Layer		Gravelly Sand /sand Layer		Rock Layer
			Top	Bottom	Top	Bottom	Top	Bottom	Top	Bottom	Top	Bottom	Top	Bottom	Top
BH1	5.40	Depth	0	6.0	6.0	14.7	14.7	16.5	16.5	25.0	25.0	35.0	N/O	N/O	35.0
		RL	+5.40	-0.60	-0.60	-9.30	-9.30	-11.1	-11.1	-19.6	-19.6	-29.6	N/O	N/O	-29.6
BH2	6.00	Depth	0	6.00	6.00	19.0	19.0	23.5	23.5	27.0	27.0	33.0	33.0	37.0	37.0
		RL	+6.00	0	0	-13.0	-13.0	-17.5	-17.5	-21.0	-21.0	-27.0	-27.0	-31.0	-31.0
BH3	5.10	Depth	0	10.0	10.0	11.8	11.8	13.0	13.0	23.5	23.5	31.4	N/O	N/O	31.4
		RL	+5.10	-4.90	-4.90	-6.70	-6.70	-7.90	-7.90	-18.4	-18.4	-26.3	N/O	N/O	-26.3
BH4	5.50	Depth	0	10	10	14.6	14.6	16.1	16.1	26.0	26.0	35.5	N/O	N/O	35.5
		RL	+5.50	-4.50	-4.50	-9.10	-9.10	-10.6	-10.6	-20.5	-20.5	-30.0	N/O	N/O	-30.0
BH5	6.00	Depth	0	5.00	5.00	17.2	17.2	24.2	24.2	25.6	25.6	35.2	N/O	N/O	35.2
		RL	+6.00	+1.00	+1.00	-11.2	-11.2	-18.2	-18.2	-19.6	-19.6	-29.2	N/O	N/O	-29.2
BH6	6.00	Depth	0	8.00	8.00	17.0	17.0	22.0	22.0	26.7	26.7	36.5	N/O	N/O	36.5
		RL	+6.00	-2.00	-2.00	-11.0	-11.0	-16.0	-16.0	-20.7	-20.7	-30.5	N/O	N/O	-30.5

Note: "N/O" indicates "Not Observed"

All depth and reduced Level are in meters

Table 3.3 Q1 Tower - Summary of Stratigraphy

Borehole		Medium Dense/Fill Sand Layer		Very Dense Sand Layer		Sandy Clay Layer		Clayey Sand Layer		Gravelly Sand		Rock Layer
		Top	Bottom	Top	Bottom	Top	Bottom	Top	Bottom	Top	Bottom	Top
BH1	Depth	0	7.0	7.0	26.8	26.8	31.1	31.1	35.4	35.4	40.05	40.05
BH2	Depth	0	4.0	4.0	27.0	27.0	30.7	30.7	36.8	36.8	38.75	38.75
BH3	Depth	0	7.80	7.80	27.0	27.0	31.7	31.7	36.0	36.0	40.7	40.7

Note: All depth and reduced are in meters

Table 3.4 Circle on Cavill - Summary of Stratigraphy

Borehole	Surface Level		Medium Dense Sand Layer		Very Dense Sand Layer		Peat Layer		Very Dense Sand Layer		Stiff Clay Layer		Gravelly Sand /sand Layer		Rock Layer
			Top	Bottom	Top	Bottom	Top	Bottom	Top	Bottom	Top	Bottom	Top	Bottom	Top
FP1	2.30	Depth	0	5.50	5.50	12.6	12.6	14.0	14.0	23.5	23.5	27.5	27.5	36.6	36.6
		RL	+2.30	-3.20	-3.20	-10.30	-10.3	-11.7	-11.7	-21.2	-21.2	-25.2	-25.2	-34.3	-34.3
FP2	2.60	Depth	0	4.00	4.0	13.7	13.7	16.8	16.8	22.0	22.0	30.0	30.0	35.9	35.9
		RL	+2.6	-1.40	-1.40	-11.1	-11.1	-14.2	-14.2	-19.4	-19.4	-27.4	-27.4	-33.3	-33.3
FP3	2.90	Depth	0	8.50	8.50	13.7	13.7	17.3	17.3	23.1	23.1	28.7	28.7	35.6	35.6
		RL	+2.9	-5.60	-5.60	-10.8	-10.8	-14.4	-14.4	-20.2	-20.2	-25.8	-25.8	-32.7	-32.7
FP4	3.30	Depth	0	8.50	8.50	13.9	13.9	15.6	15.6	25.0	25.0	30.1	30.1	37.9	37.9
		RL	+3.30	-5.20	-5.20	-10.6	-10.6	-12.3	-12.3	-21.7	-21.7	-26.8	-26.8	-34.6	-34.6
FP5	1.97	Depth	0	8.00	8.00	12.2	12.2	14.0	14.0	23.50	23.50	28.0	28.0	33.6	33.6
		RL	+1.97	-6.03	-6.03	-10.2	-10.2	-12.0	-12.0	-21.5	-21.5	-26.0	-26.0	-31.6	-31.6
FP6	4.46	Depth	0	11.5	11.5	14.0	14.0	16.0	16.0	24.5	24.5	28.3	28.3	38.2	38.2
		RL	+4.46	-7.04	-7.04	-9.54	-9.54	-11.5	-11.5	-20.0	-20.0	-23.8	-23.8	-33.7	-33.7
FP7	6.00	Depth	0	8.00	8.00	18.0	18.0	23.1	23.1	25.9	25.9	36.0	36.0	40.5	40.5
		RL	+6.0	-2.00	-2.00	-12.0	-12.0	-17.1	-17.1	-19.9	-19.9	-30.0	-30.0	-34.5	-34.5

Note: All depth and reduced are in meters

Table 3.5 SOLAIRE - Summary of Stratigraphy

Borehole	Surface Level		Medium Dense Sand Layer		Very Dense Sand Layer		Peat Layer		Very Dense Sand Layer		Stiff Clay Layer		Gravelly Sand /sand Layer		Rock Layer
			Top	Bottom	Top	Bottom	Top	Bottom	Top	Bottom	Top	Bottom	Top	Bottom	Top
GA1	3.501	Depth	0	4.6	4.6	14.7	14.7	18.9	18.9	23.4	23.4	29.5	29.5	30.8	30.8
		RL	+3.5	-1.10	-1.10	-11.2	-11.2	-15.4	-15.4	-19.9	-19.9	-26.0	-26.0	-27.3	-27.3
GA2	3.587	Depth	0	5.60	5.60	14.3	14.3	17.5	17.5	23.0	23.0	29.85	29.85	30.9	30.9
		RL	+3.6	-2.0	-2.0	-10.7	-10.7	-13.9	-13.9	-19.4	-19.4	-26.3	-26.3	-27.3	-27.3
GA3	3.453	Depth	0	5.6	5.6	14.5	14.5	18.7	18.7	22.9	22.9	28.2	28.2	29.0	29.0
		RL	+3.5	-2.10	-2.10	-11.0	-11.0	-15.2	-15.2	-19.4	-19.4	-24.7	-24.7	-25.5	-25.5
GA4	3.488	Depth	0	5.4	5.4	14.7	14.7	18.5	18.5	22.9	22.9	28.3	28.3	30.6	30.6
		RL	+3.5	-1.90	-1.90	-11.2	-11.2	-15.0	-15.0	-19.4	-19.4	-24.8	-24.8	-27.1	-27.1
BH1	4.2	Depth	0	6.0	6.0	14.9	14.9	19.1	19.1	28.9	N/O	N/O	N/O	N/O	28.9
		RL	+4.2	-1.8	-1.8	-10.7	-10.7	-14.9	-14.9	-24.7	N/O	N/O	N/O	N/O	-24.7
BH2	5.9	Depth	0	6.8	6.8	16.3	16.3	17.6	17.6	25.2	25.2	33.7	33.7	34	34
		RL	+5.9	-0.9	-0.9	-10.4	-10.4	-11.7	-11.7	-19.3	-19.3	-27.8	-27.8	-28.1	-28.1

Note: "N/O" indicates "Not Observed"

All depth and reduced are in meters

BH1 and BH2 is the previous Borehole record which investigated in 2003

Table 3.6 SPT Hammer Efficiencies (Adapted from Clayton, 1990)

Country	Hammer Type	Hammer Release Mechanism	Hammer Efficiency E_m
Argentina	Donut	Cathead	0.45
Brazil	Pin weight	Hand dropped	0.72
China	Automatic	Trip	0.60
	Donut	Hand dropped	0.55
	Donut	Cathead	0.50
Colombia	Donut	Cathead	0.50
Japan	Donut	Tombi trigger	0.78-0.85
	Donut	Cathead 2 turns + special release	0.65-0.67
UK	Automatic	Trip	0.73
US	Safety	2 turns on cathead	0.55-0.60
	Donut	2 turns on cathead	0.45
Venezuela	Donut	Cathead	0.43
Gold Coast, AU	Automatic	Trip	0.73

Table 3.7 Borehole, Sampler, and Rod Correction Factors (after Skempton, 1986)

Factor	Equipment Variables	Value
Borehole diameter factor, C_B	65-115 mm	1.0
	150 mm	1.05
	200 mm	1.15
Sampling method factor, C_S	Standard sampler	1.00
	Sampler without liner	1.20
Rod length factor, C_R	3 – 4 m	0.75
	4-6 m	0.85
	6-10 m	0.95
	>10 m	1.00

Table 3.8(a) ARTIQUE: Summarised Average SPT N , N_{60} , $(N_1)_{60}$

	Loose to Medium Dense Sand	Dense Sand	Peat/Clay	Lower Dense Sand	Lower Stiff Clay	Rock
Depth (m)	0-7.5	7.5-15.7	15.7-19.2	19.2-25.6	25.6-35.1	35.1-N/A
Thickness (m)	7.5	8.2	3.5	6.4	9.9	-
N	13	48	12	48	27	-
N_{60}	12	43	10	44	24	-
$(N_1)_{60}$	13	33	7	27	13	-

Note: N – measured SPT N value

N_{60} – SPT N value corrected for field procedures

$(N_1)_{60}$ – SPT N value corrected for field Procedures and overburden pressure

Table 3.8(b) Q1 Tower: Summarised Average SPT N , N_{60} , $(N_1)_{60}$

	Loose to Medium Dense Sand	Dense Sand	Sandy Clay	Clayey Sand	Gravelly Sand	Rock
Depth (m)	0-6.3	6.3-26.9	26.9-31.2	31.2-36.1	36.1-39.8	39.8-N/A
Thickness (m)	6.3	20.6	4.3	4.9	3.7	-
N	20	50	44	36	50	-
N_{60}	18	46	40	33	46	-
$(N_1)_{60}$	22	32	22	17	22	-

Note: N – measured SPT N value

N_{60} – SPT N value corrected for field procedures

$(N_1)_{60}$ – SPT N value corrected for field Procedures and overburden pressure

Table 3.8(c) Circle on Cavill: Summarised Average SPT N , N_{60} , $(N_1)_{60}$

	Loose to Medium Dense Sand	Dense Sand	Peat/Clay	Lower Dense Sand	Lower Stiff Clay	Gravelly Sand	Rock
Depth (m)	0-7.7	7.7-14.0	14.0-16.7	16.7-23.9	23.9-29.8	29.8-36.9	36.9-N/A
Thickness (m)	7.7	6.3	2.7	7.2	5.9	7.1	-
N	16	48	10	47	18	49	-
N₆₀	15	44	9	43	16	44	-
(N₁)₆₀	19	40	7	30	10	24	-

Note: N – measured SPT N value

N_{60} – SPT N value corrected for field procedures

$(N_1)_{60}$ – SPT N value corrected for field Procedures and overburden pressure

Table 3.8(d) SOLAIRE: Summarised Average SPT N , N_{60} , $(N_1)_{60}$

	Loose to Medium Dense Sand	Dense Sand	Peat/Clay	Lower Dense Sand	Lower Stiff Clay	Gravelly Sand	Rock
Depth (m)	0-5.7	5.7-14.9	14.9-18.4	18.4-24.4	24.4-29.9	29.9-31.1	31.1-N/A
Thickness (m)	5.7	9.2	3.9	6	5.5	1.2	-
N	14	49	10	44	23	50	-
N₆₀	13	45	9	40	21	46	-
(N₁)₆₀	17	39	7	26	12	25	-

Note: N – measured SPT N value

N_{60} – SPT N value corrected for field procedures

$(N_1)_{60}$ – SPT N value corrected for field Procedures and overburden pressure

Table 3.9 SPT N vs. ϕ Relationships

N value (blows/300 mm)	Relative Density	ϕ (degrees)	
		Peck <i>et al</i> (1974)	Meyerhof (1956)
0 – 4	Very Loose	< 28	< 30
4 – 10	Loose	28 – 30	30 – 35
10 – 30	Medium	30 – 36	35 – 40
30 – 50	Dense	36 – 41	40 – 45
> 50	Very Dense	> 41	> 45

Table 3.10 Approximate s_u versus N Relationship (after Terzaghi and Peck, 1967)

N Value (blows/300 mm)	Consistency	Approximate S_u (kPa)
0 - 2	Very Soft	< 12.5
2 - 4	Soft	12.5 – 25
4 - 8	Medium	25 – 50
8 - 15	Stiff	50 – 100
15 - 30	Very Stiff	100 - 200
> 30	Hard	> 200

Table 3.11 Typical Ranges of Drained Modulus for Sand (Kulhawy and Mayne, 1990)

Consistency	Normalized Elastic Modulus, E_d (MPa)
	Typical

Loose	10 – 20
Medium	20 – 50
Dense	50 – 100

Table 3.12 Suggested Average Values of E_s for Driven Piles in Sand

Sand Density	Range of relative density, D_r	Range of E_s (MPa)
Loose	< 0.4	27.5 – 55
Medium	0.4 – 0.6	55 – 70
Dense	>0.6	70 – 110

Table 3.13 Typical Ranges of Undrained Modulus for Clay (Kulhawy & Mayne, 1990)

Consistency	Normalized Undrained Modulus, E_d (MPa)
Soft	1.5 – 4
Medium	4 – 8
Stiff	8 – 20

Table 3.14 Required Parameters for the Analysis of Piled Rafts for Elastic Analysis

Soil Parameters	Structure Element Parameters	Interface Parameters
Unsaturated unit weight, γ_{unsat} Saturated unit weight, γ_{sat} Young's Modulus, E Poisson Ratio, ν	Young's modulus, E_p Axial Stiffness, EA Flexural Rigidity, EI Poisson Ratio, ν	Cohesion, \bar{c} (constant) Friction, $\bar{\phi}$ Interface strength, R_{inter}

Table 4.1 Summarised Material Properties of the Raft

Thickness (m)	Normal Stiffness EA (kN/m)	Flexural rigidity EI (kNm²/m)	Poisson's ration, ν
0.25	7.5 E+06	3.91 E+04	0.2
0.40	1.2 E+07	1.60 E+05	0.2
0.80	2.4 E+07	1.28 E+06	0.2
1.50	4.5 E+07	8.44 E+06	0.2
3.00	9.0 E+07	6.75 E+07	0.2

Table 4.2 Summarised Material Properties of the Pile

Parameter	Name	Value	Unit
Pile Diameter	Ø	0.7	m
Young's Modulus	E	3.0 E+07	kN/m ²
Equivalent Young's Modulus	E _{qu}	8.2 E+06	kN/m ²
Normal stiffness	EA	1.2 E+07	kN/m

Flexural rigidity	EI	3.5 E+05	kNm ² /m
Poisson's Ratio	ν	0.2	-

Table 4.3 Suggested Cohesion, c Value in PLAXIS (Huybrechts and Whenham, 2004)

Soil Material	I _p (%)	Φ' (deg)	C (kN/m ²)
Crushed rock		47+/-7	0
Clean gravel	0	40+/-5	0
Loamy gravel	2-6	36+/-4	~ 0
Clayey gravel	7-12	34+/-4	~ 0
Clean sand poorly graded	0	40+/-4	0
Well graded clean sand	0	36+/-6	0
Slightly Loamy sand	2 - 6	34+/-4	~ 0
Slightly clayey sand	6 -12	32+/-3	~ 0
Clayey sand	9 - 15	27+/-3	5+/-5
Loam	2 - 6	33+/-4	~ 0
Clayey loam	4 - 10	30+/-4	15+/-10
Loamy clay	12 - 18	27+/-4	20+/-10
Clay	~ 20	20+/-4	20+/-10
	~ 40	15+/-4	25+/-10
	~ 60	11+/-4	too variable
	> 100	< 8	too variable

Table 4.4 Newton-Cotes Integrations

	ξ_i	w_i
2 nodes	± 1	1
3 nodes	$\pm 1, 0$	1/3, 4/3
4 nodes	$\pm 1, \pm 1/3$	1/4, 3/4
5 nodes	$\pm 1, \pm 1/2, 0$	7/45, 32/45, 12/45

Table 4.5 Parameters Used in PLAXIS Analysis

Parameter	Name	M. Sand	Sand	Stiff Clay	Unit
Material Model	Model	Mohr-C	Mohr-C	Mohr-C	-
Material Behaviour	Type	Drained	Drained	Drained	-
Soil unit weight above phreatic level	γ_{unsat}	16	17	16	kN/m ³
Soil unit weight below phreatic level	γ_{sat}	19	20	19	kN/m ³
Permeability in hor. direction	k_x	1.0	1.0	0.001	m/day
Permeability in ver. direction	k_y	1.0	1.0	0.001	m/day
Young's Modulus (Constant)	E_{ref}	55	120	65	MPa
Poisson Ratio, ν	ν	0.3	0.3	0.35	-
Cohesion (Constant)	c_{ref}	1	1	20	kN/m ²
Friction angle	ϕ	37	42	25	deg
Dilatancy angle	Ψ	7	12	0	deg

Strength reduction factor inter	R_{inter}	0.8	0.8	1	-
---------------------------------	-------------	-----	-----	---	---

Table 5.1 Range of Normalized Settlement for Each Raft Size

Normalized Settlement	8m×8m	15m×15m	30m×30m
I_R	1.02 ~ 1.15	0.64 ~ 0.81	0.38 ~ 0.54

Table 5.2 Value of K_R , Raft Relative Stiffness for Each Thickness

	$K_R(8m \times 8m)$	$K_R(15m \times 15m)$	$K_R(30m \times 30m)$
0.25m	2.10E-02	3.19E-03	3.99E-04
0.4m	8.62E-02	1.31E-02	1.63E-03
0.8m	6.89E-01	1.05E-01	1.31E-02
1.5m	4.54E+00	6.89E-01	8.62E-02
3.0m	3.64E+01	5.52E+00	6.89E-01

Table 5.3 Maximum Settlement of Different Size Unpiled Raft. Loads = 215 kN/m²

	8m×8m raft Settlement(mm)	15m×15m raft Settlement(mm)	30m×30m raft Settlement(mm)
0.25m	32.8	43.0	57.4
0.4m	32.3	42.9	57.4
0.8m	31.7	41.8	57.3
1.5m	31.5	40.5	55.8
3.0m	31.5	40.1	53.2

Table 5.4 Summarised Relative Stiffness Zone for Different Size Raft Foundation

	Flexible Raft	Relative Flexible	Rigid
8m×8m	$t_R < 0.25m$	$0.25m < t_R < 1.5m$	$t_R > 1.5m$
15m×15m	$t_R < 0.4m$	$0.4m < t_R < 3.0m$	$t_R > 3.0m$
30m×30m	$t_R < 0.8m$	$0.8m < t_R < 6m$	$t_R > 6m$

Table 5.5 Normalized Differential Settlement for Each Raft Size

	$t_R = 0.25m$	$t_R = 0.4m$	$t_R = 0.8m$	$t_R = 1.5m$	$t_R = 3.0m$
--	---------------	--------------	--------------	--------------	--------------

Δw^* (8m×8m)	0.12	0.1	0.018	0.003	0.0004
Δw^* (15m×15m)	0.23	0.21	0.20	0.03	0.005
Δw^* (30m×30m)	0.32	0.31	0.27	0.18	0.05

Table 5.6a Maximum Normalized Bending Moment for Each Thickness. 8m×8m Unpiled Raft

Thickness (m)	Max. Normalized Bending Moment
0.25	0.164
0.4	0.471
0.8	0.896
1.5	1.00
3.0	1.02

Table 5.6b Maximum Normalized Bending Moment for Each Thickness. 15m×15m Unpiled Raft

Thickness (m)	Max. Normalized Bending Moment
---------------	--------------------------------

0.25	0.035
0.4	0.111
0.8	0.584
1.5	1.067
3.0	1.225

Table 5.6c Maximum Normalized Bending Moment for Each Thickness. 30m×30m Unpiled Raft

Thickness (m)	Max. Normalized Bending Moment
0.25	0.007
0.4	0.02
0.8	0.095
1.5	0.477
3.0	1.077

Table 5.7 Effect of Raft Thickness: Maximum Settlement in Piled Raft

Thickness(m)	Max. Settlement (mm)
0.25	64.00
0.4	63.3
0.8	62.6
1.5	62.3
3.0	62.2

Table 5.8 Effect of Raft Thickness: Maximum Bending Moment in Piled Raft

Thickness (m)	Max. Bending Moment (kNm)
0.25	-107
0.4	-160
0.8	-321
1.5	-446
3.0	-485

Table 5.9(a) Effect of Raft Thickness: Maximum Axial Force on Pile 1 (at the edge)

Thickness (m)	Max. Axial Force(MN)
0.25	1.19
0.4	1.267

0.8	1.35
1.5	1.41
3.0	1.411

Table 5.9(b) Effect of Raft Thickness: Maximum Axial Force Pile 2 (at the centre)

Thickness(m)	Max. Axial Force(MN)
0.25	1.064
0.4	1.035
0.8	0.967
1.5	0.923
3.0	0.909

Table 5.10 Effect of Pile Spacing: Piled Raft Maximum Settlement. Load=215kN/m²

S/D	Max. Settlement (mm)
3	22
4	26
5	29
6	34

7	36
---	----

Table 5.11 Effect of Pile Spacing: Piled Raft Maximum Bending Moment. Load=215kN/m²

S/D	Max. Bending Moment (MNm)
3	-0.197
4	-0.329
5	-0.369
6	-0.423
7	-0.440

Table 5.12(a) Effect of Pile Spacing: Maximum axial force on Pile 1 (at the edge). Load=215kN/m²

S/D	Max. Axial Force(MN)
3	0.265
4	0.453
5	0.552
6	0.743
7	0.835

Table 5.12(b) Effect of Pile Spacing: Maximum axial force on Pile 2 (at the centre). Load=215kN/m²

S/D	Max. Axial Force(MN)
3	0.475
4	0.541
5	0.571

6	0.620
7	0.640

Table 5.13(a) Effect of Pile Spacing: Maximum Bending Moment on Pile 1 (at the edge). Load=215kN/m²

S/D	Max. Bending Moment(kNm)
3	-91.4
4	-159
5	-187.5
6	-231.2
7	-246.2

Table 5.13(b) Effect of Pile Spacing: Maximum Bending Moment on Pile 2 (at the centre). Load=215kN/m²

S/D	Max. Bending Moment(kNm)
3	-28.9
4	-48.9
5	-58.0
6	-68.0
7	-69.4

Table 5.14 Effect of Pile Spacing: Piled Raft Maximum Settlement. Load=430kN/m²

S/D	Max. Settlement (mm)
3	41
4	53
5	60
6	69
7	74

Table 5.15 Effect of Pile Spacing: Piled Raft Maximum Bending Moment. Load=430kN/m²

S/D	Max. Bending Moment (MNm)
3	-0.262
4	-0.526
5	-0.603
6	-0.740
7	-0.771

Table 5.16(a) Effect of Pile Spacing: Maximum axial force on Pile 1 (at the edge). Load=430kN/m²

S/D	Max. Axial Force(MN)
3	0.917
4	1.066
5	1.148
6	1.227

7	1.286
---	-------

Table 5.16(b) Effect of Pile Spacing: Maximum axial force on Pile 2 (at the centre). Load=430kN/m²

S/D	Max. Axial Force(MN)
3	0.611
4	0.981
5	1.178
6	1.539
7	1.727

Table 5.17(a) Effect of Pile Spacing: Maximum Bending Moment on Pile 1 (at the edge). Load=430kN/m²

S/D	Max. Bending Moment(kNm)
3	-137.3
4	-247.9
5	-285.9

6	-371.7
7	-387.2

Table 5.17(b) Effect of Pile Spacing: Maximum Bending Moment on Pile 2 (at the centre). Load=430kN/m²

S/D	Max. Bending Moment(kNm)
3	-43.7
4	-79.7
5	-90.05
6	-110.3
7	-114.1

Table 5.18 Effect of Pile Spacing: Piled Raft Maximum Settlement. Load=645kN/m²

S/D	Max. Settlement (mm)
3	62
4	83
5	92
6	108
7	115

Table 5.19 Effect of Pile Spacing: Piled Raft Maximum Bending Moment. Load=645kN/m²

S/D	Max. Bending Moment (MNm)
3	-0.343
4	-0.749
5	-0.872
6	-1.073
7	-1.147

Table 5.20(a) Effect of Pile Spacing: Maximum axial force on Pile 1 (at the edge). Load=645kN/m²

S/D	Max. Axial Force(MN)
3	1.352
4	1.573
5	1.667
6	1.807
7	1.923

Table 5.20(b) Effect of Pile Spacing: Maximum axial force on Pile 2 (at the centre). Load=645kN/m²

S/D	Max. Axial Force(MN)
3	0.956
4	1.506
5	1.794
6	2.338
7	2.602

Table 5.21(a) Effect of Pile Spacing: Maximum Bending Moment on Pile 1 (at the edge). Load=645kN/m²

S/D	Max. Bending Moment(kNm)
3	-183.1
4	-33.67
5	-398.3
6	-513.9
7	-533.7

Table 5.21(b) Effect of Pile Spacing: Maximum Bending Moment on Pile 2 (at the centre). Load=645kN/m²

S/D	Max. Bending Moment(kNm)
3	-58
4	-112
5	-127.6
6	-161.1
7	-162.6

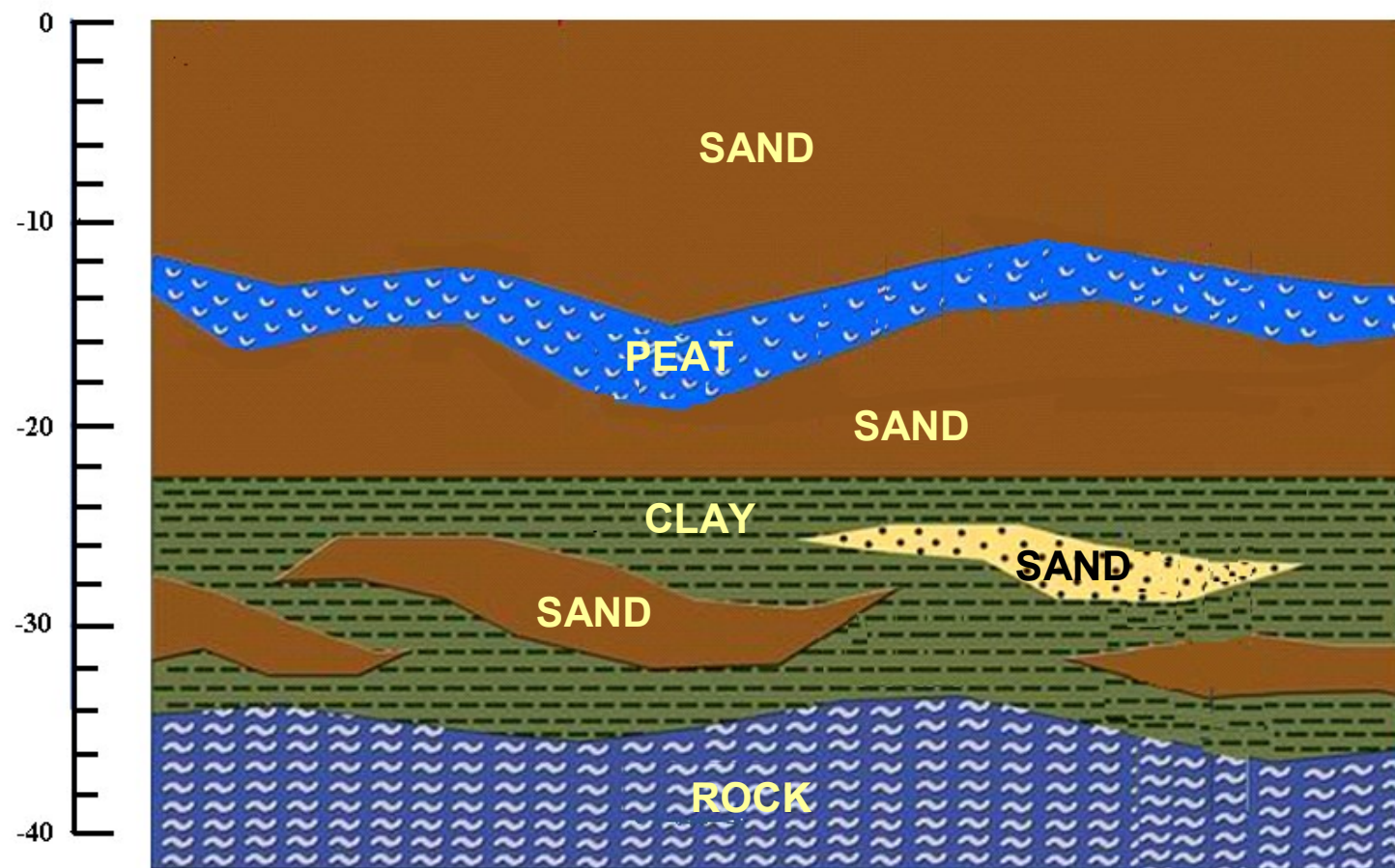


Figure 2.1 Gold Coast Subsoil Profile

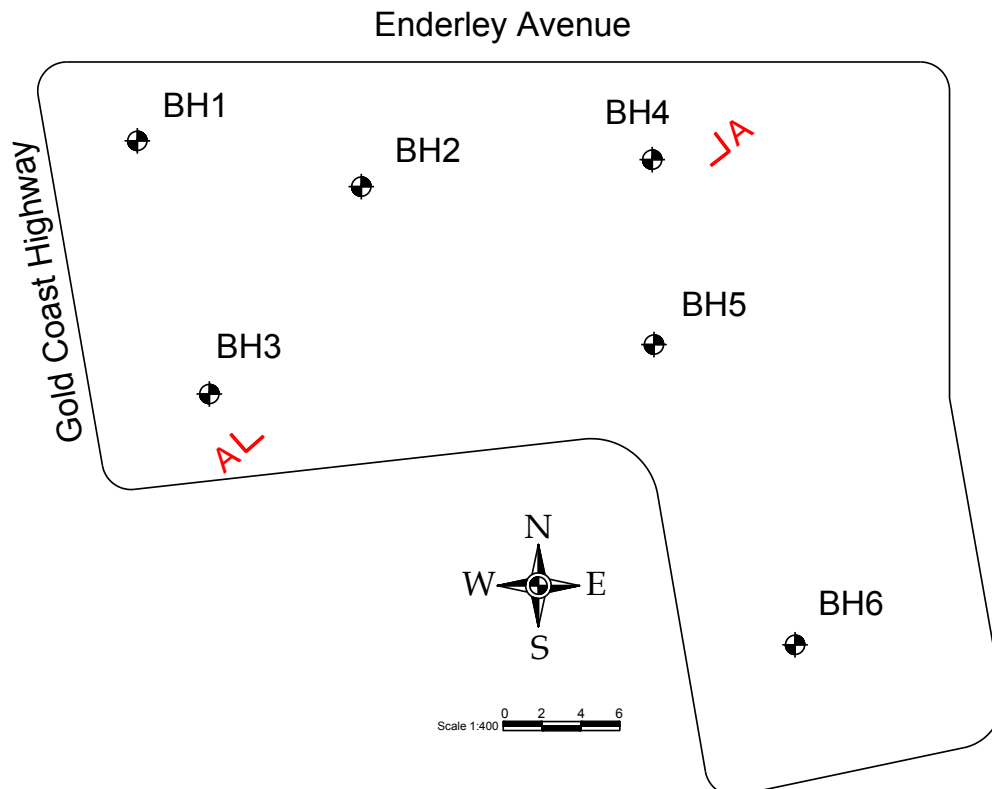


Figure 3.1(a) ARTIQUE – Borehole Location Plan (APPROX.)

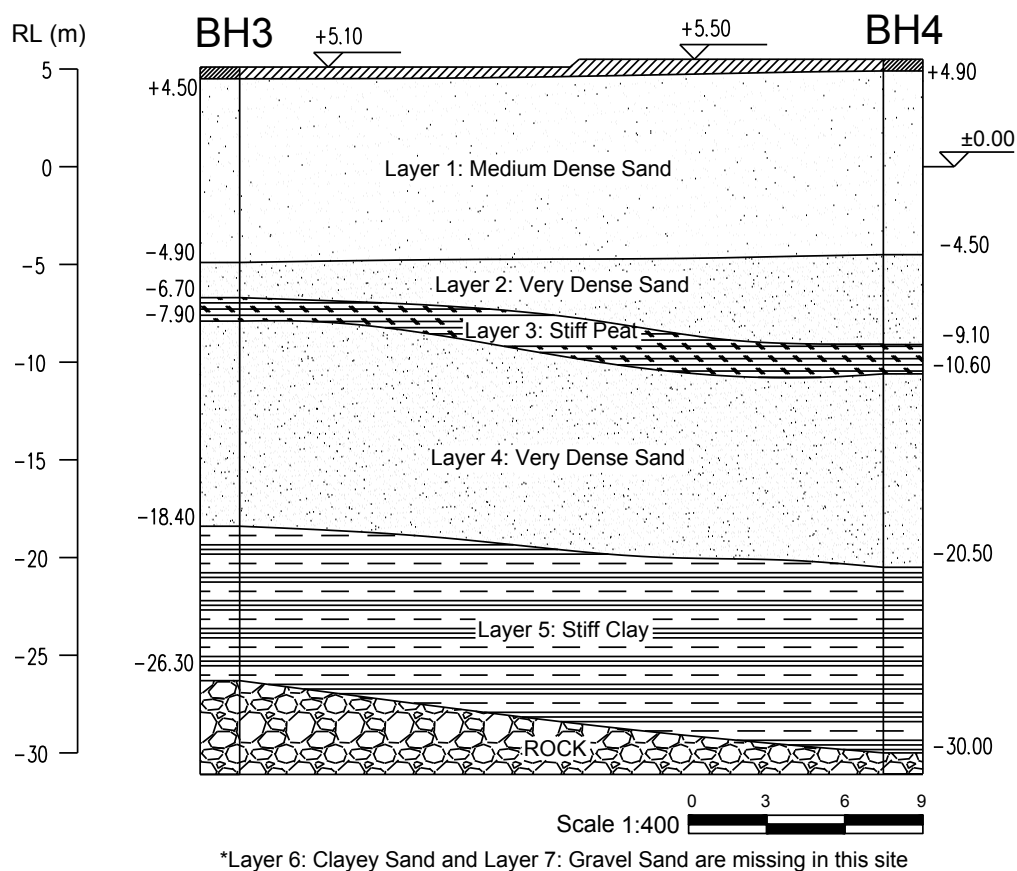


Figure 3.1(b) ARTIQUE – Soil Profile along Section A-A'

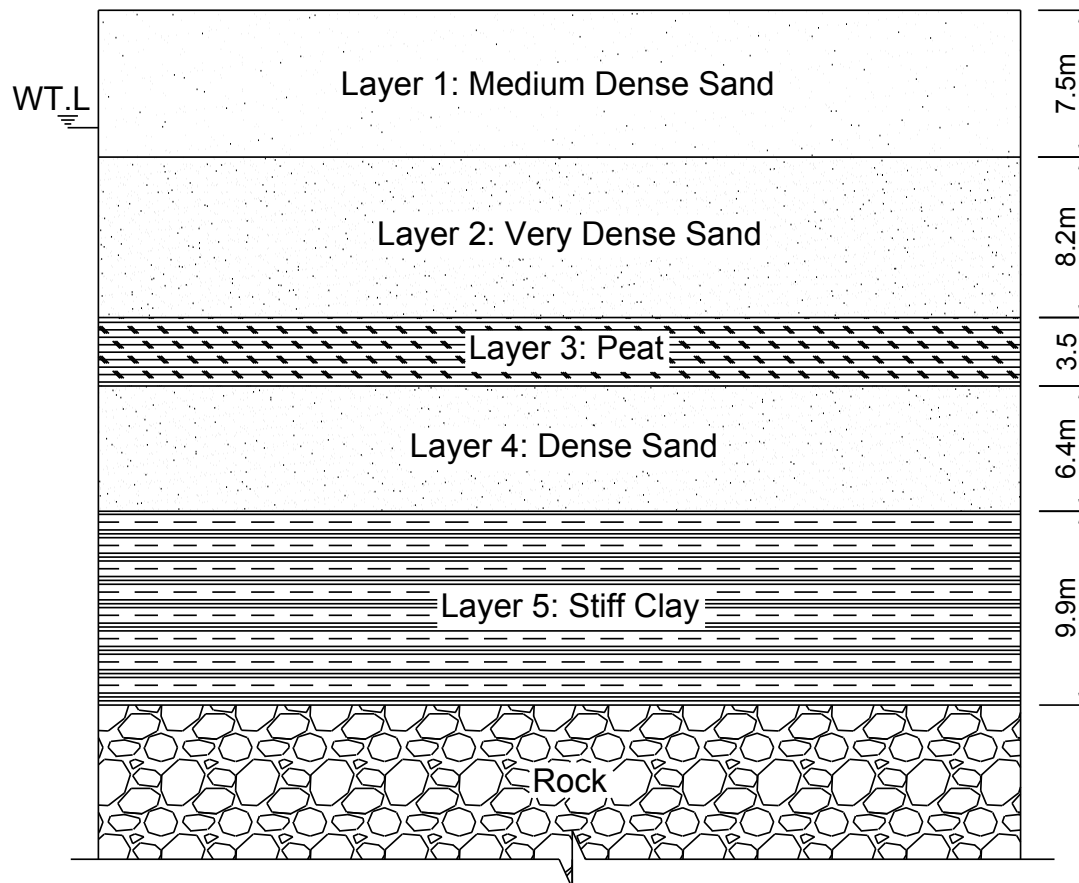


Figure 3.2 ARTIQUE – General Site Soil Profile

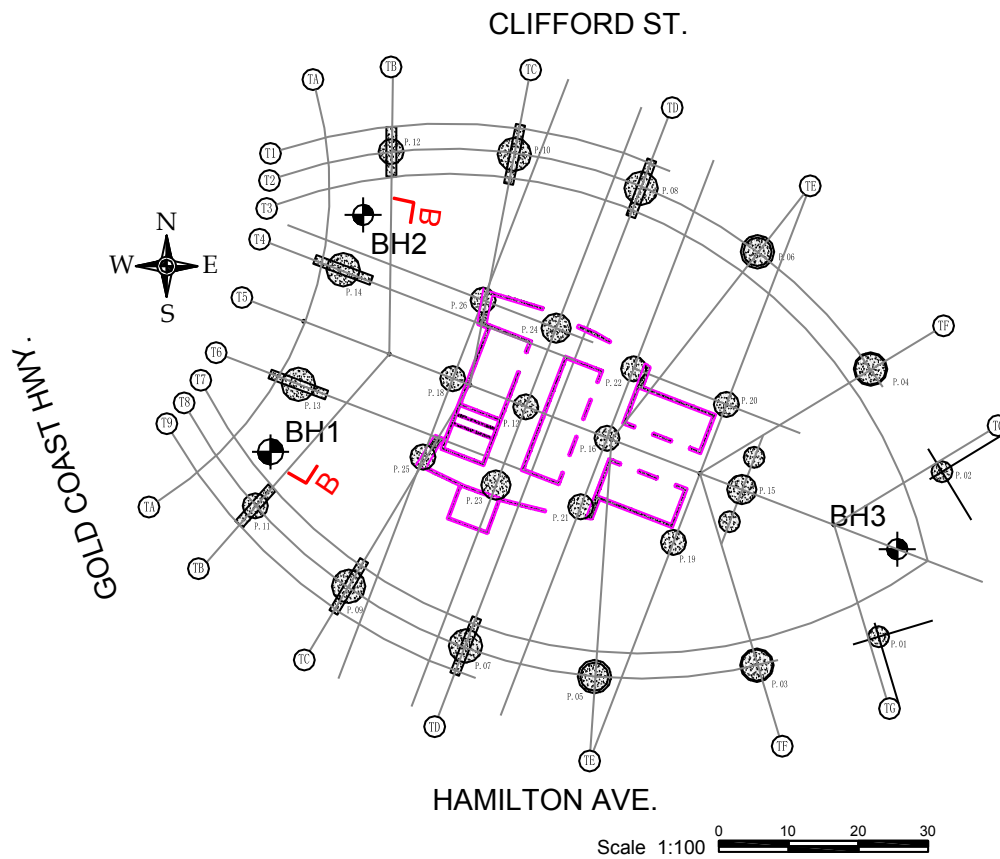
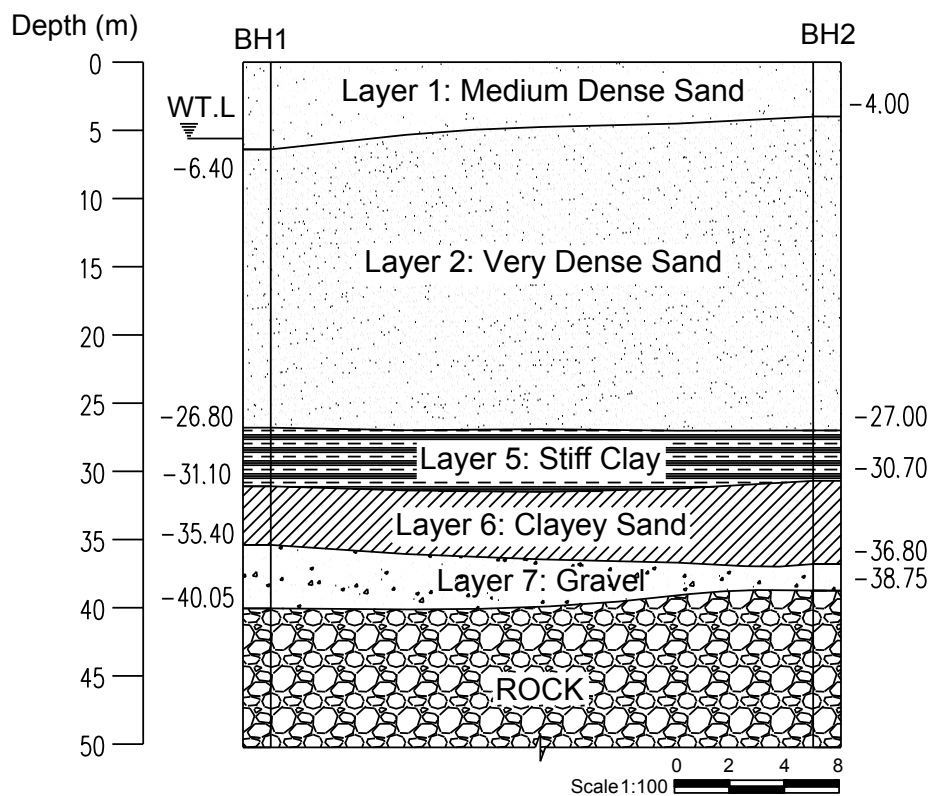


Figure 3.3a Q1 - Borehole and Pile Location Plan



*Layer 3: peat is missing
Figure 3.3b Q1 - Soil Profile along Section B-B'

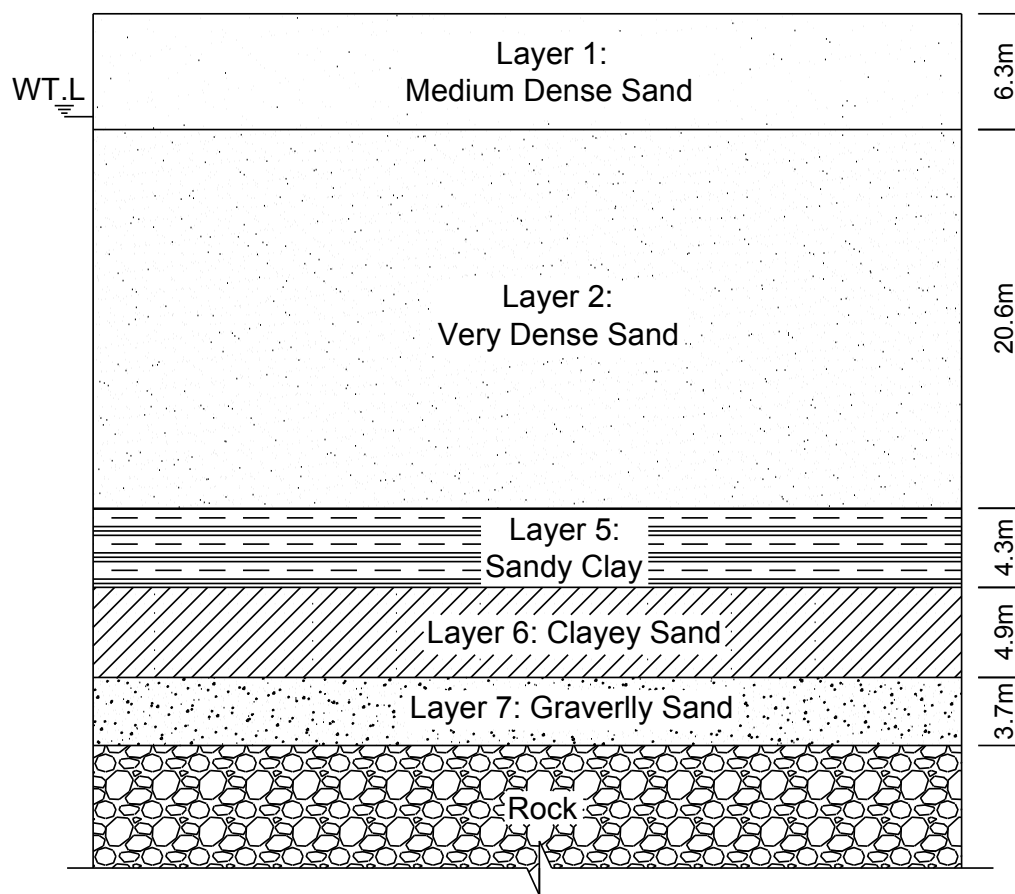


Figure 3.4 Q1 – General Site Soil Profile

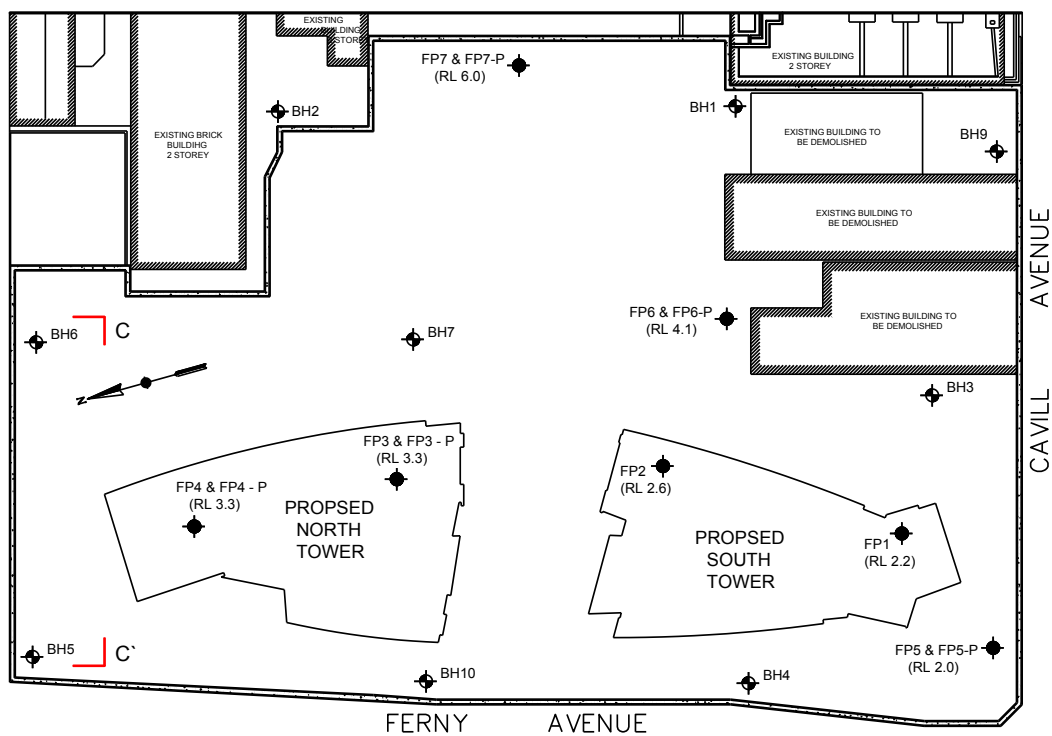


Figure 3.5a Circle on Cavill - Borehole Location Plan (APPROX-)

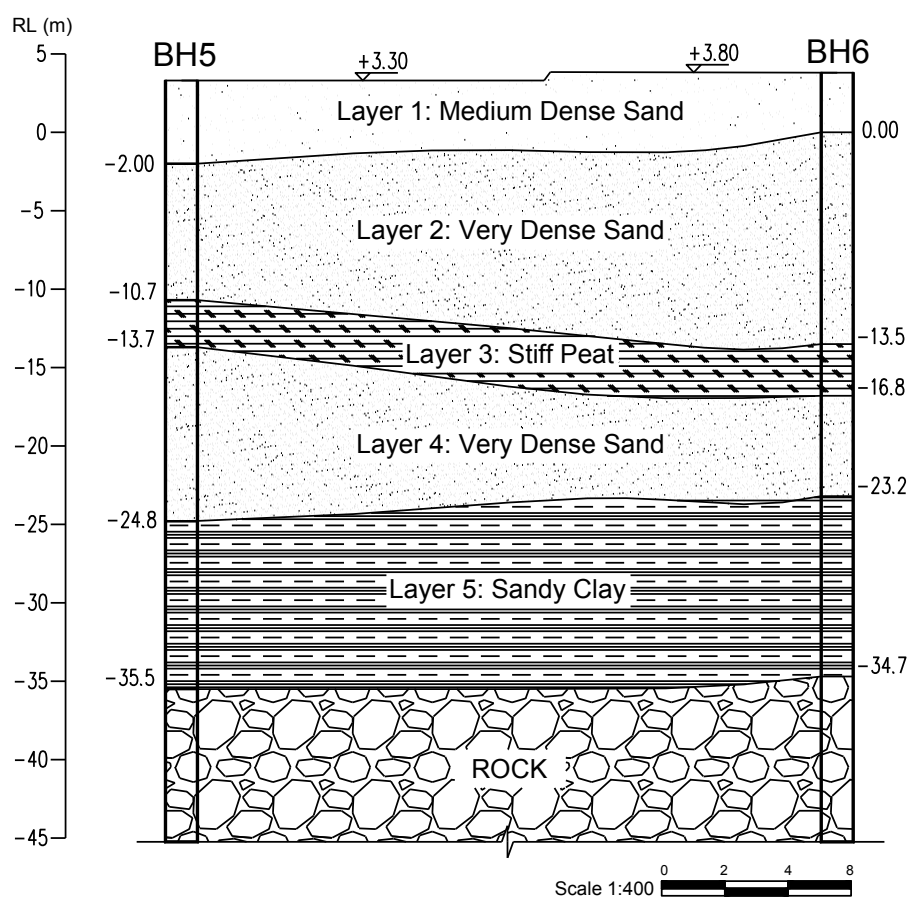


Figure 3.5b Circle on Cavill - Soil Profile along Section C-C'

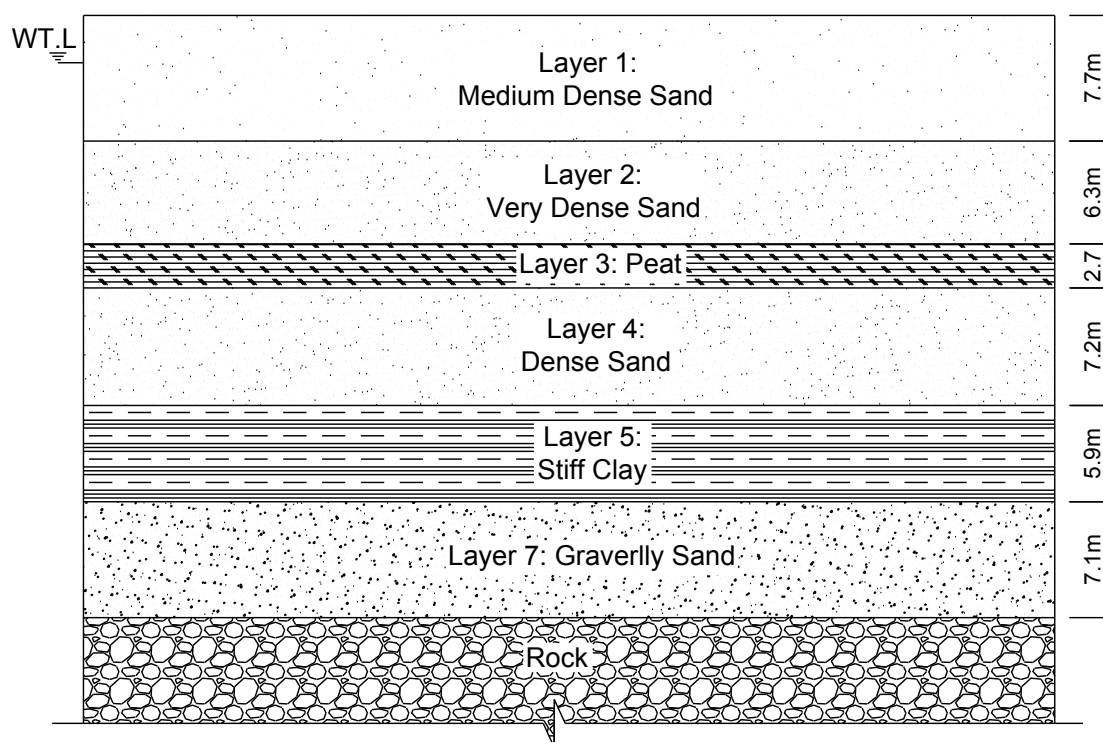


Figure 3.6 Circle on Cavill - General Site Soil Profile

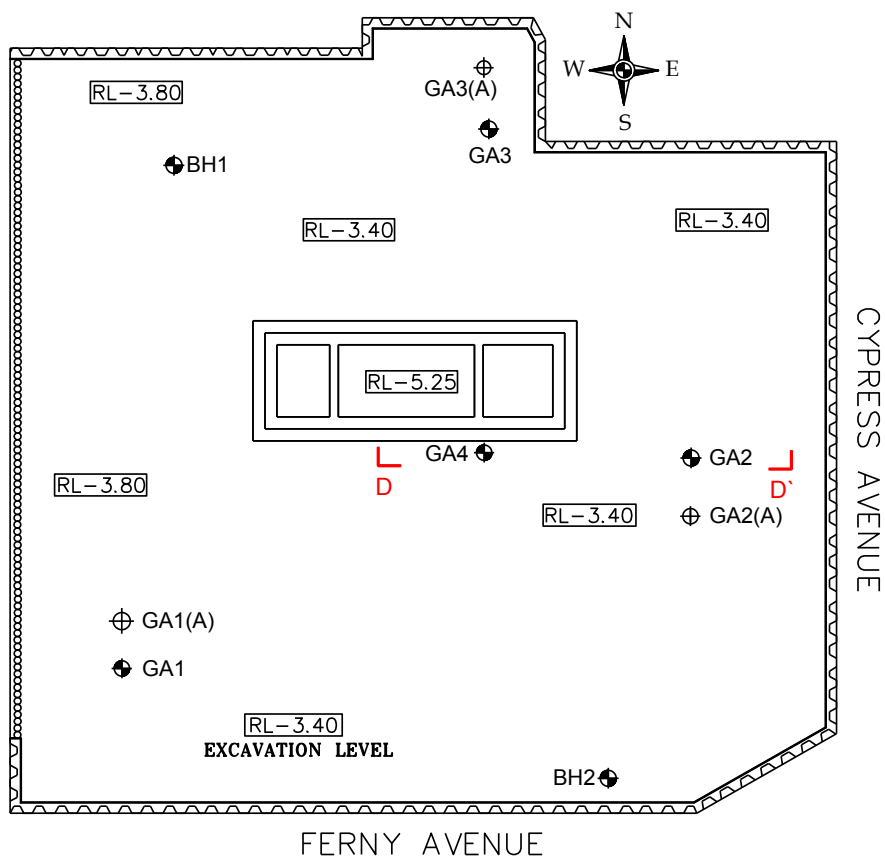


Figure 3.7a SOLAIRE - Borehole Location Plan (APPROX-)

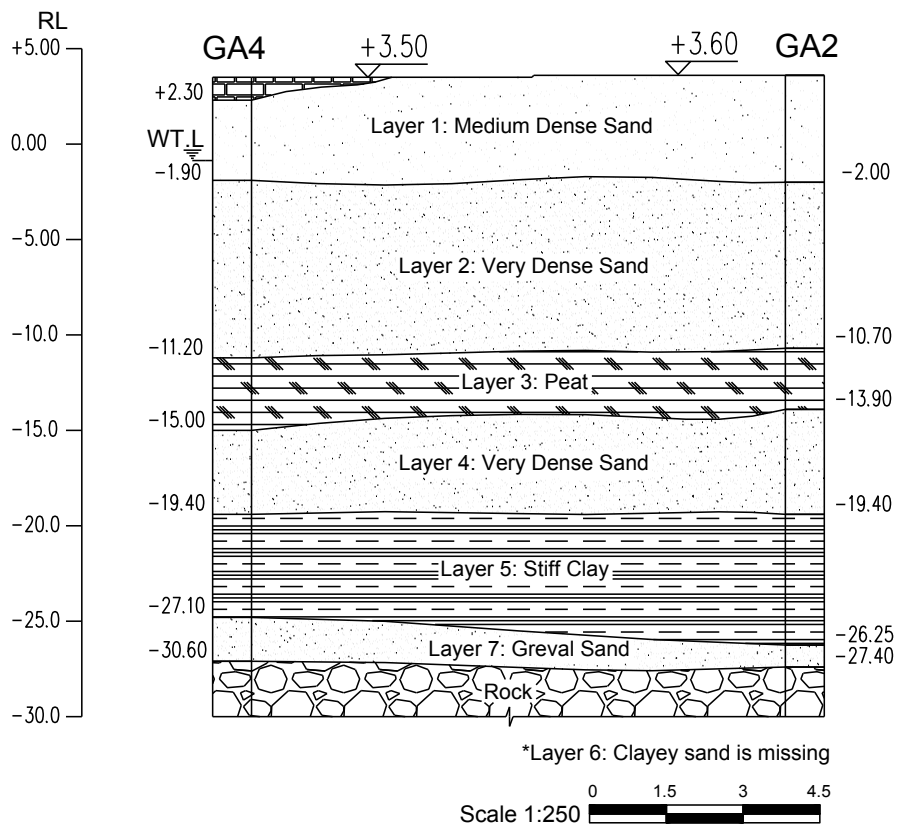


Figure 3.7b SOLAIRE - Soil Profile along Section D-D'

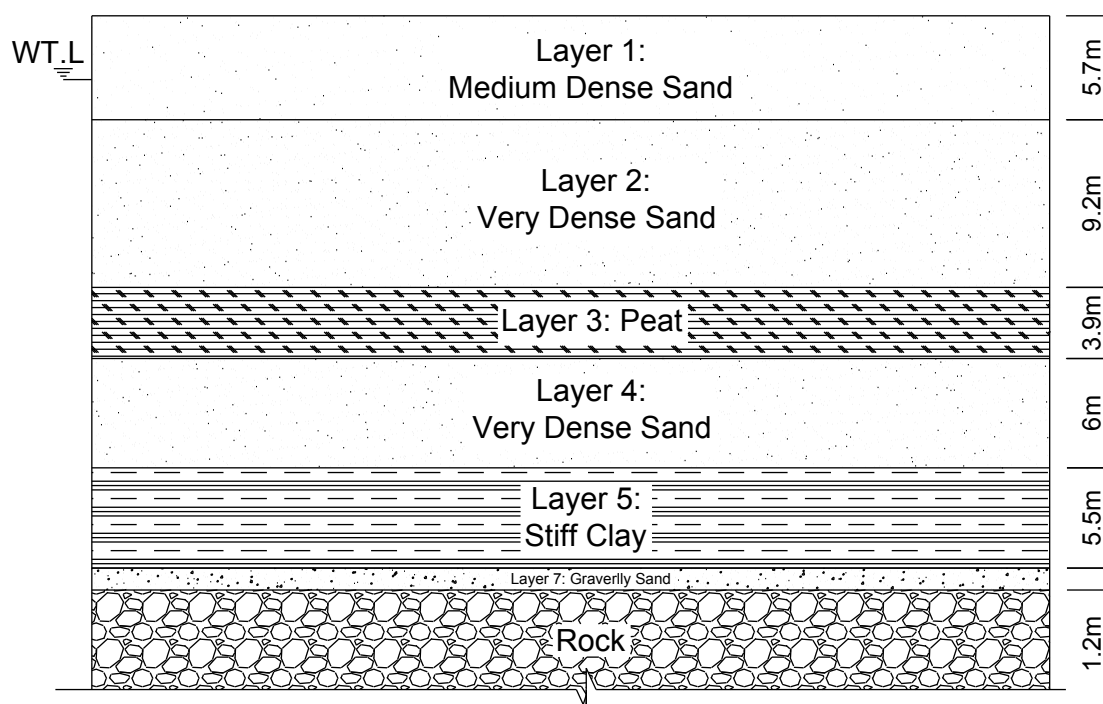


Figure 3.8 SOLAIRE – General Site Soil Profile

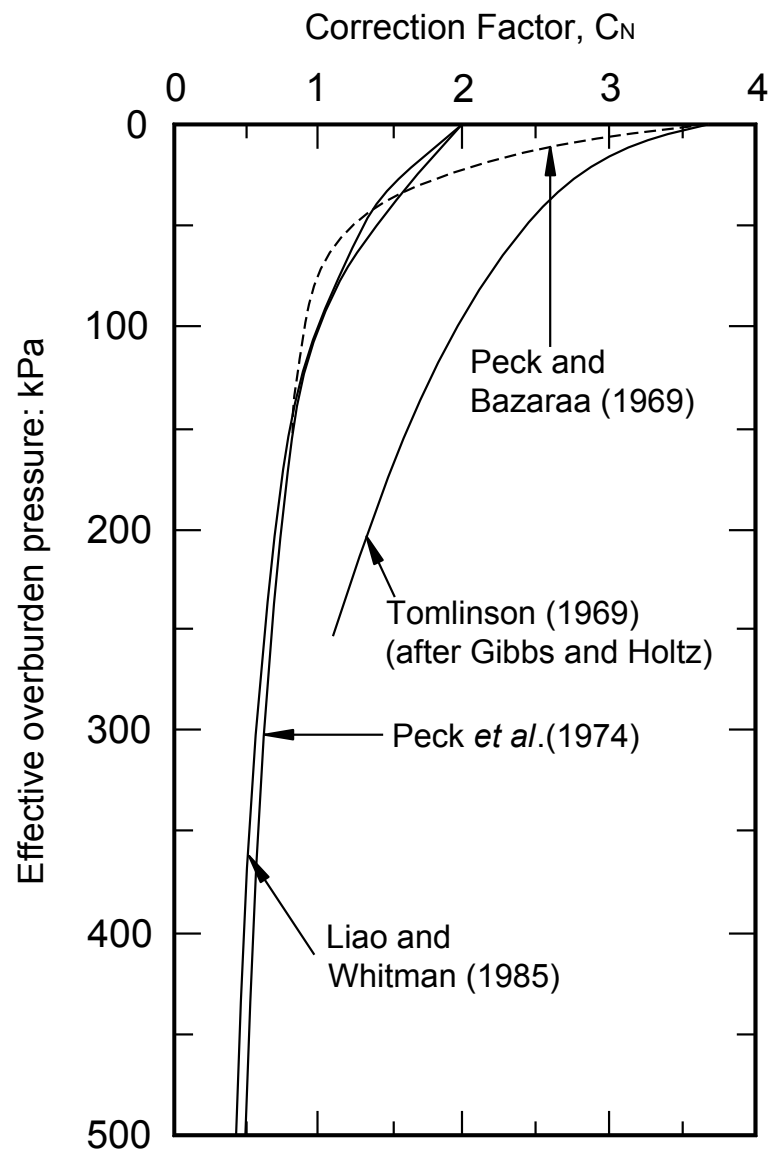
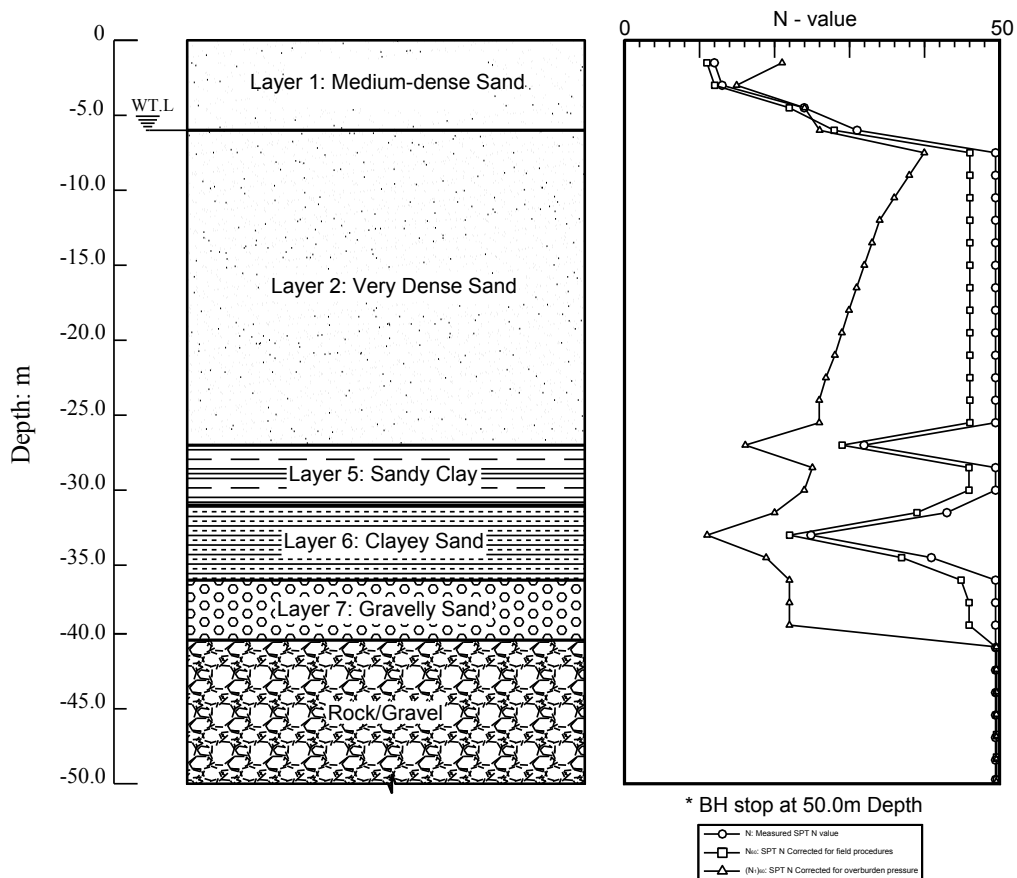
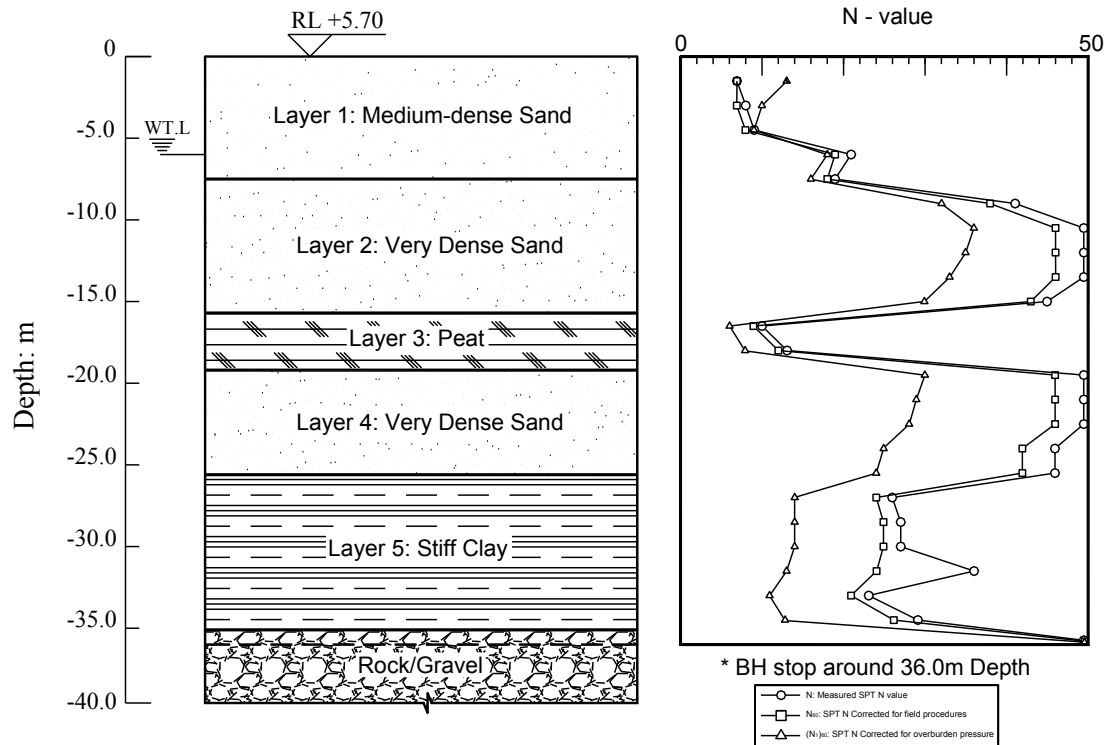


Figure 3.9 Correction Factor for influence of effective overburden pressure on SPT “N” value



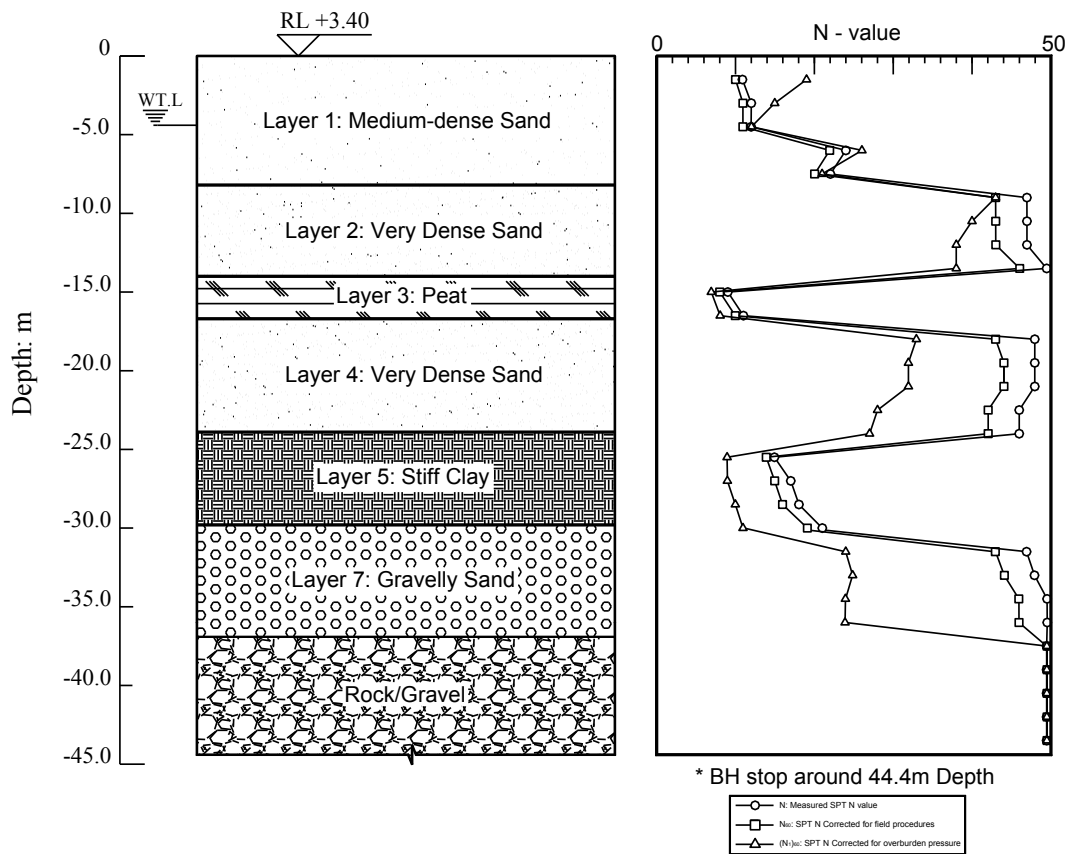


Figure 3.10 (c) Circle on Cavill: SPT N value vs. Depth

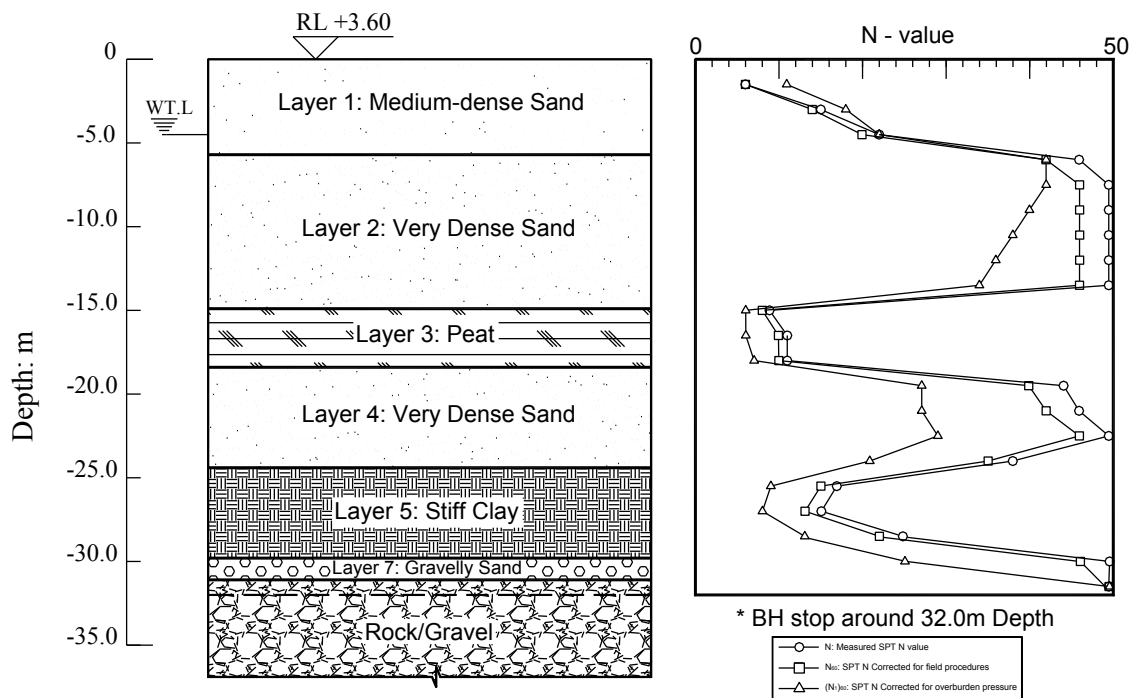


Figure 3.10 (d) SOLAIRE: SPT N value vs. Depth

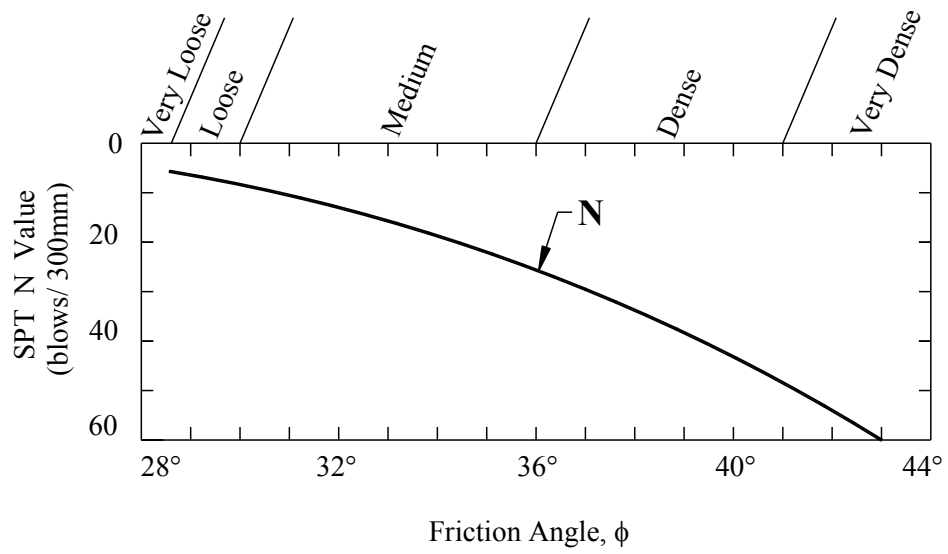


Figure 3.11 N versus ϕ (after Peck *et al*, 1974)

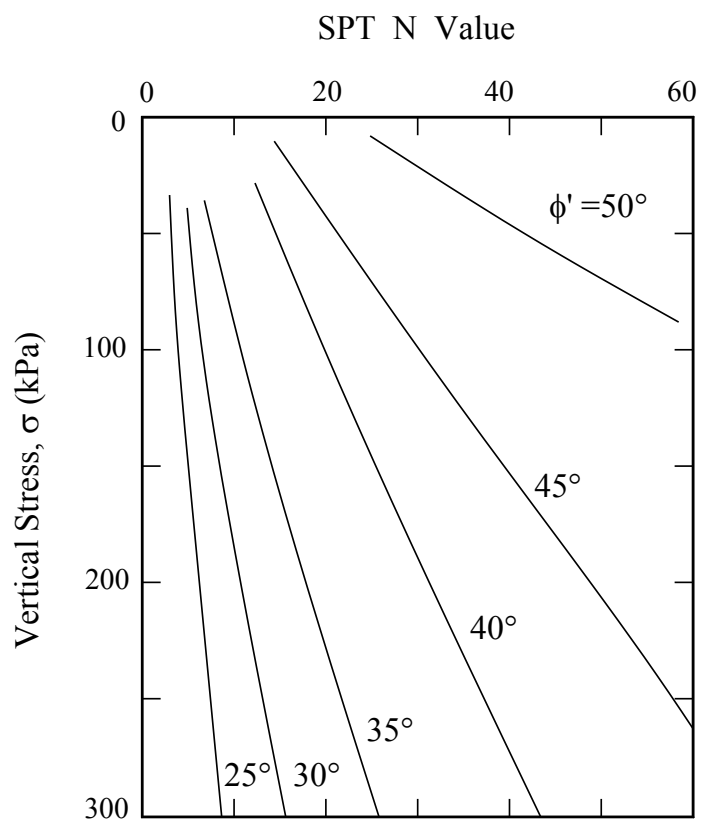


Figure 3.12 N versus ϕ' and Overburden Pressure (after Schmertmann, 1975)

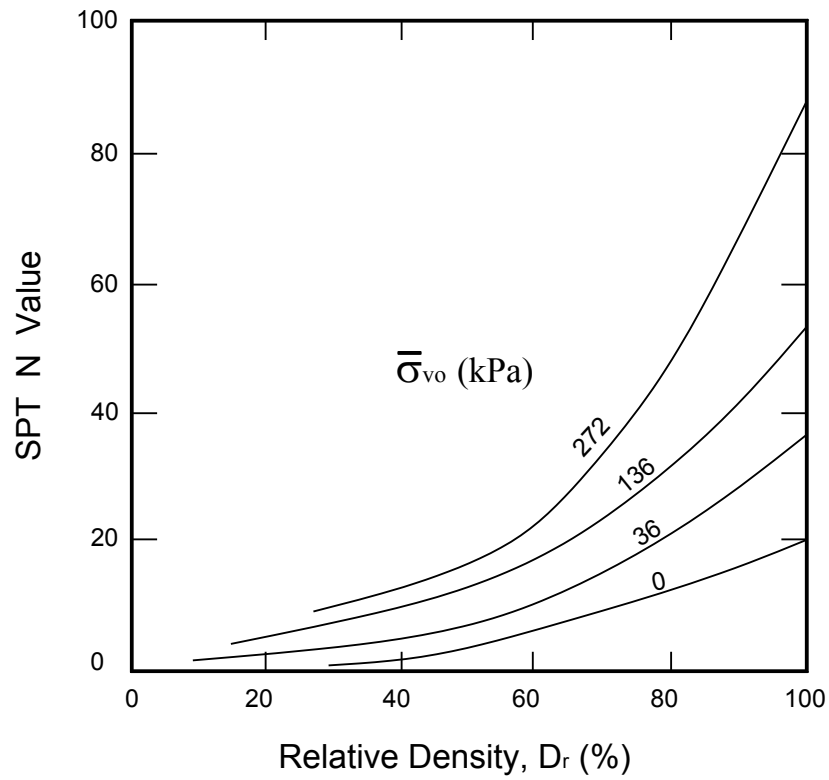


Figure 3.13 (a) Effective of overburden Stress and Relative Density, D_r on SPT N Value (after Gibbs and Holtz, 1957)

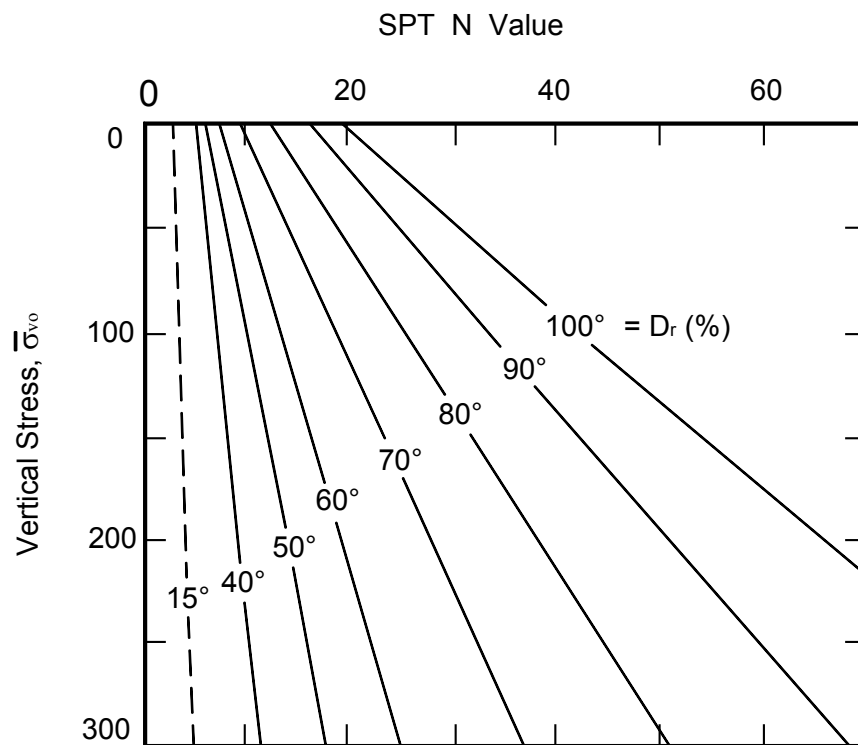


Figure 3.13 (b) Relative Density - N - Stress Relationship (after Holtz and Gibbs, 1979)

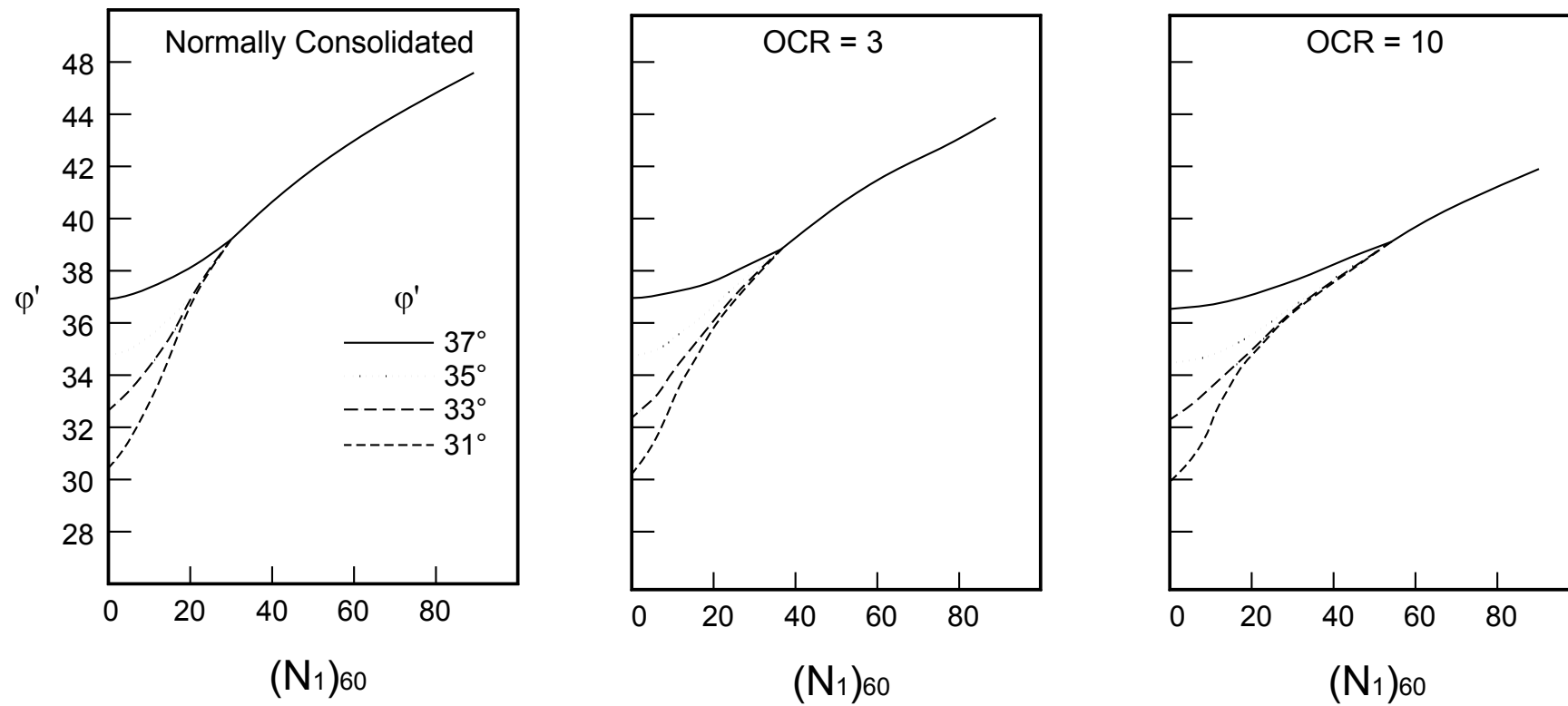


Figure 3.13 (c) Variation of ϕ' and $(N_1)_{60}$ with ϕ_{cs} and OCR (after Stroud, 1989)

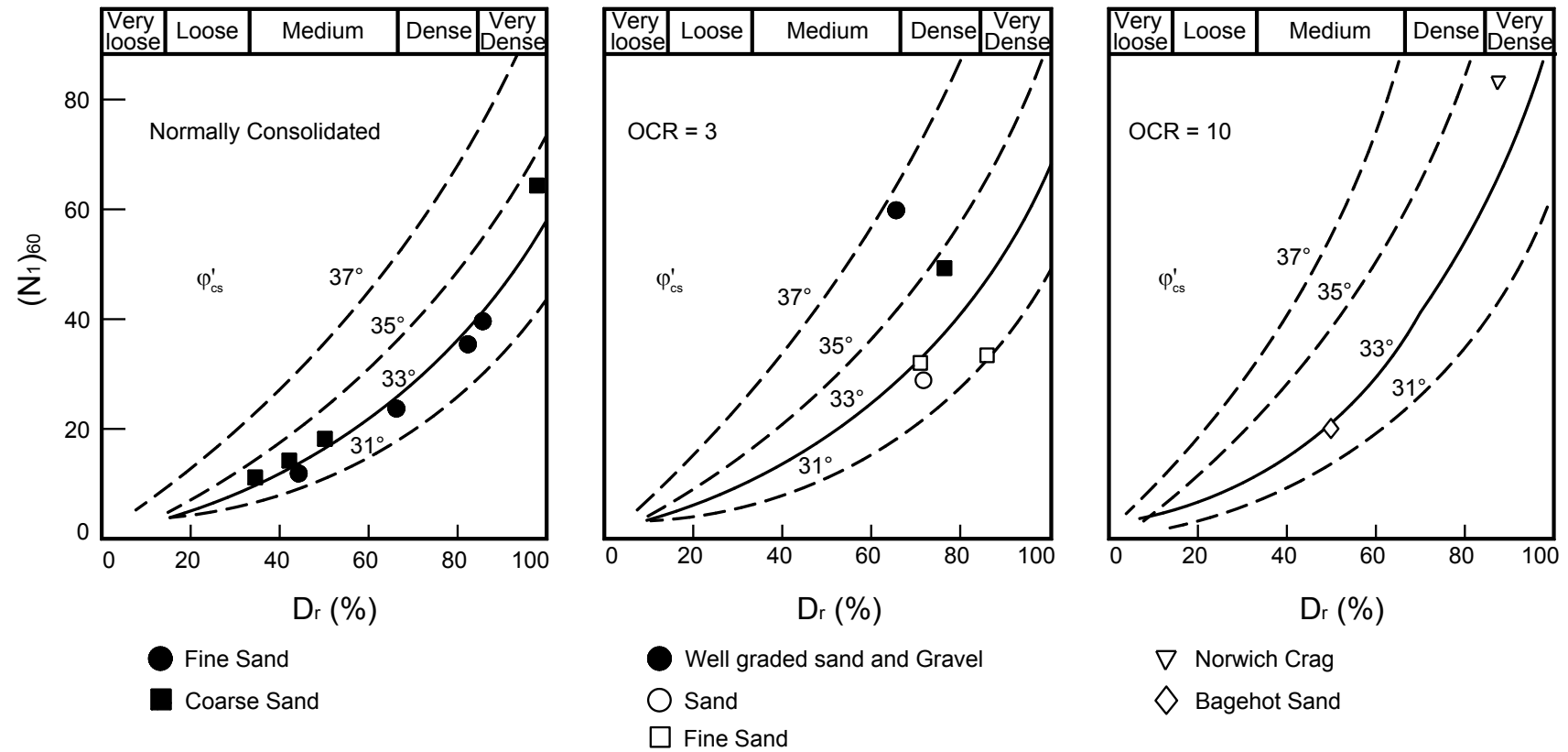


Figure 3.13 (d) Variation of ϕ' and Relative Density D_r with ϕ'_{cs} and OCR (after Stroud, 1989)

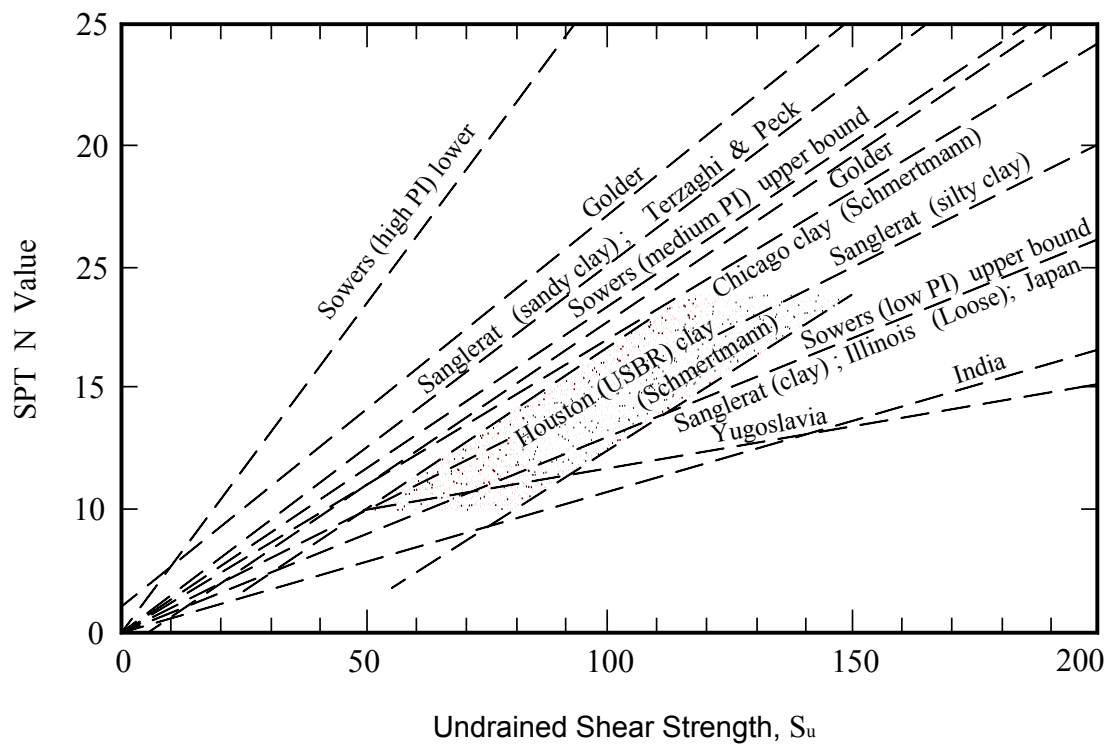


Figure 3.14 Selected Relationships between N and S_u (Djoenaidi, 1985)

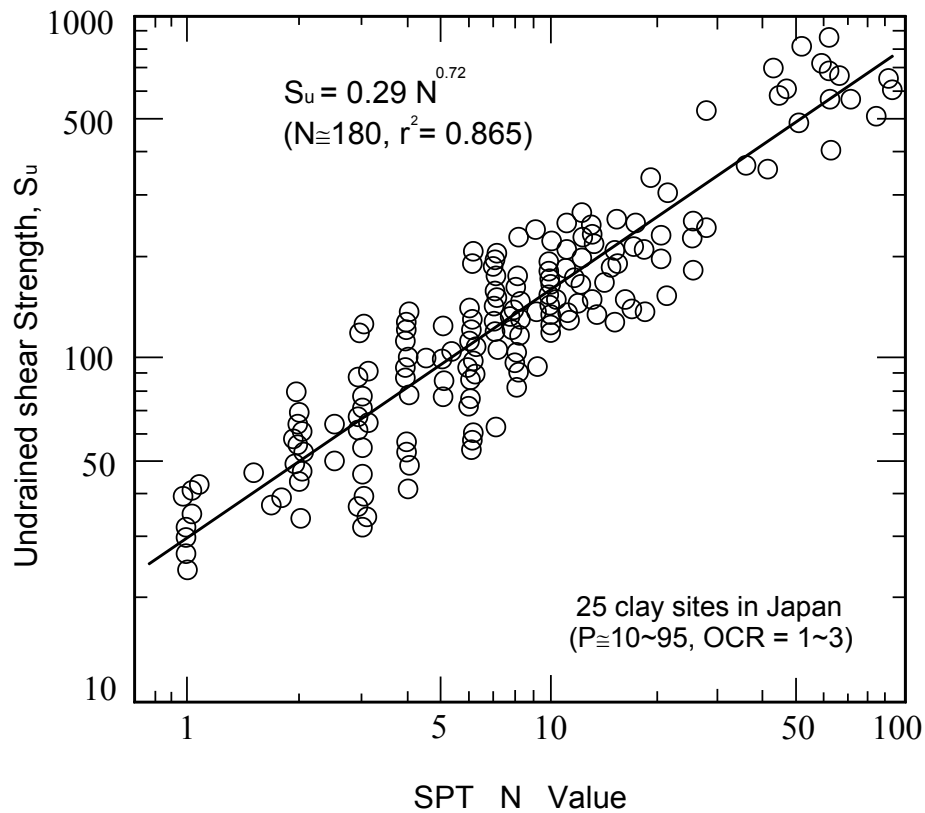


Figure 3.15 Relationships between S_u and SPT N Value (after Hara et al, 1974)

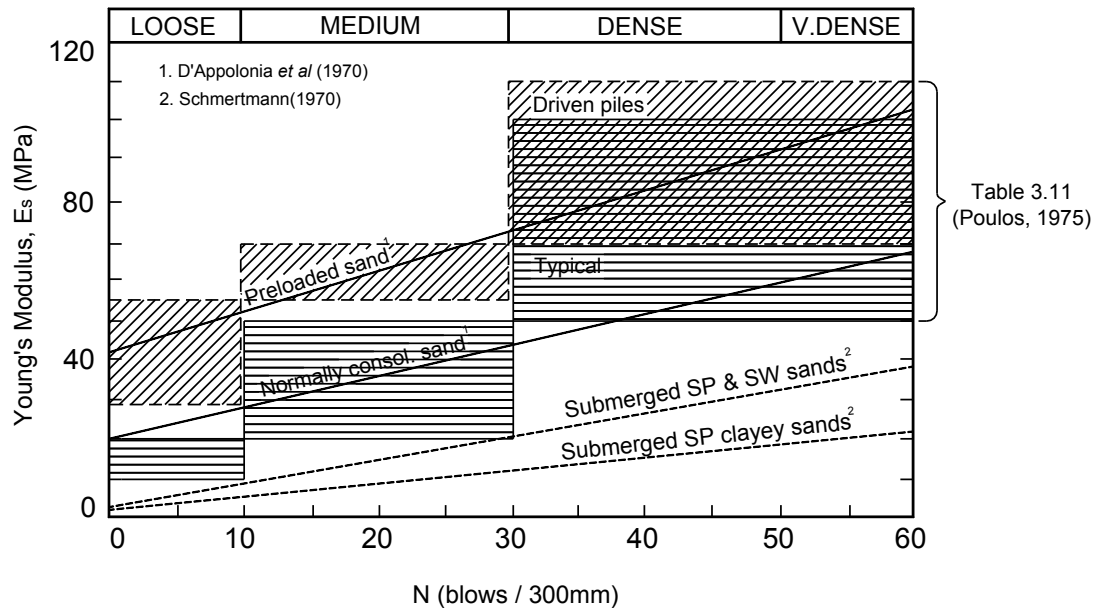


Figure 3.16 Comparative plots of Drained Modulus correlations for sand (Callanna and Kulhawy, 1985)

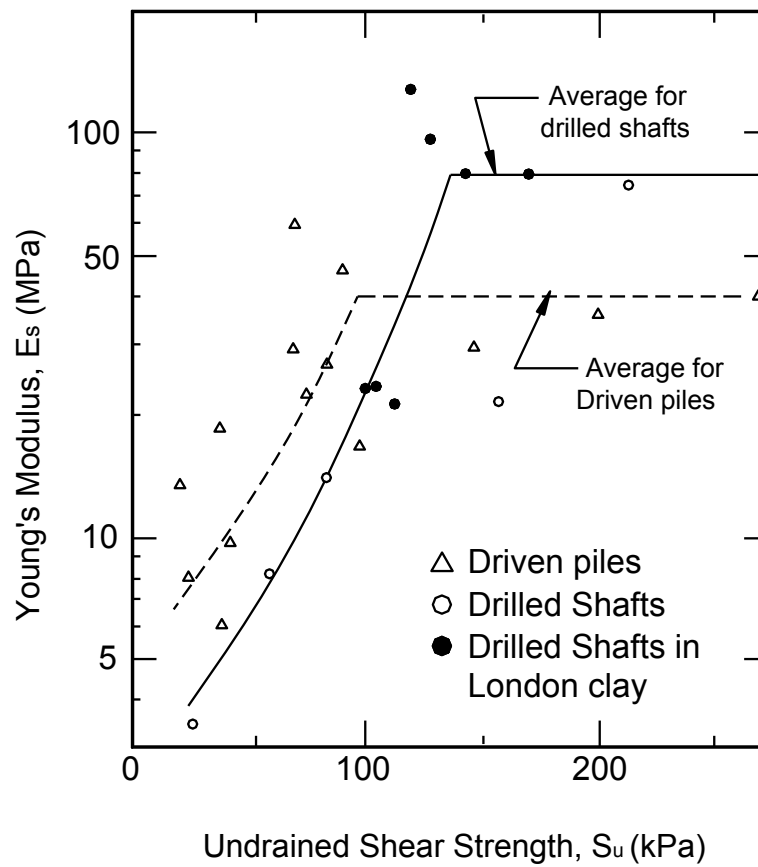


Figure 3.17 Backfigured soil modulus E_s for piles in clay (after Poulos and Davis, 1980)

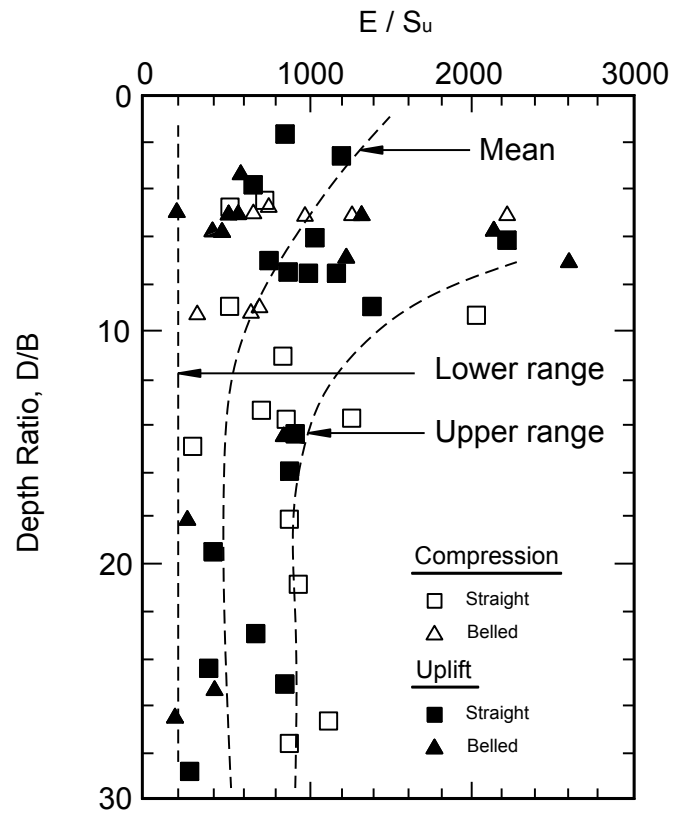
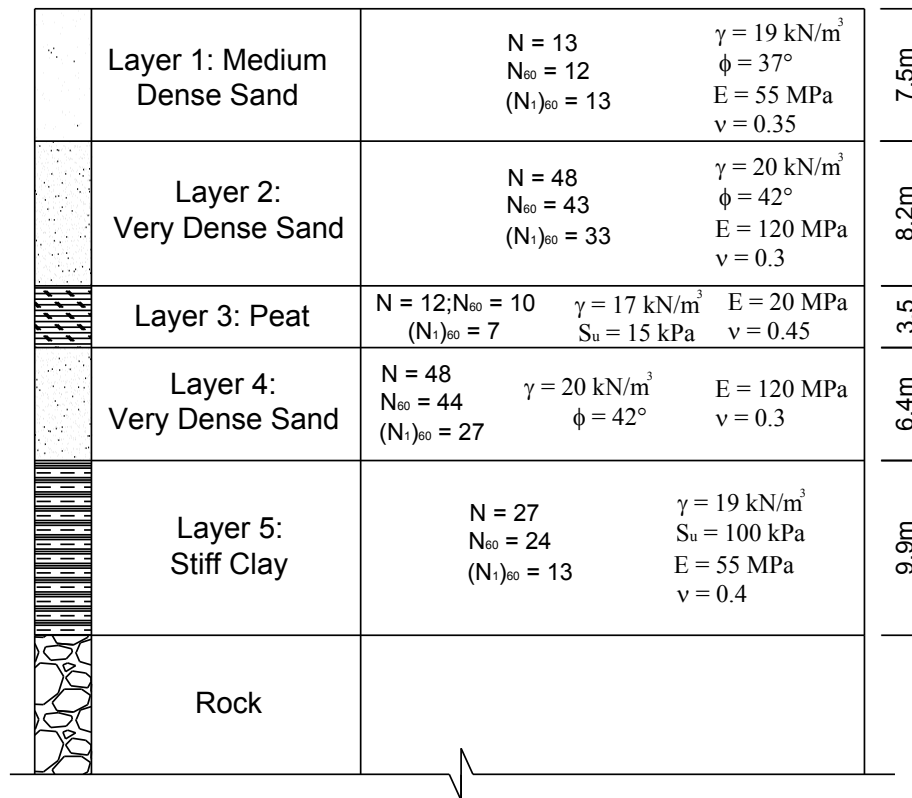
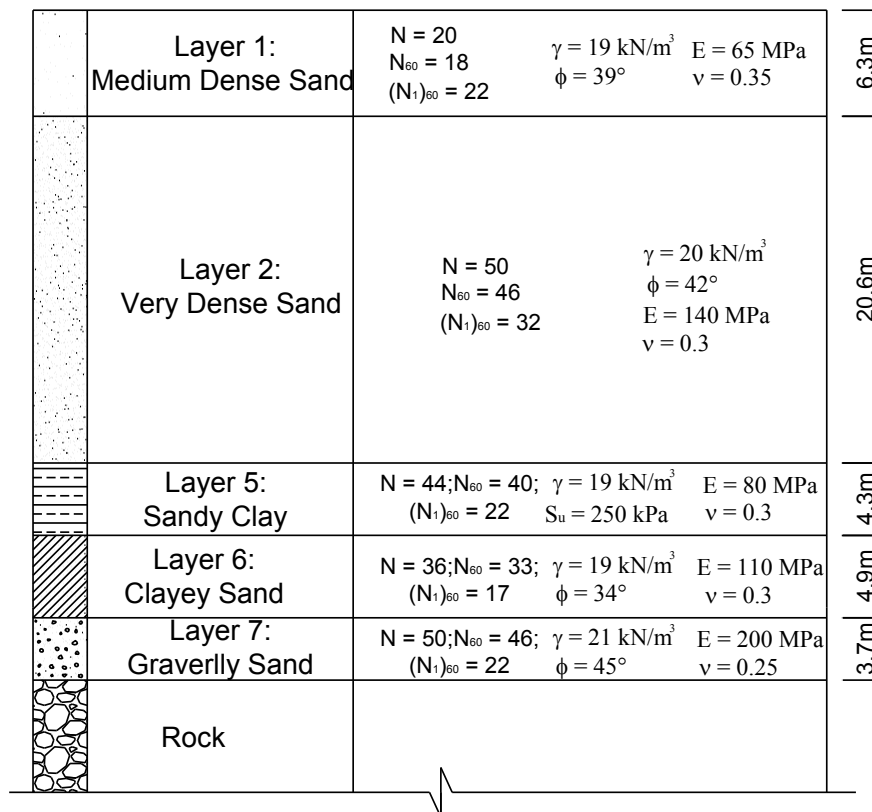


Figure 3.18 Undrained Modulus for Drilled shafts in compression and uplift (Callanand and Kulhawy, 1985)







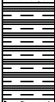
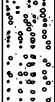

* Layer 6: Clayey Sand and Layer 7: Gravel Sand are missing in this site

Figure 3.19 (a) ARTIQUE: Summarised soil parameters for each soil layers





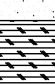

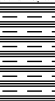


* Layer 3: Peat is missing in this site

Figure 3.19 (b) Q1 TOWER: Summarised soil properties for each soil layers

	Layer 1: Medium Dense Sand	$N = 16$ $N_{60} = 15$ $(N_1)_{60} = 19$	$\gamma = 19 \text{ kN/m}^3$ $\phi = 35^\circ$ $E = 60 \text{ MPa}$ $\nu = 0.3$	7.7m
	Layer 2: Very Dense Sand	$N = 48$ $N_{60} = 44$ $(N_1)_{60} = 40$	$\gamma = 20 \text{ kN/m}^3$ $\phi = 42^\circ$ $E = 120 \text{ MPa}$ $\nu = 0.3$	6.3m
	Layer 3: Peat	$N = 10; N_{60} = 9; (N_1)_{60} = 7$	$\gamma = 17 \text{ kN/m}^3; S_u = 60 \text{ kPa}; \nu = 0.45; E = 20 \text{ MPa}$	2.7m
	Layer 4: Very Dense Sand	$N = 47$ $N_{60} = 43$ $(N_1)_{60} = 30$	$\gamma = 20 \text{ kN/m}^3$ $\phi = 41^\circ$ $E = 120 \text{ MPa}$ $\nu = 0.3$	7.2m
	Layer 5: Stiff Clay	$N = 18$ $N_{60} = 16$ $(N_1)_{60} = 10$	$\gamma = 18 \text{ kN/m}^3$ $S_u = 80 \text{ kPa}$ $E = 20 \text{ MPa}$ $\nu = 0.45$	5.9m
	Layer 7: Gravelly Sand	$N = 49$ $N_{60} = 44$ $(N_1)_{60} = 24$	$\gamma = 21 \text{ kN/m}^3$ $\phi = 45^\circ$ $E = 200 \text{ MPa}$ $\nu = 0.25$	7.1m
	Rock			

* Layer 6: Clayey Sand is missing in this site

Figure 3.19(c) Circle on Cavill: Summarised soil properties for each soil layers

	Layer 1: Medium Dense Sand	$N = 14$ $N_{60} = 13$ $(N_1)_{60} = 17$	$\gamma = 19 \text{ kN/m}^3$ $\phi = 37^\circ$ $E = 60 \text{ MPa}$ $\nu = 0.35$	5.7m
	Layer 2: Very Dense Sand	$N = 49$ $N_{60} = 45$ $(N_1)_{60} = 39$	$\gamma = 19 \text{ kN/m}^3$ $\phi = 42^\circ$ $E = 140 \text{ MPa}$ $\nu = 0.3$	9.2m
	Layer 3: Peat	$N = 10; N_{60} = 9;$ $(N_1)_{60} = 7$	$\gamma = 17 \text{ kN/m}^3$ $E = 25 \text{ MPa}$ $S_u = 55 \text{ kPa}$ $\nu = 0.4$	3.9m
	Layer 4: Dense Sand	$N = 44$ $N_{60} = 40$ $(N_1)_{60} = 26$	$\gamma = 20 \text{ kN/m}^3$ $\phi = 41^\circ$ $E = 120 \text{ MPa}$ $\nu = 0.3$	6m
	Layer 5: Stiff Clay	$N = 23$ $N_{60} = 21$ $(N_1)_{60} = 12$	$\gamma = 19 \text{ kN/m}$ $S_u = 100 \text{ kPa}$ $\nu = 0.35$ $E = 55 \text{ MPa}$	5.5m
	Layer 7: Gravelly Sand	$N = 50; N_{60} = 46; (N_1)_{60} = 25$	$\gamma = 21 \text{ kN/m}^3; \phi = 45^\circ; \nu = 0.25; E = 200 \text{ MPa}$	
	Rock			1.2m

* Layer 6: Clayey Sand is missing in this site

Figure 3.19(d) SOLAIRE: Summarised soil properties for each soil layers

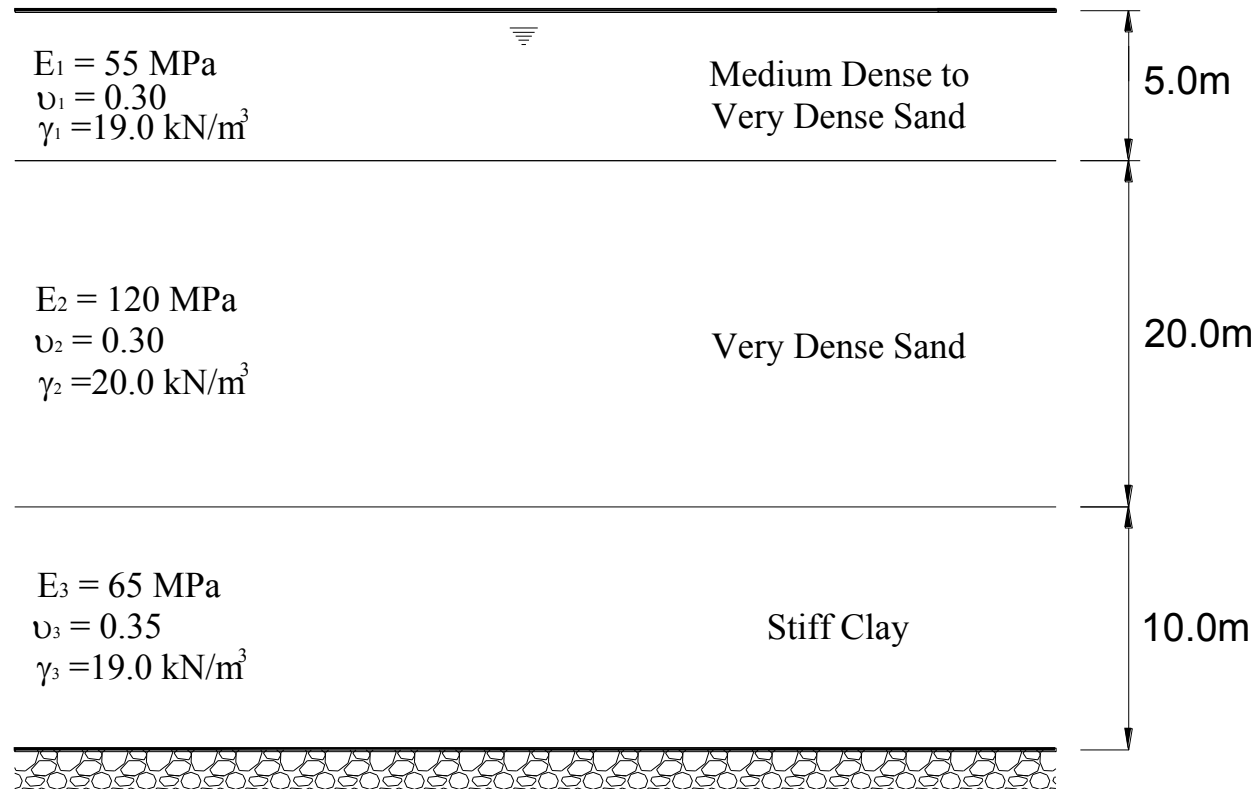
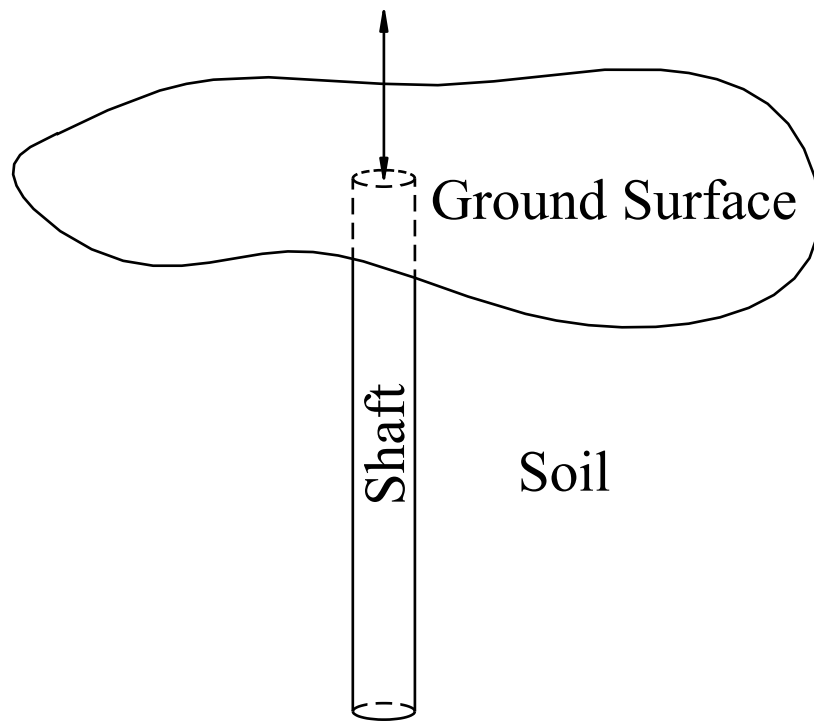
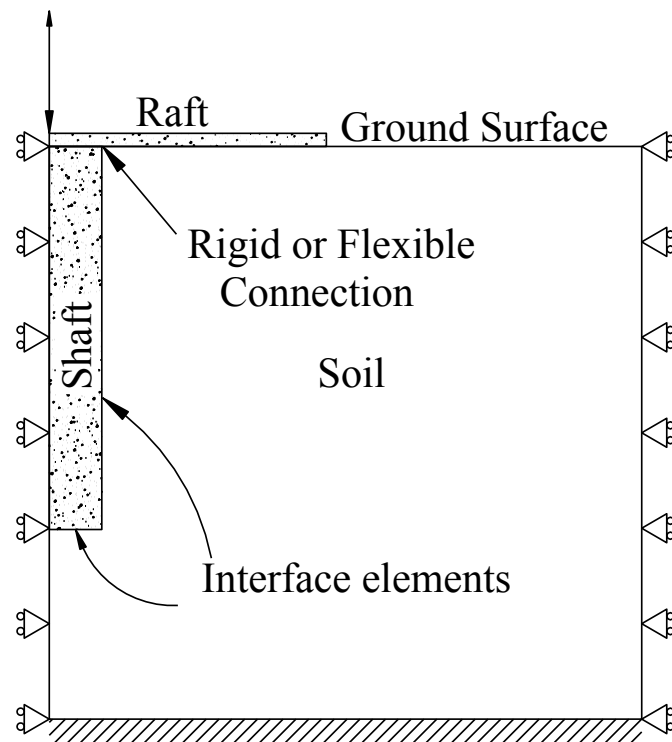


Figure 3.20 Generalised Soil Profile Adopted for Analysis



a. Basic Problem



b. Symmetric Generalisation

Figure 4.1 Finite Element Idealisation of the Pile Raft Element

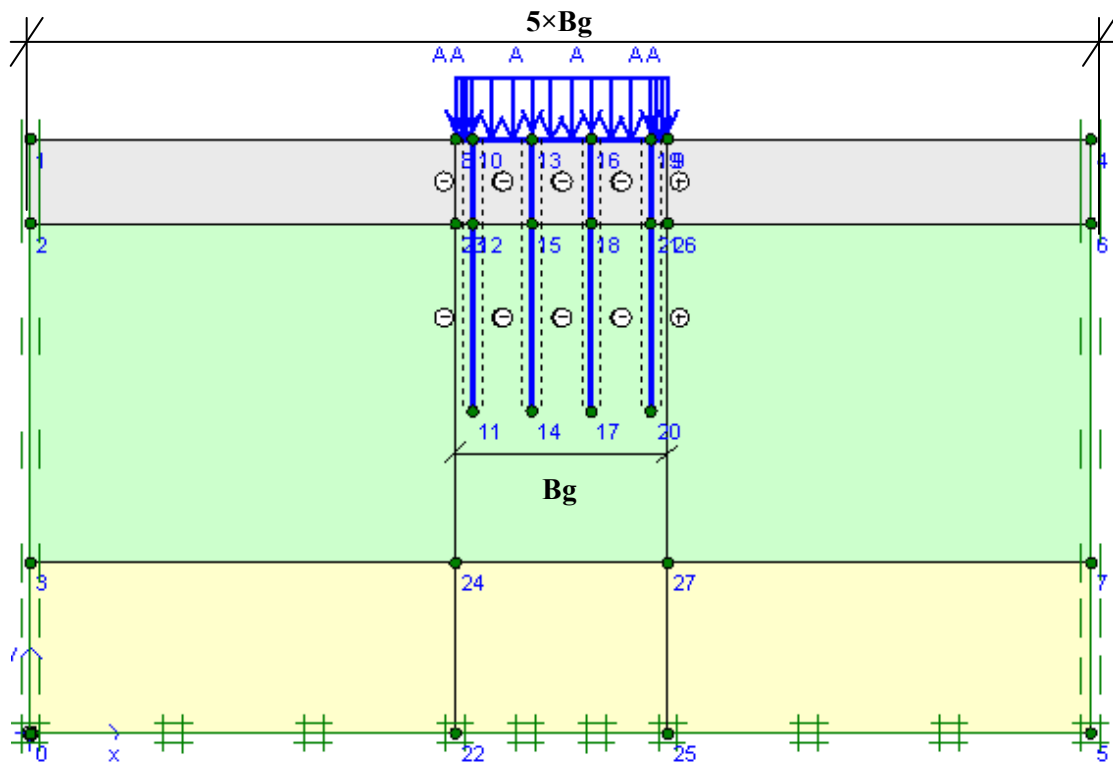


Figure 4.2 Diagrammatic View of Boundary Condition Using for Modelling

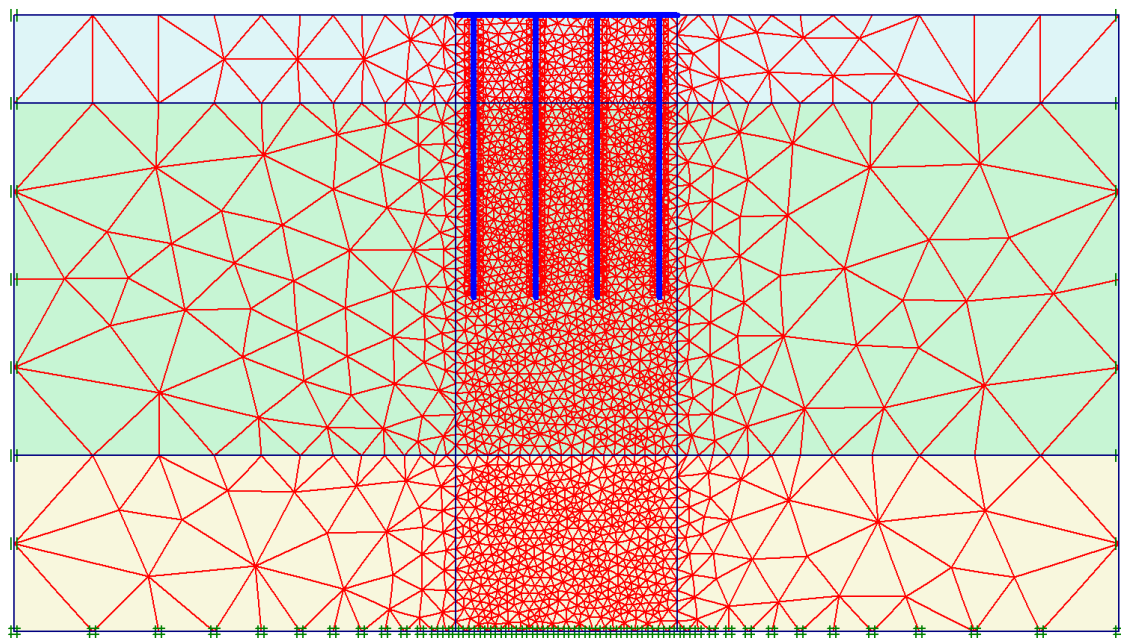


Figure 4.3 Schematic View of the Finite Element Mesh

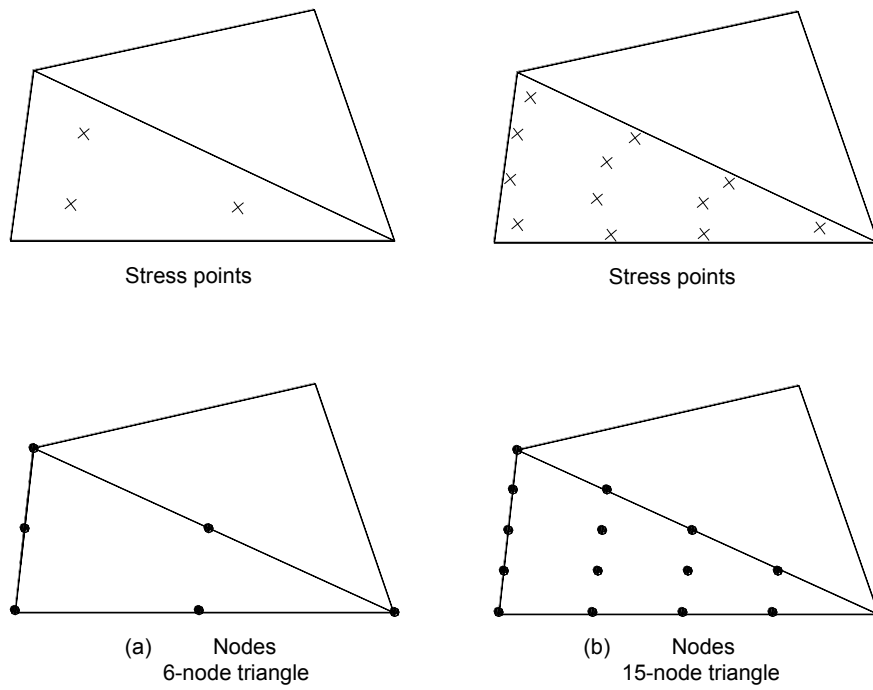


Figure 4.4 Position of Nodes and Stress Points in Soil Elements

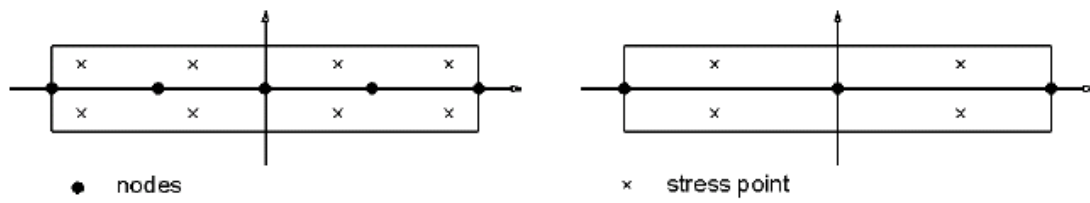


Figure 4.5 Position of Nodes and Stress Points in a 3-node and a 5-node Beam Element

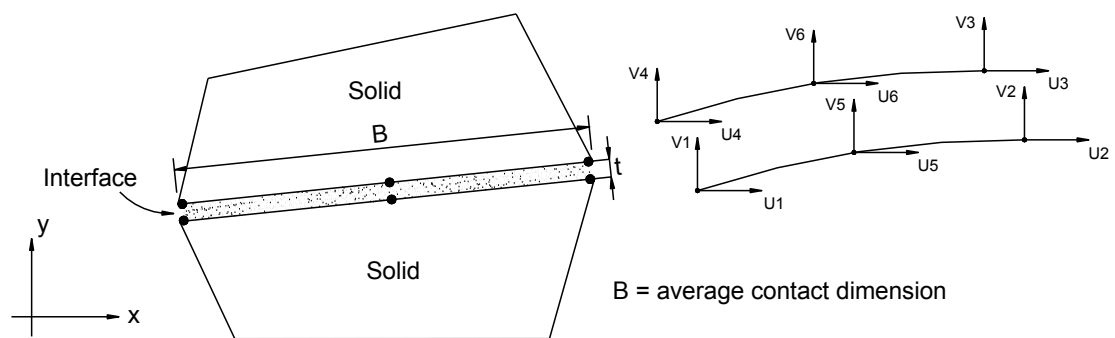


Figure 4.6 Thin Layer Interface Element

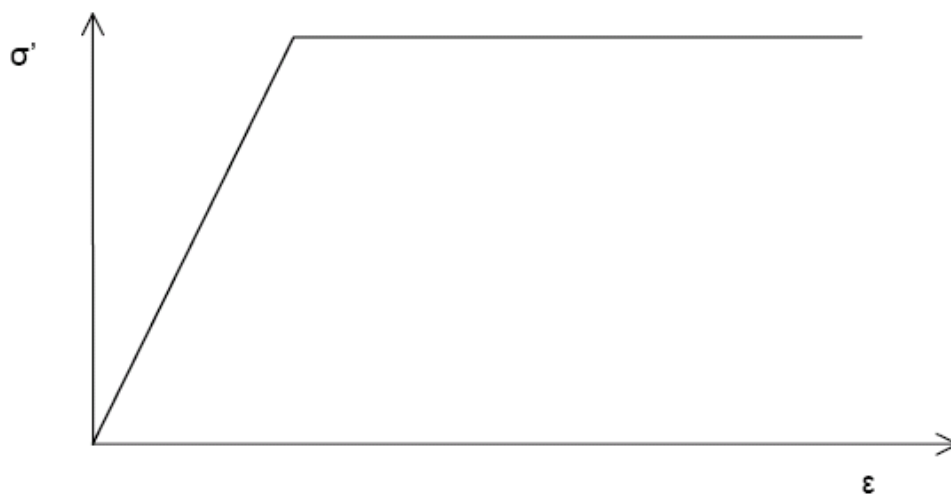


Figure 4.7 Basic Idea of an Elastic Perfectly Plastic Model

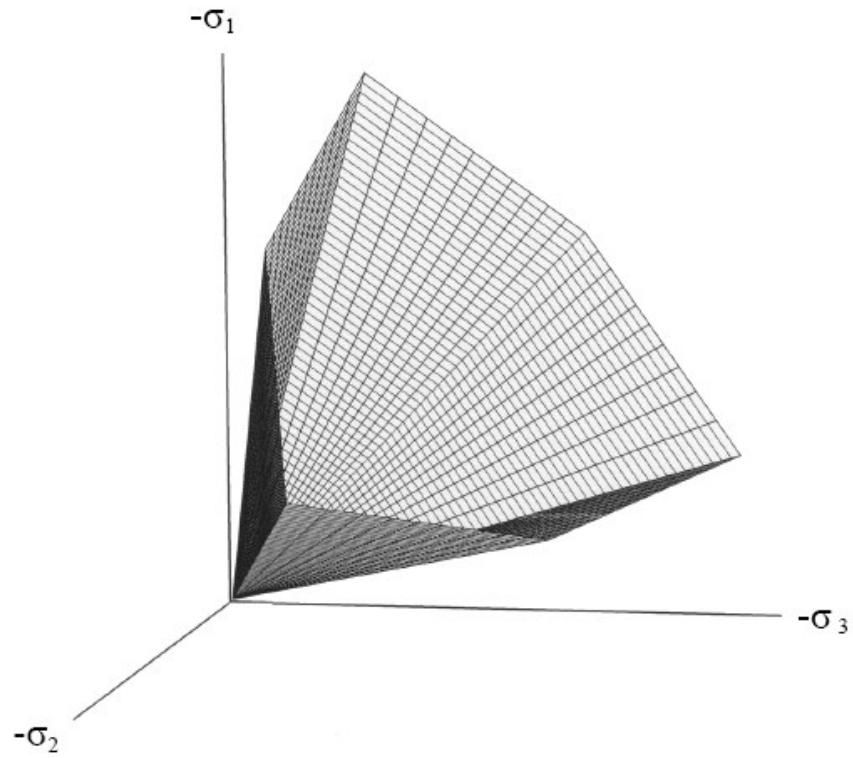


Figure 4.8 Mohr-Coulomb Yield Surface in Principal Stress Space ($c = 0$)

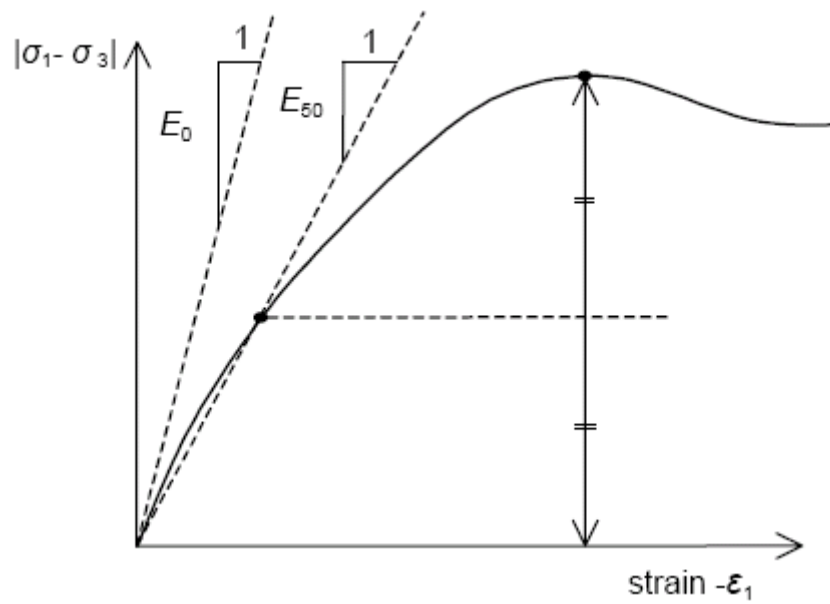
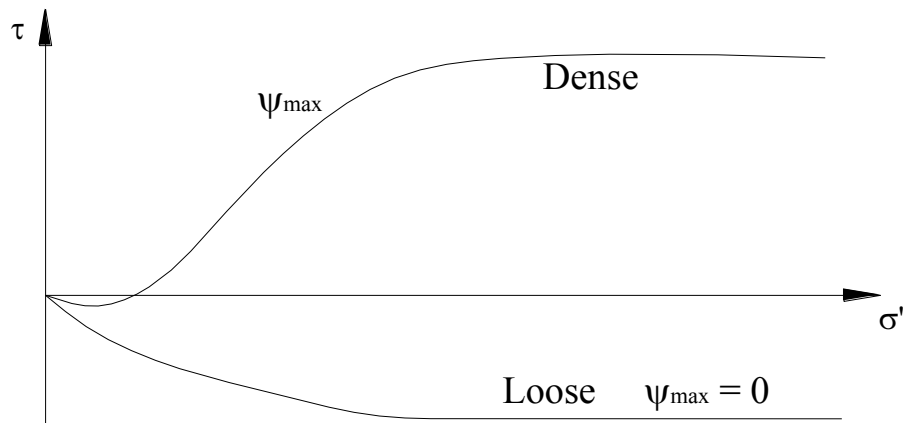
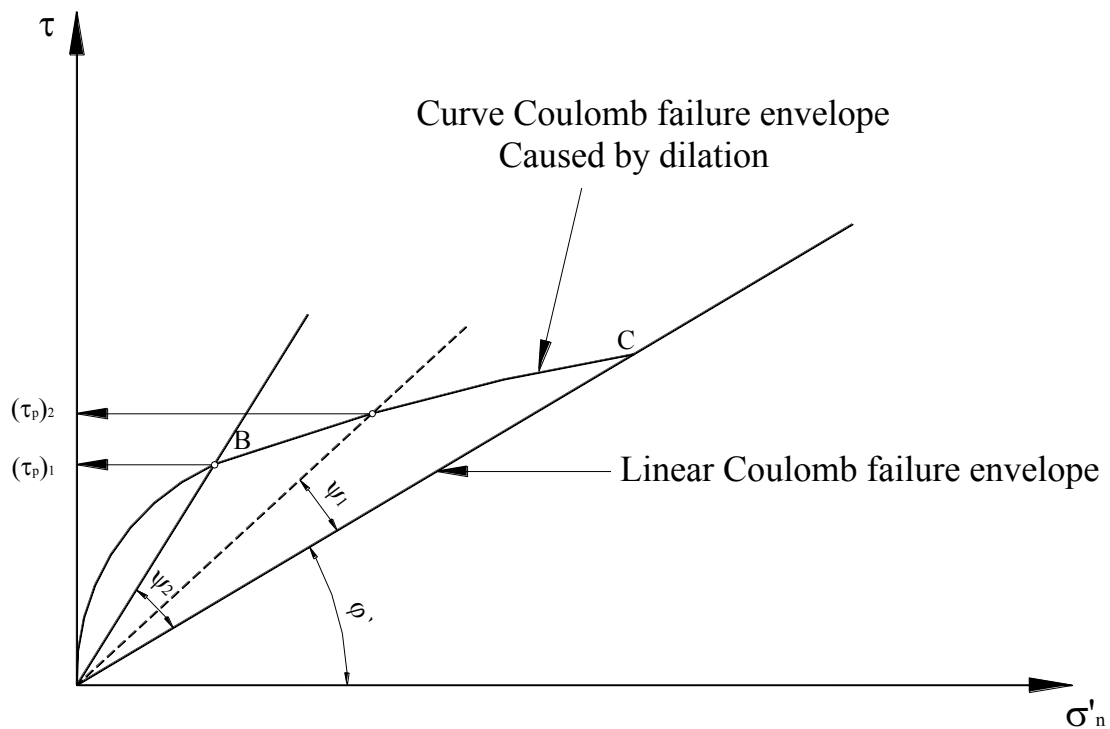


Figure 4.9 Definition of E_0 and E_{50} for Standard Drained Triaxial Test Results



(a) Dilation Angle



(b) Dilation and contraction during a direct shear test

Figure 4.10 Illustration of Dilatancy Angle

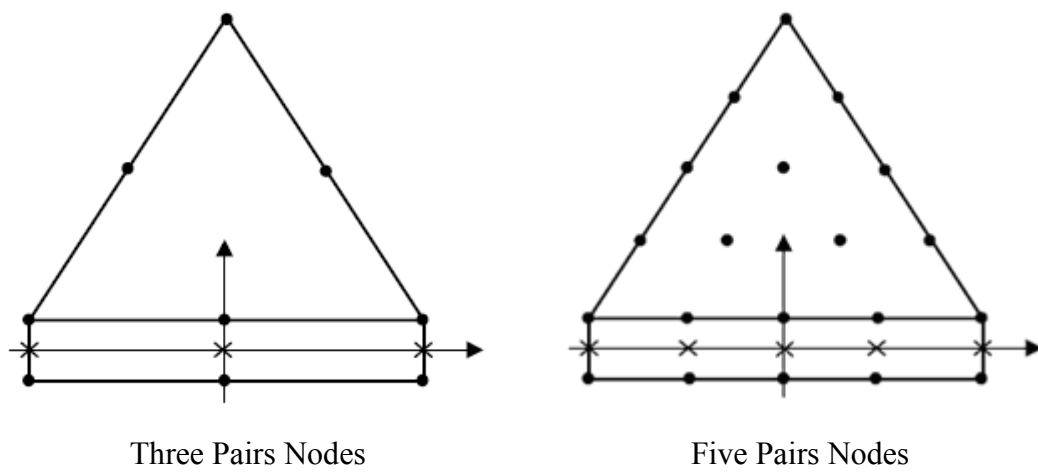


Figure 4.11 Distribution of Nodes and Stress Point in Interface Elements and Their Connection to Soil Elements

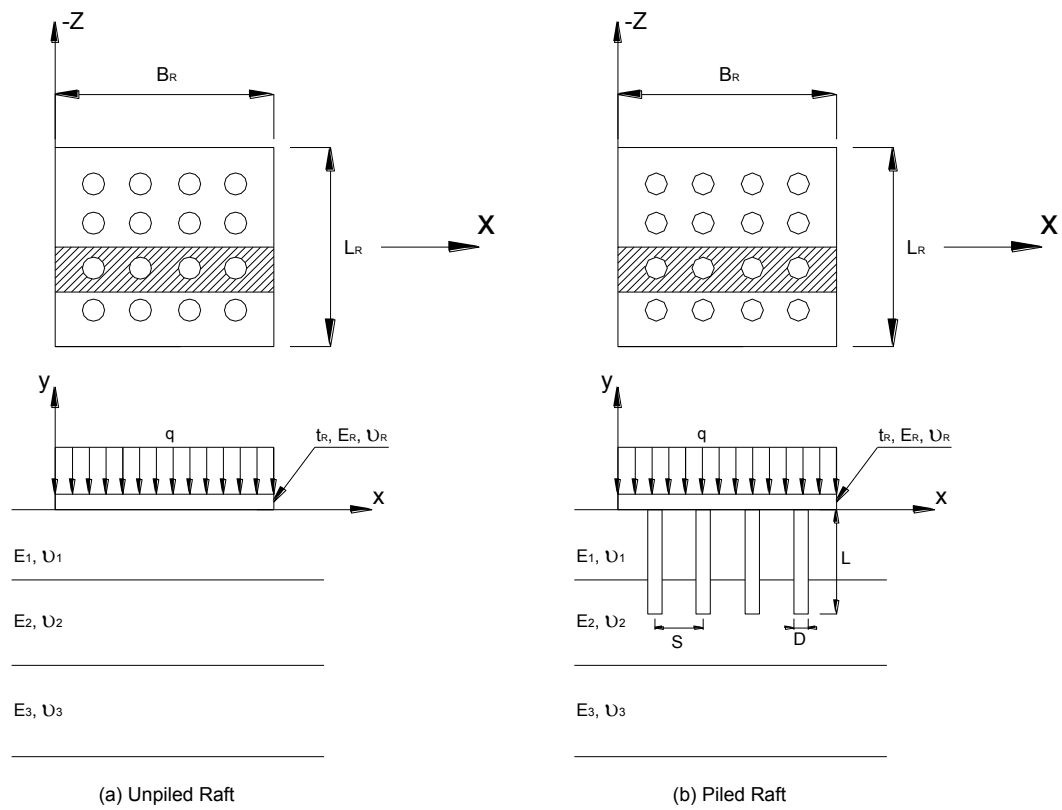


Figure 5.1 Typical Raft and Piled Raft Configurations for Analysis

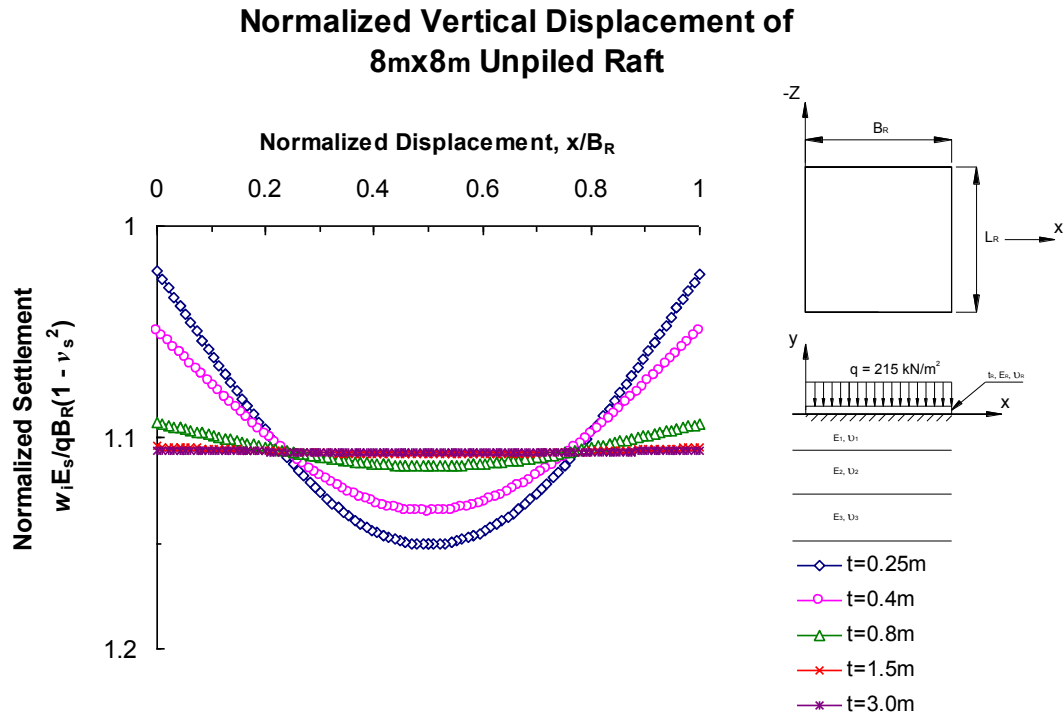


Figure 5.2(a) Normalised Vertical Displacement of 8m×8m Square Unpiled Raft

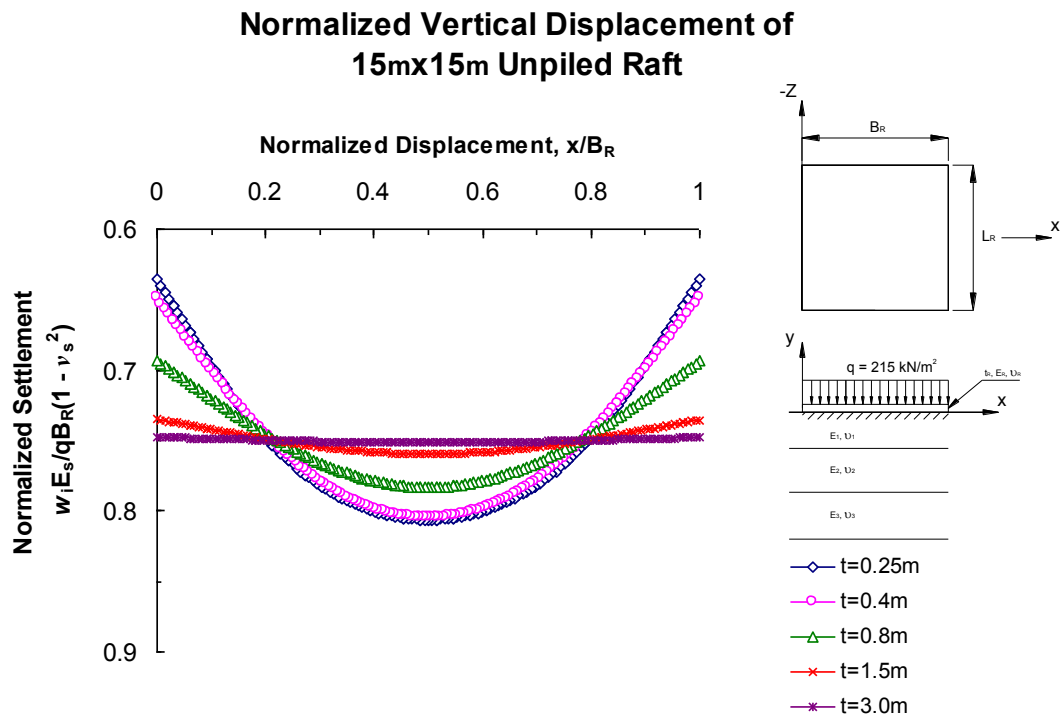


Figure 5.2 (b) Normalised Vertical Displacement of 15m×15m Square Unpiled Raft

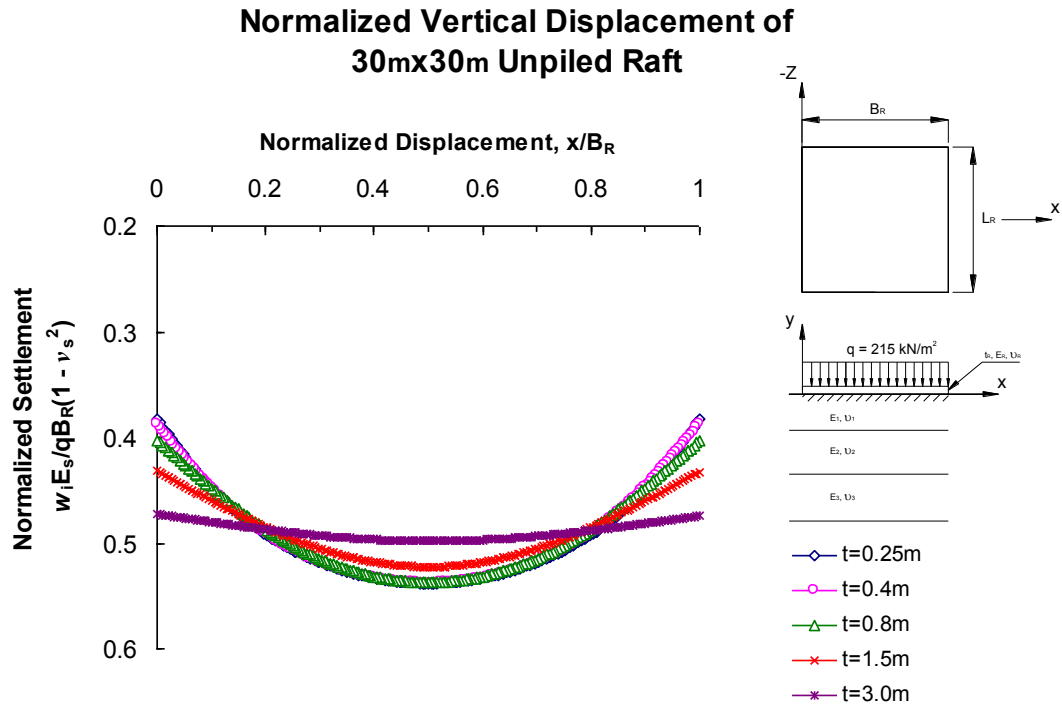


Figure 5.2 (c) Normalised Vertical Displacement of 30m×30m Square Unpiled Raft

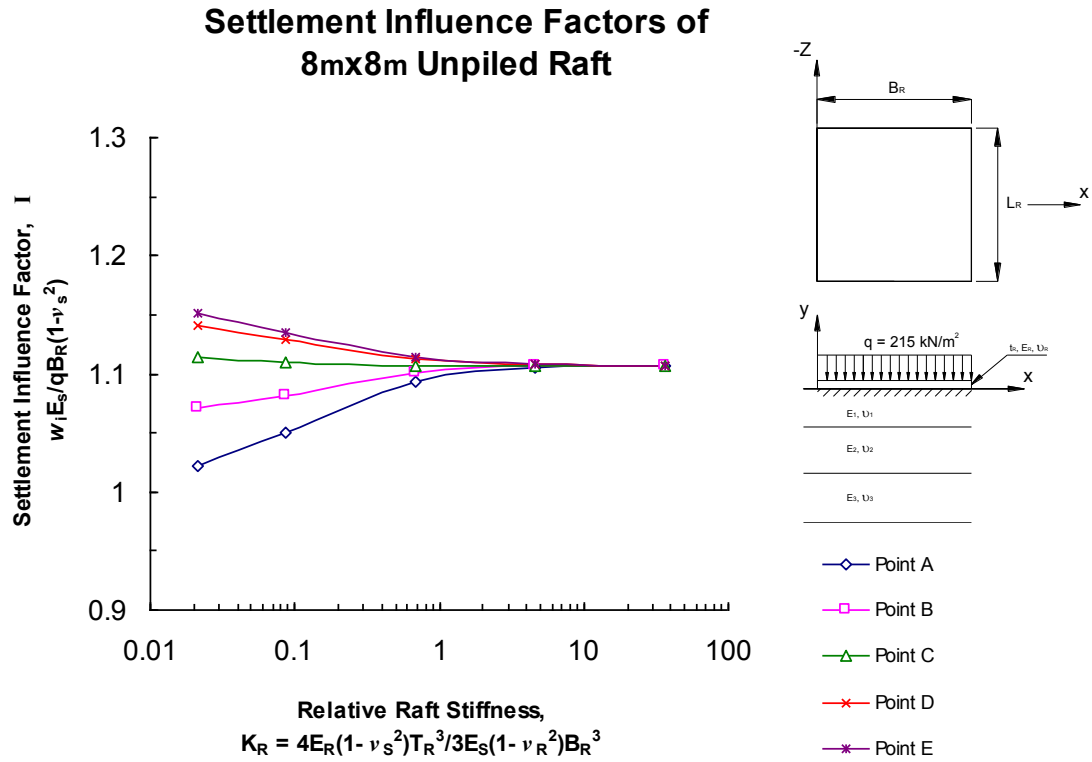


Figure 5.3 (a) Settlement Influence Factors of 8m×8m Square Unpiled Raft

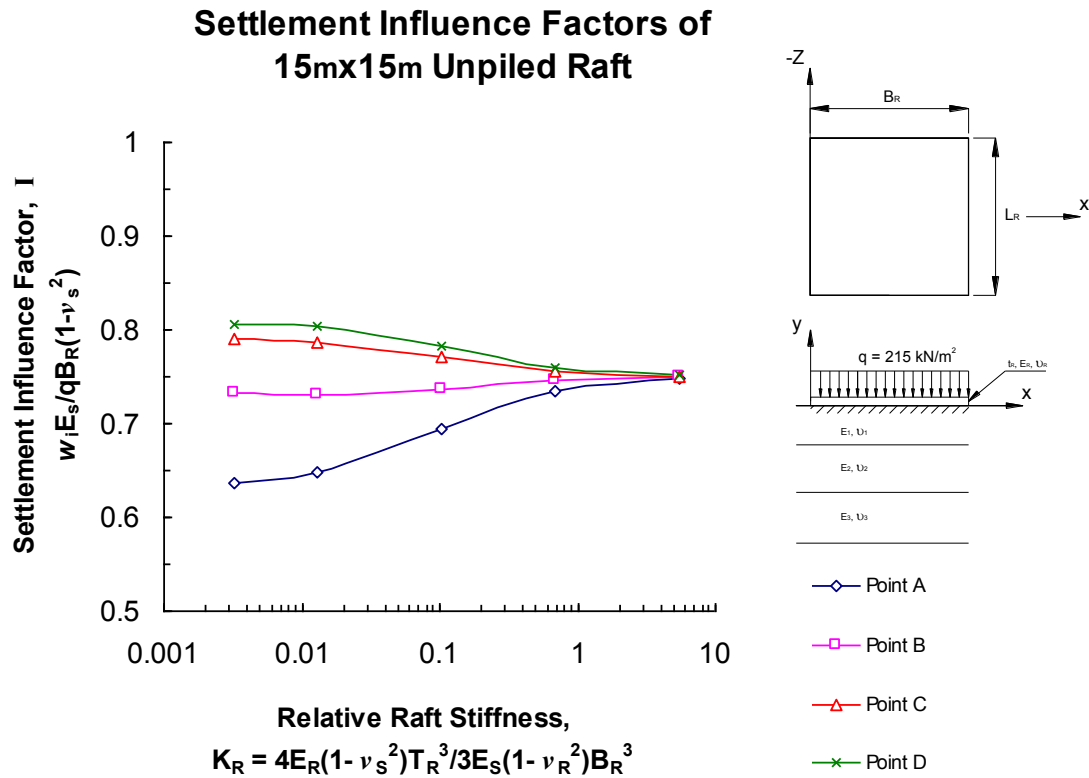


Figure 5.3 (b) Settlement Influence Factors of 15m×15m Square Unpiled Raft

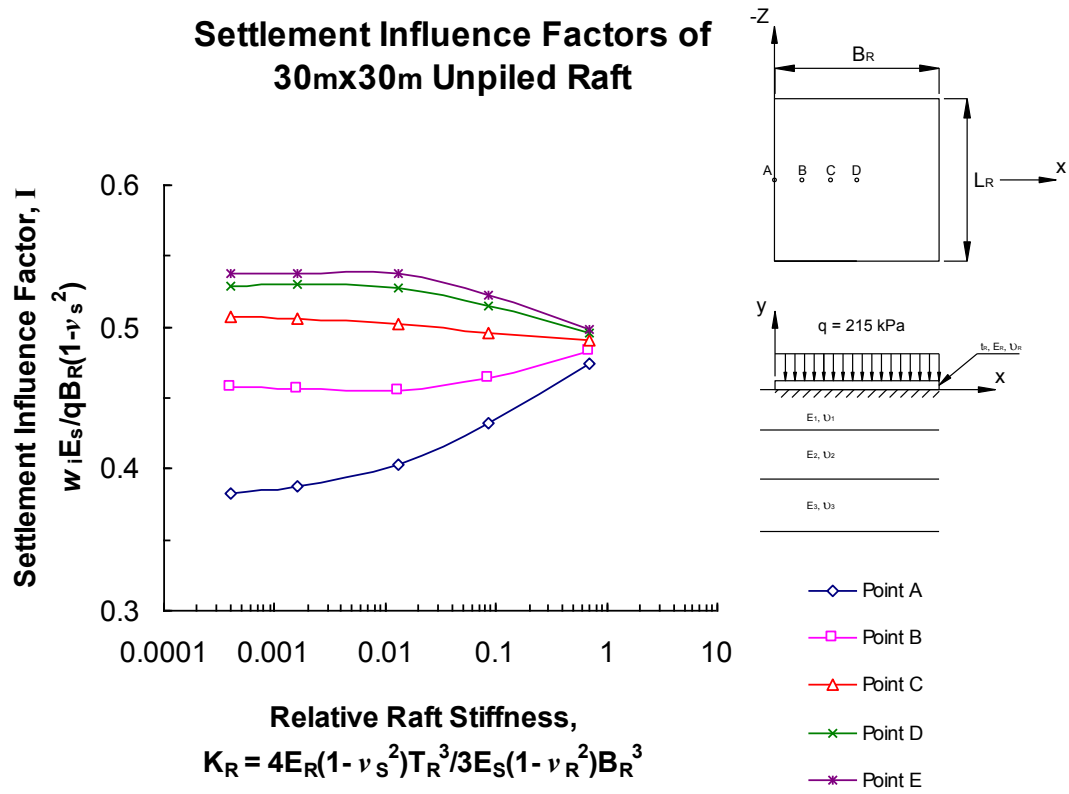


Figure 5.3 (c) Settlement Influence Factors of 30m×30m Square Unpiled Raft

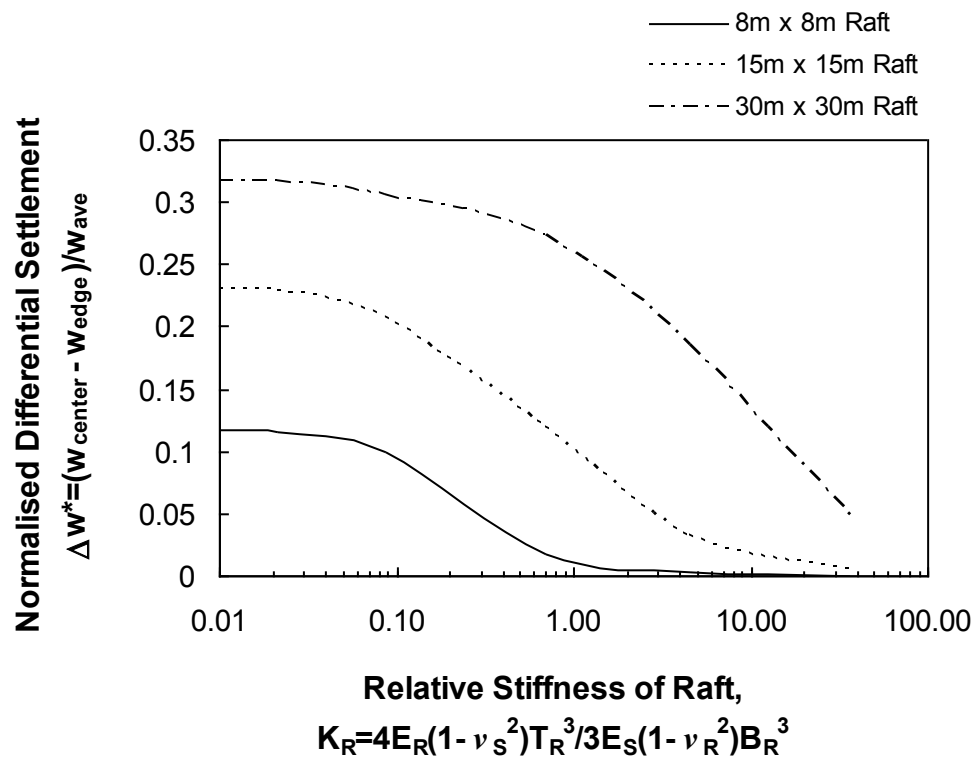


Figure 5.4 Variation of Normalized Differential Settlement with Stiffness

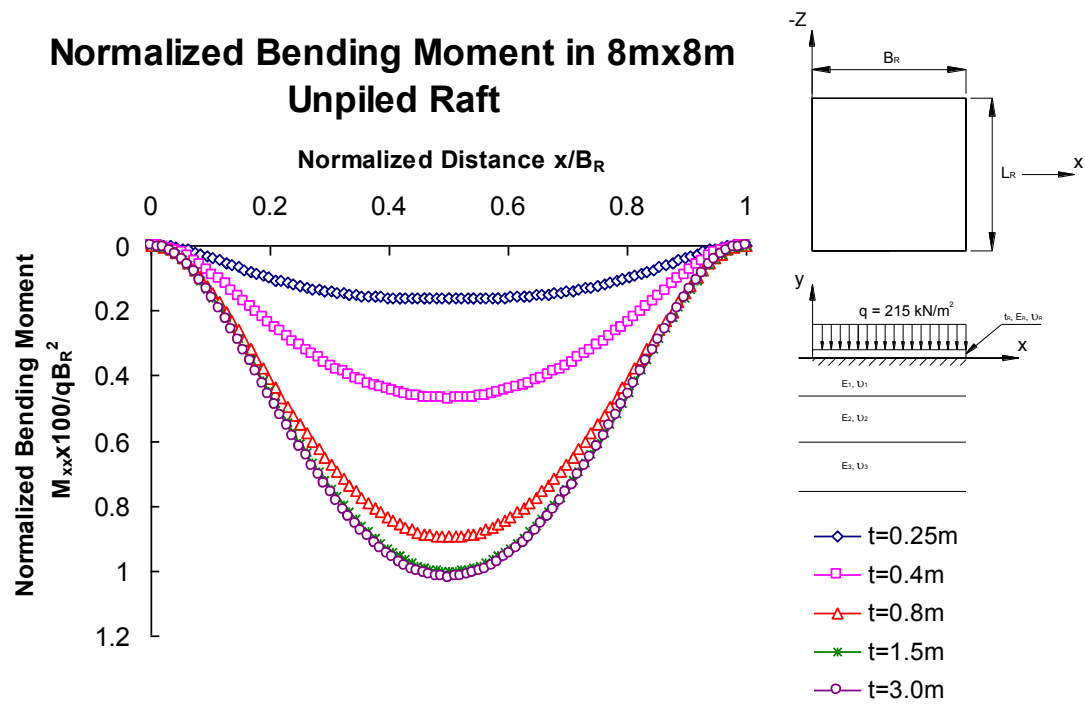


Figure 5.5 (a) Normalised Bending Moment in 8m×8m Unpiled Raft

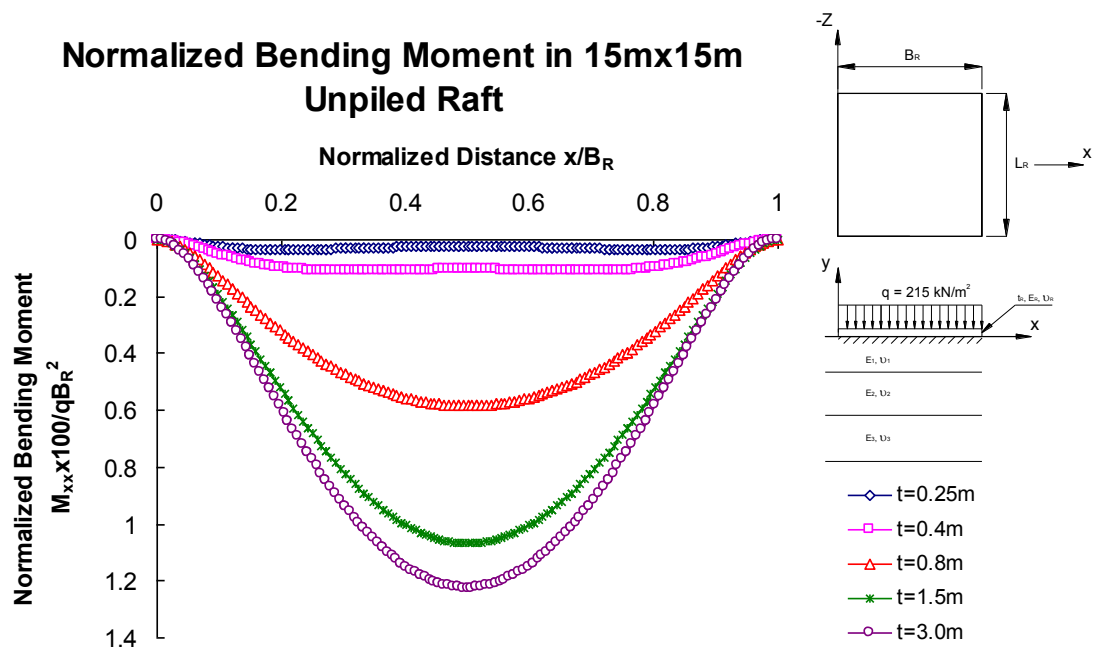


Figure 5.5 (b) Normalised Bending Moment in 15m×15m Unpiled Raft

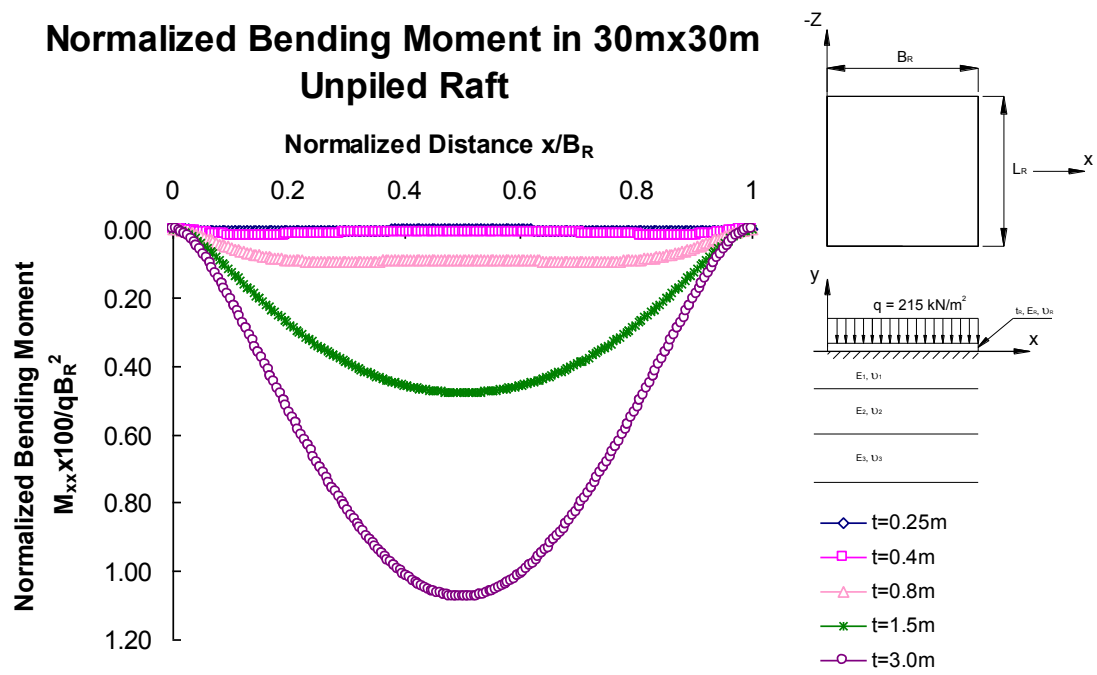


Figure 5.5 (c) Normalised Bending Moment in 30m×30m Unpiled Raft

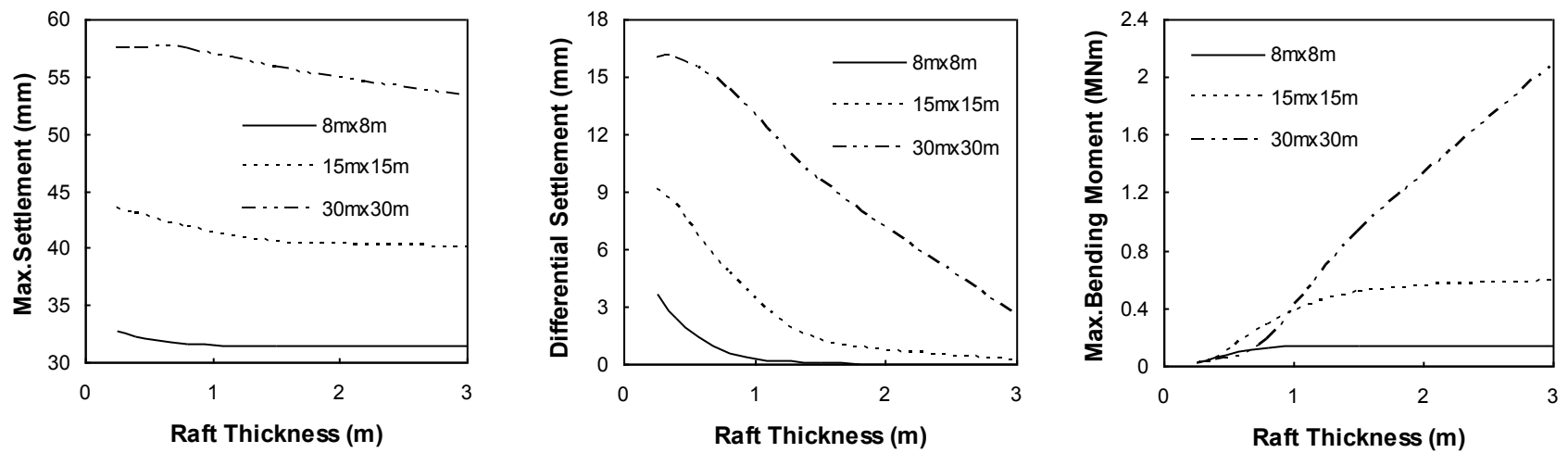


Figure 5.6 Effect of Thickness on Unpile Raft Performance. Load = 215 kN/m²

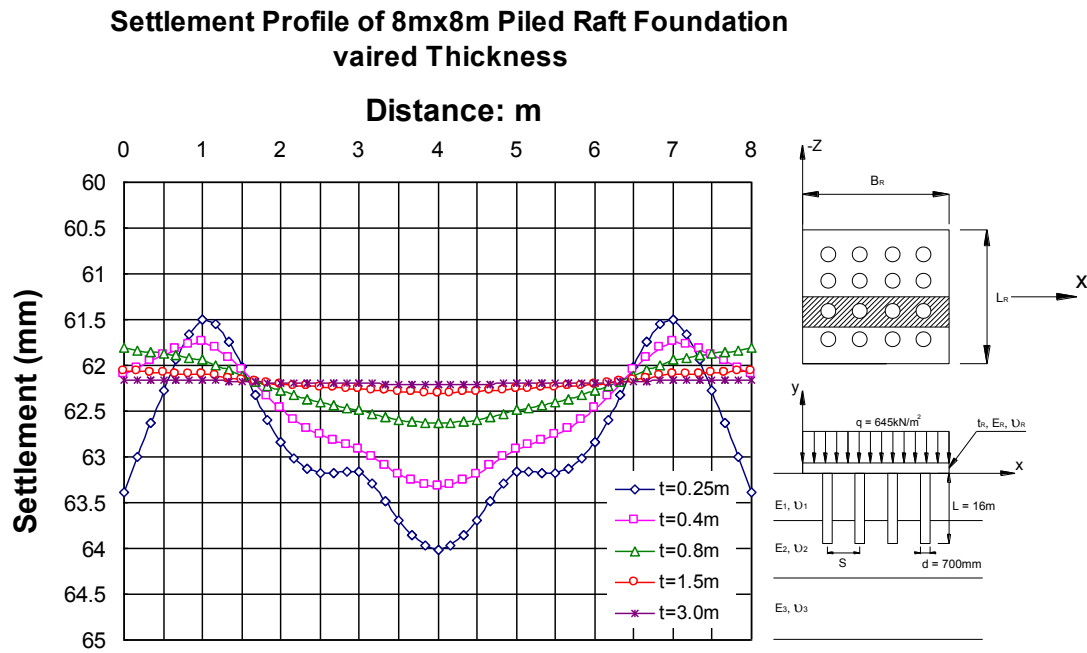


Figure 5.7 Effect of raft thickness on Computed Settlement of piled raft

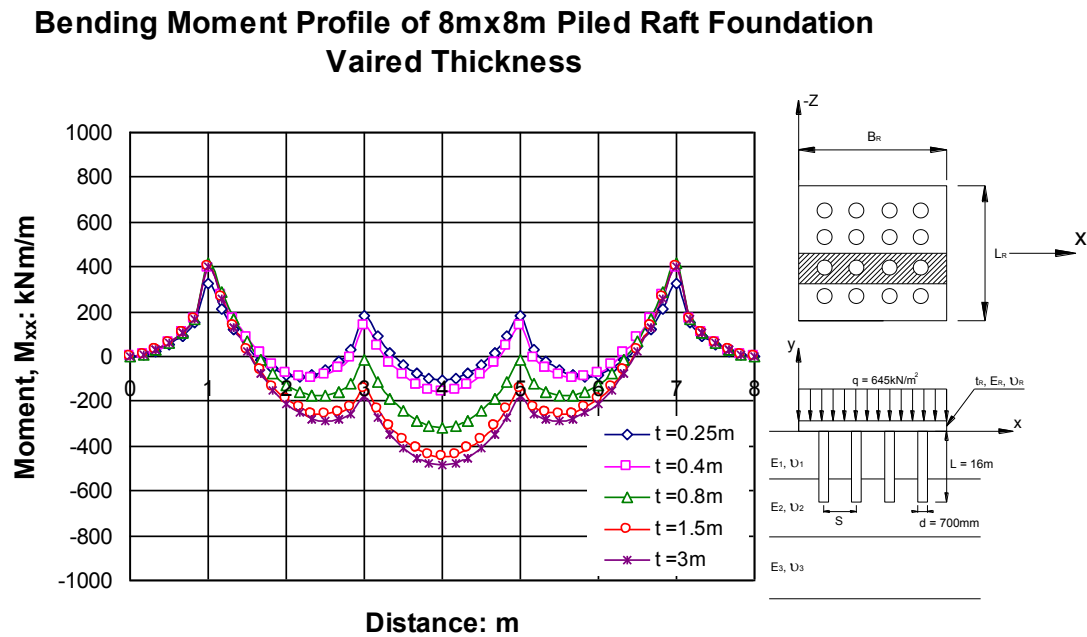


Figure 5.8 Effect of raft thickness on Bending Moment of piled raft

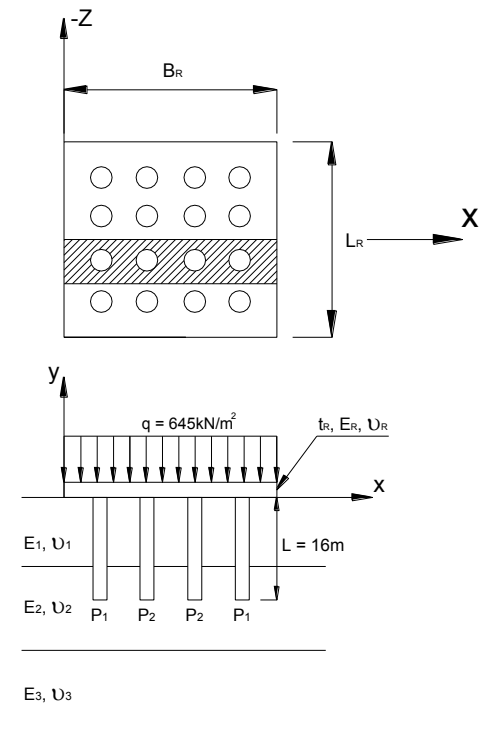
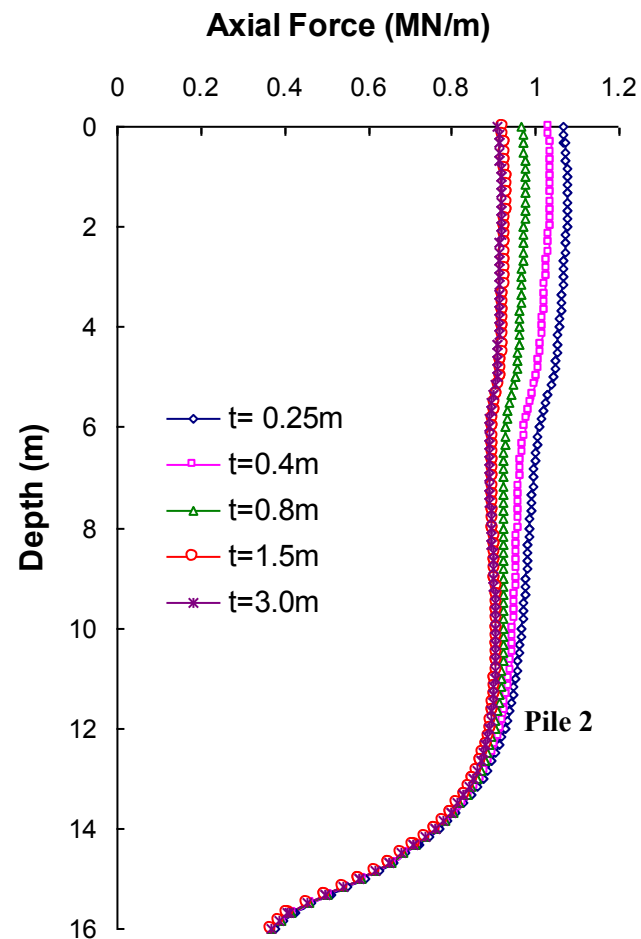
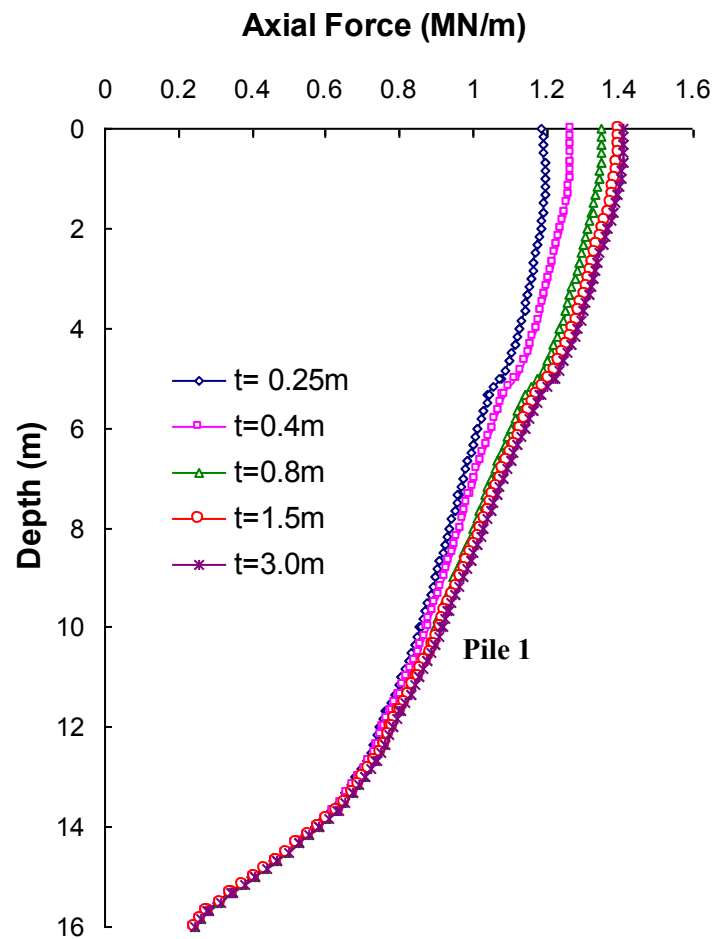


Figure 5.9 Effect of Raft Thickness on Pile Axial Force

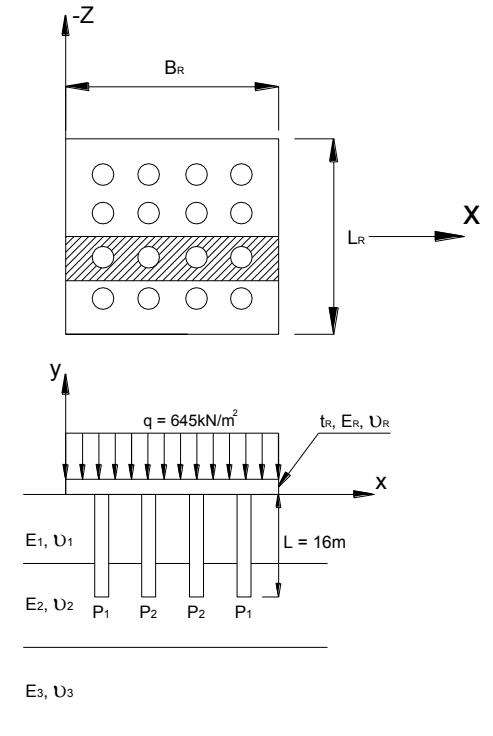
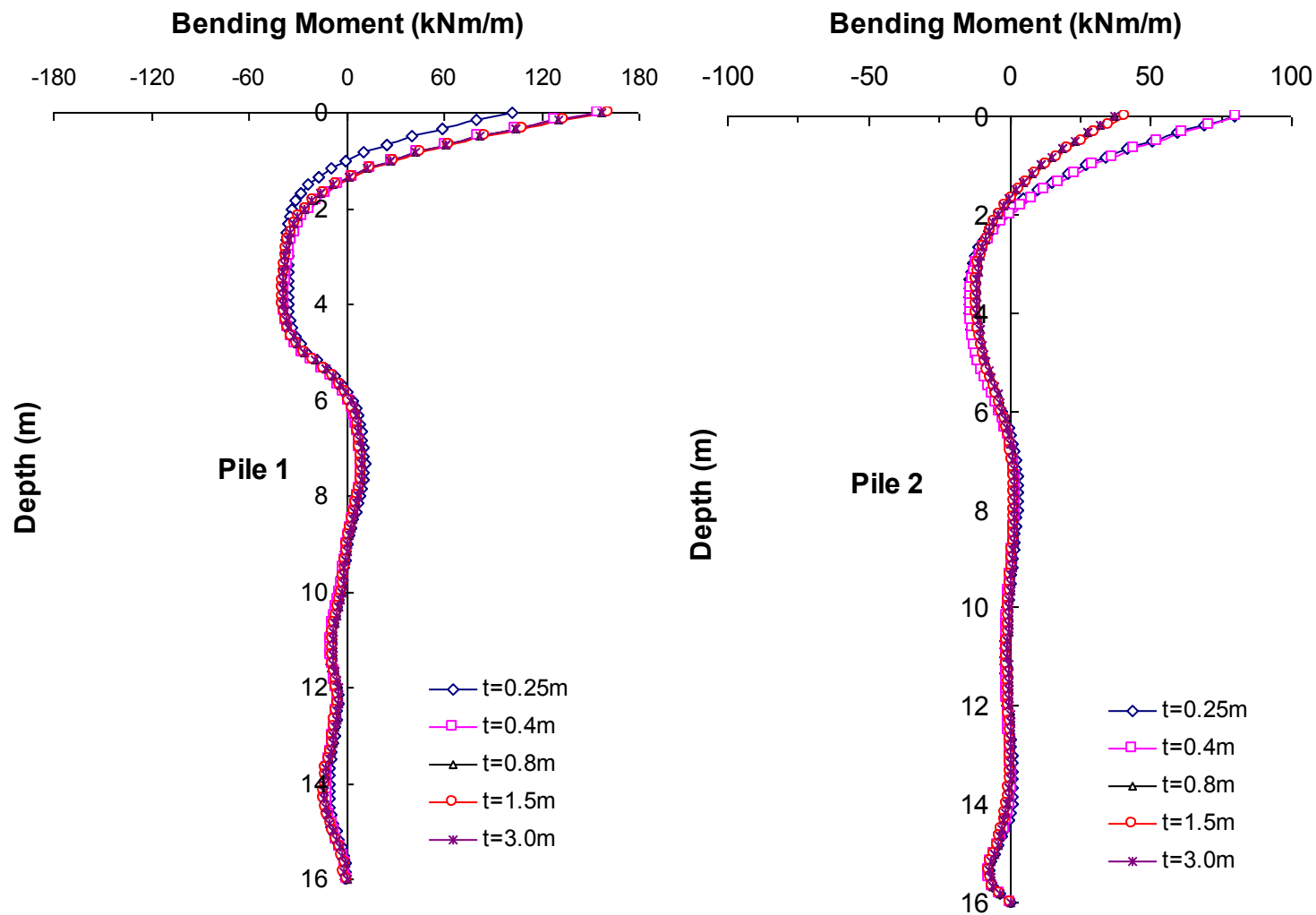


Figure 5.10 Effect of raft Thickness on Pile Bending Moment

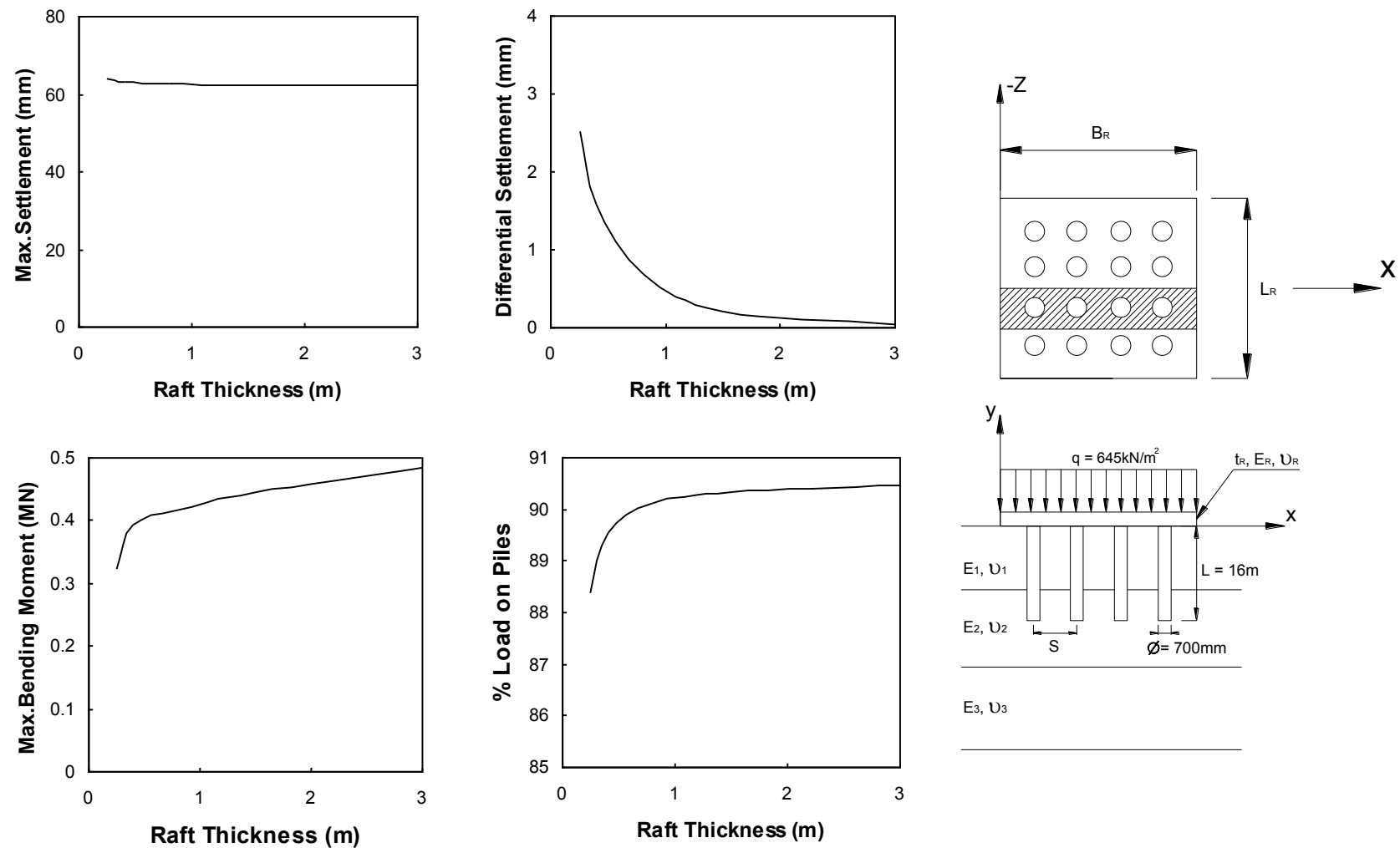


Figure 5.11 Summarized Effect of Raft Thickness on Piled Raft Performance. Raft with 16 Piles, 16m long. Load = 645 kPa

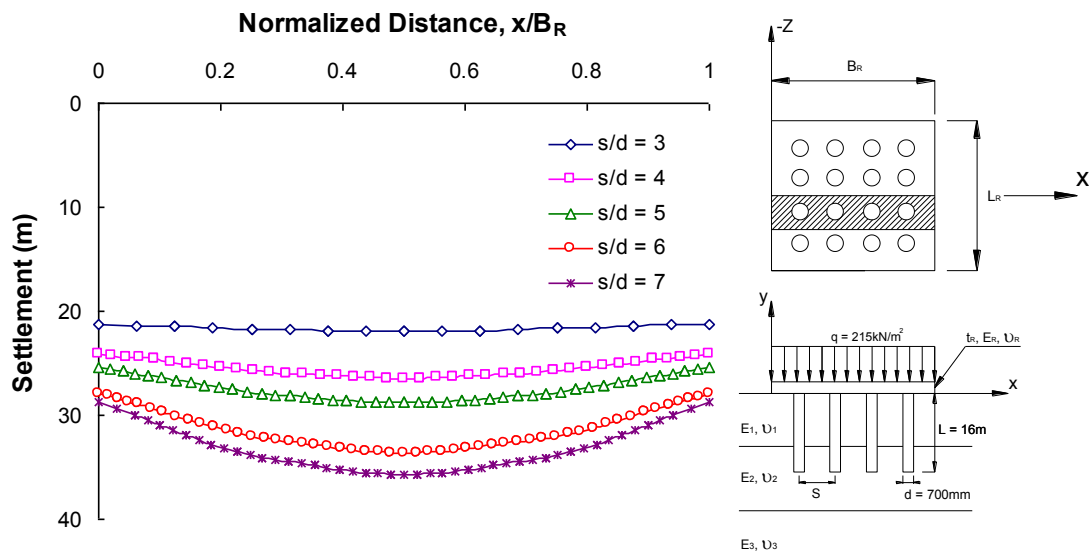


Figure 5.12 Comparison of Piled Raft Settlement Response for Different Spacing of Piles. $Q = 215 \text{ kN/m}^2$

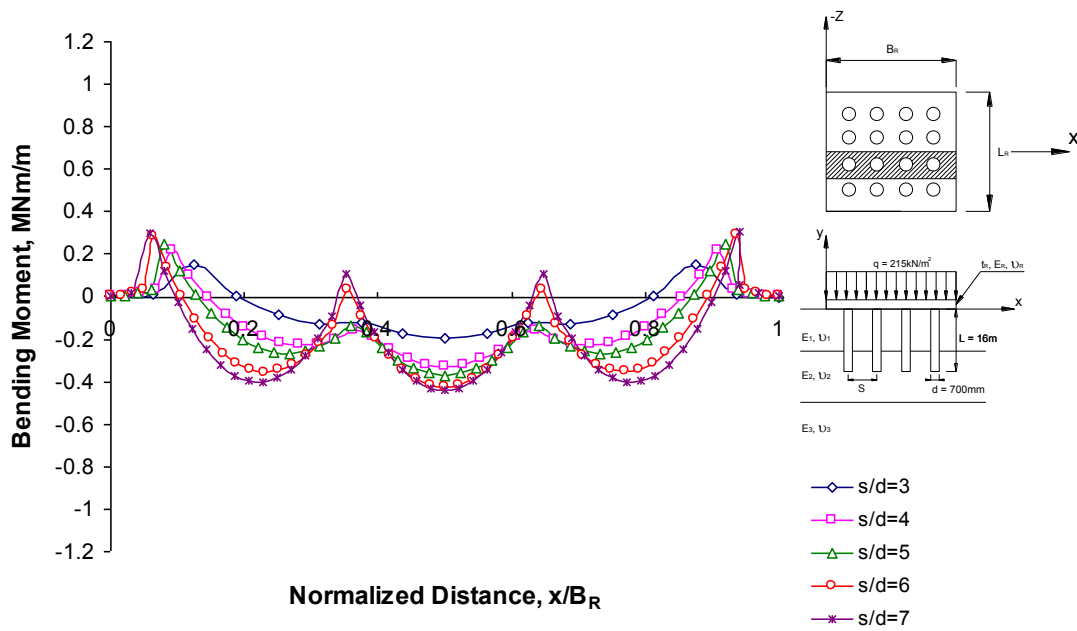


Figure 5.13 Comparison of Piled Raft Bending Moment Response for Different Spacing of Piles. $q = 215 \text{ kN/m}^2$

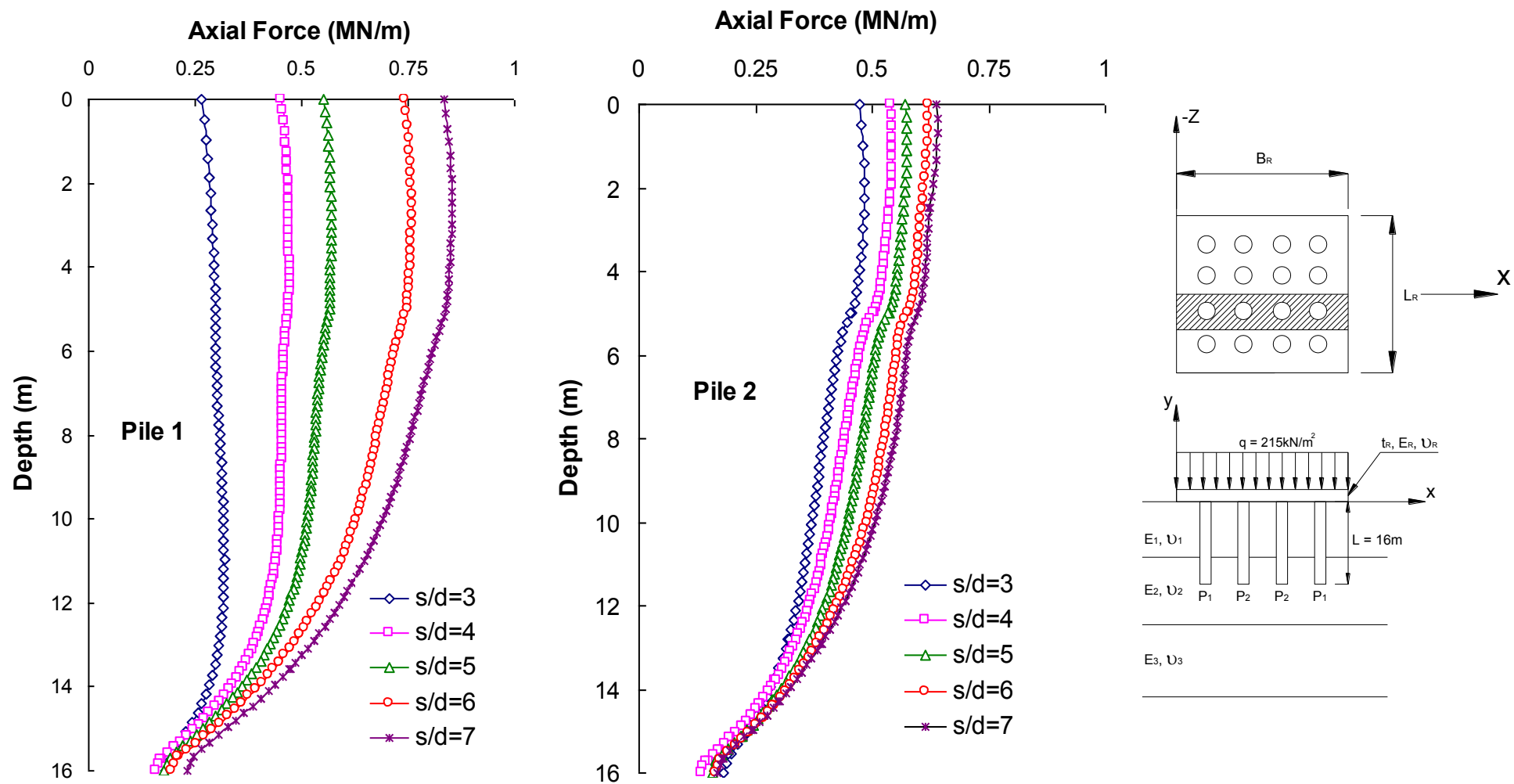


Figure 5.14 Effect of Pile Spacing on Pile Axial Load. $q = 215 \text{ kN/m}^2$

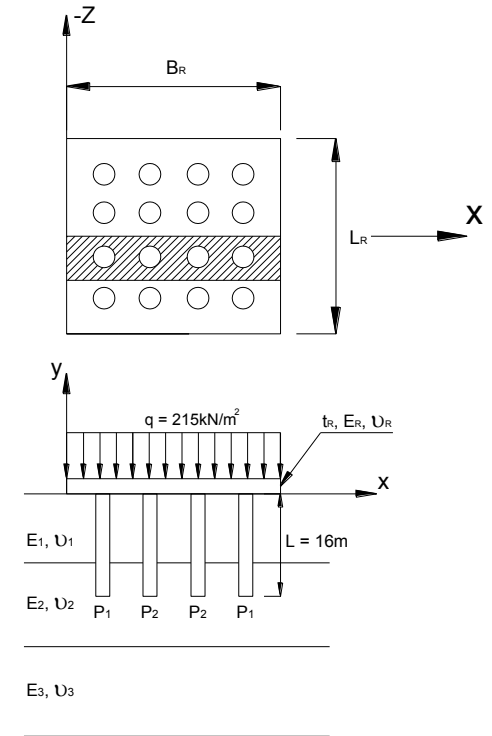
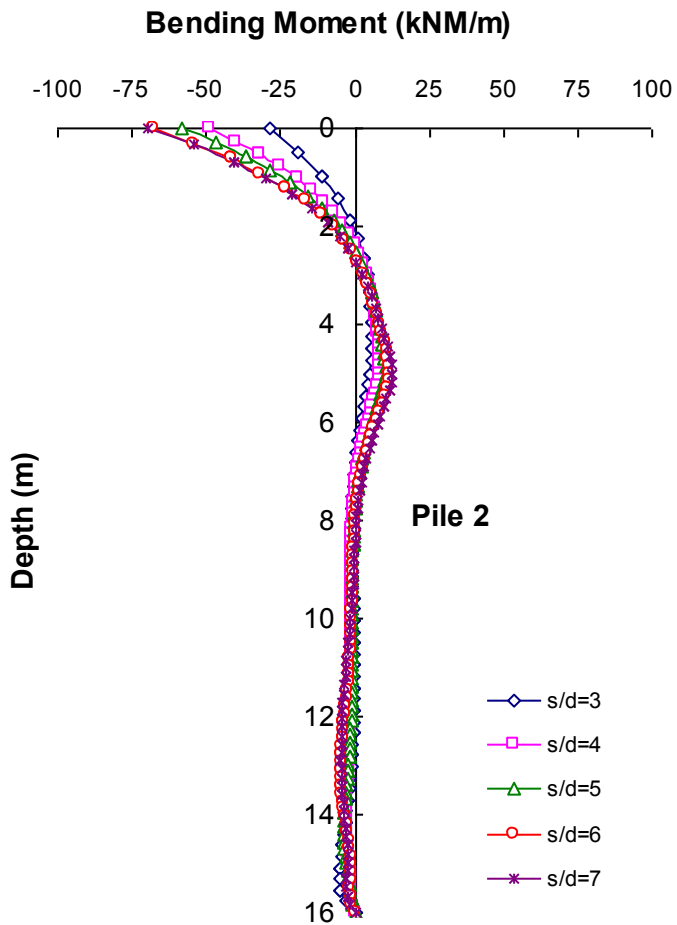
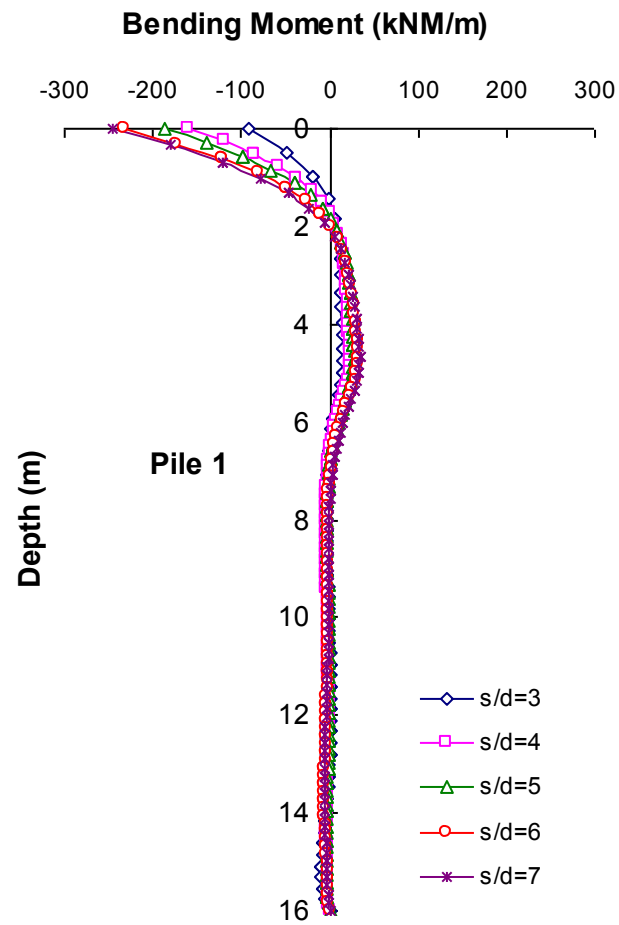


Figure 5.15 Effect of Pile Spacing on Pile Bending Moment. $q = 215 \text{ kN/m}^2$

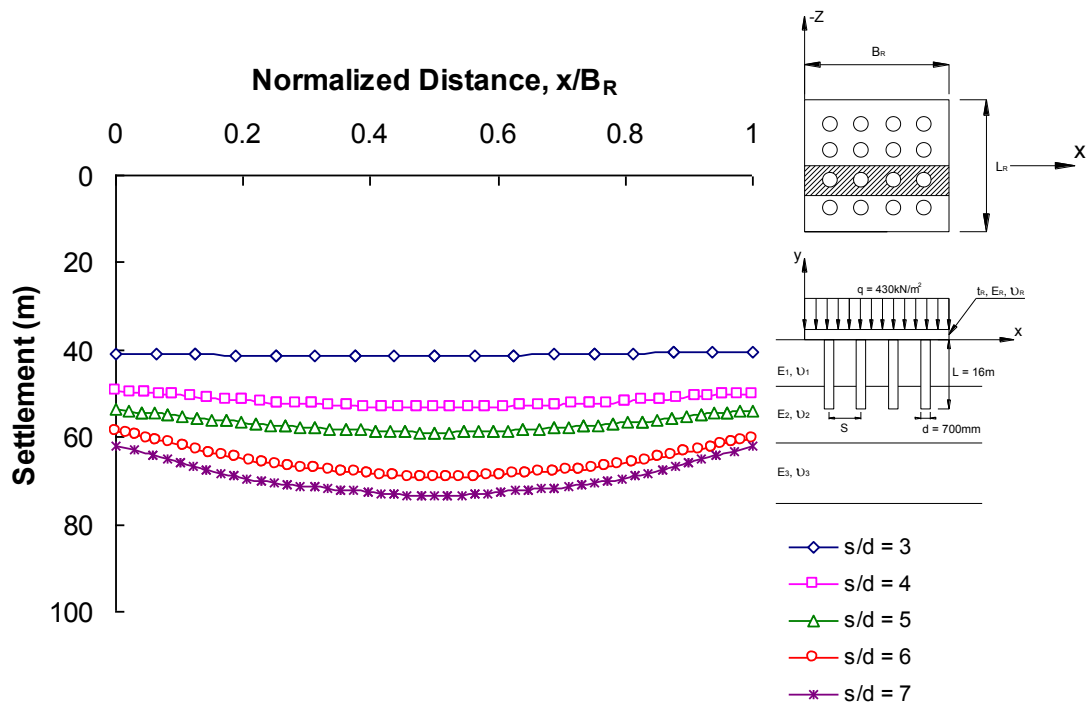


Figure 5.16 Comparison of the Piled Raft Settlement Response for Different Spacing of Piles. $Q = 430 \text{ kN/m}^2$

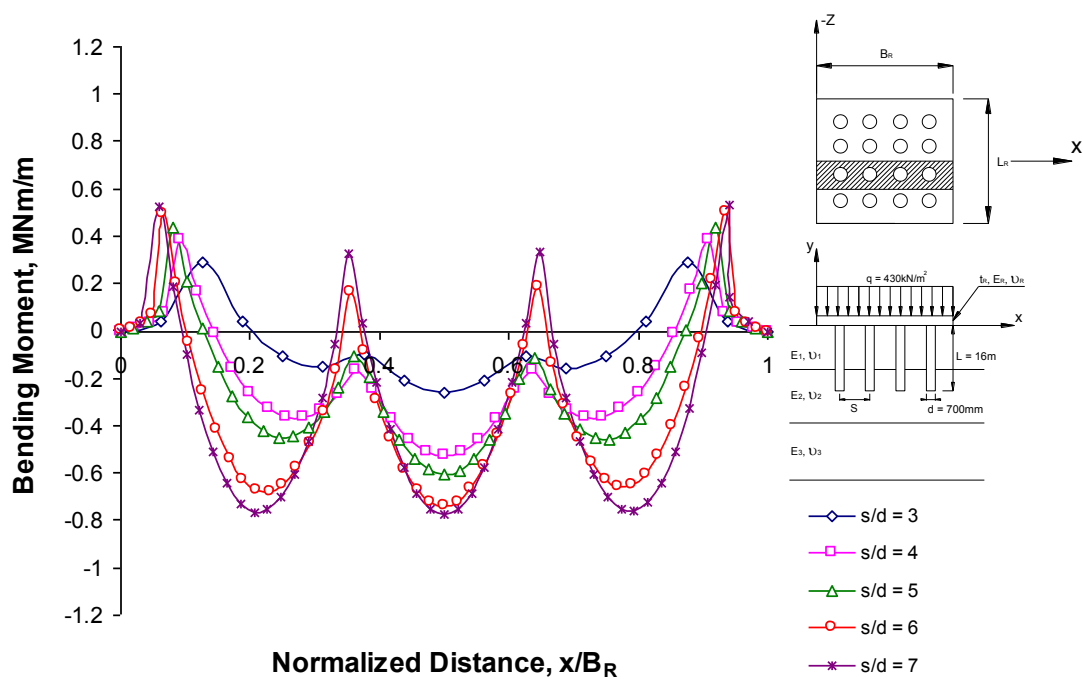


Figure 5.17 Comparison of Piled Raft Bending Moment Response for Different Spacings of Piles. $q = 430 \text{ kN/m}^2$

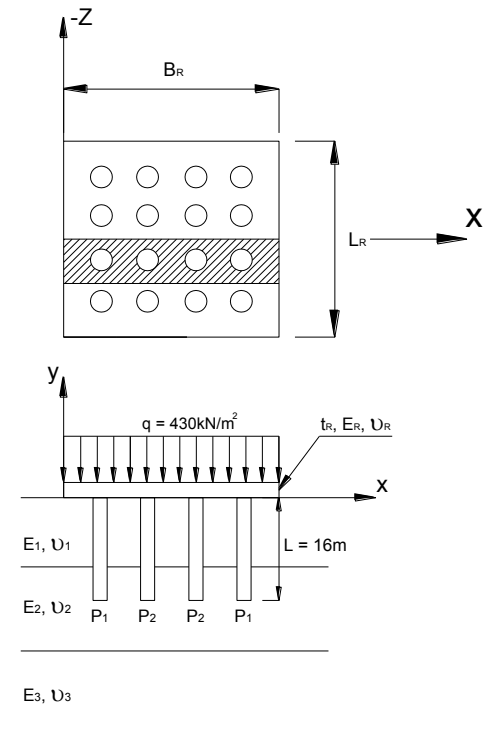
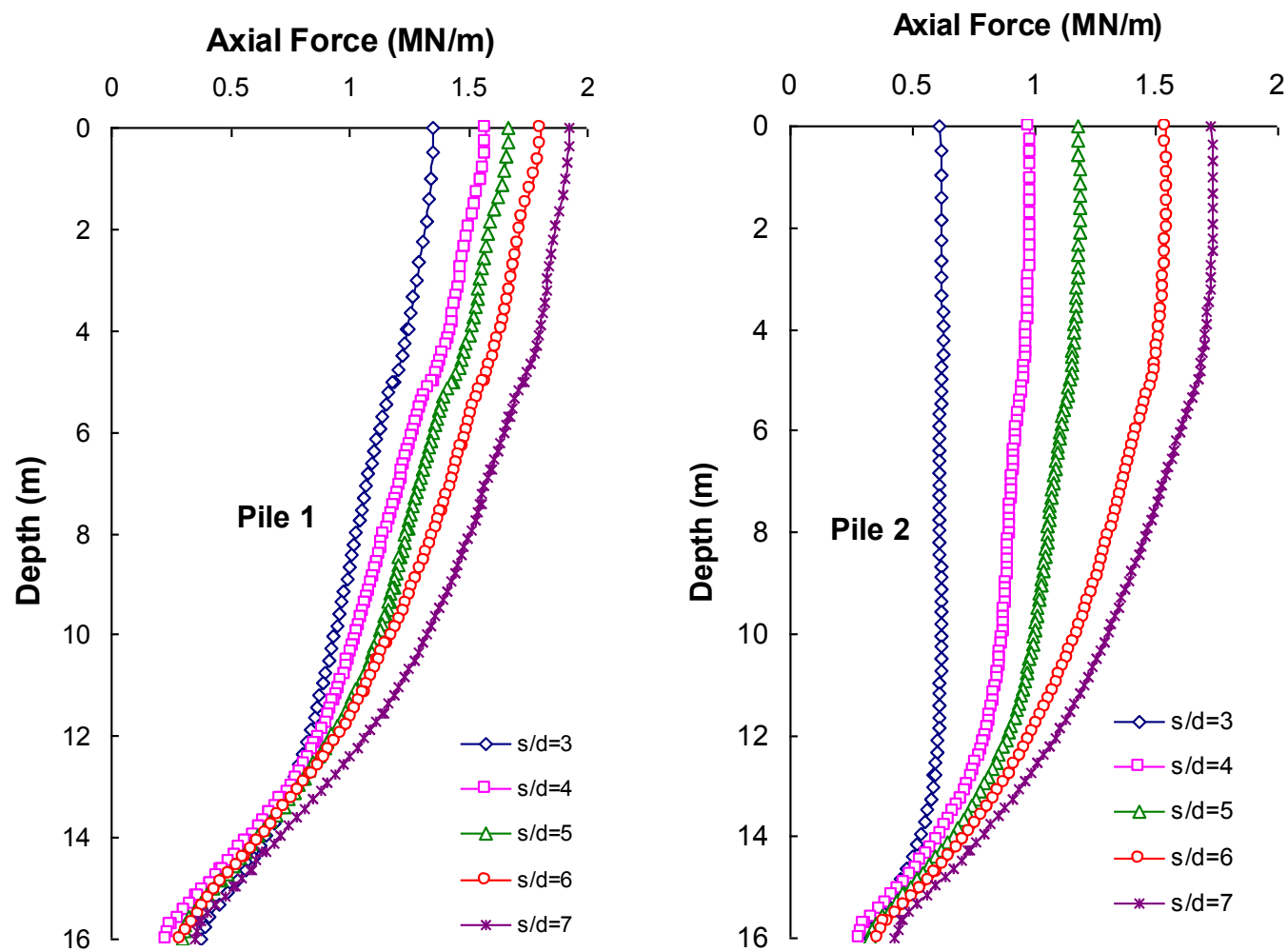


Figure 5.18 Effect of Pile Spacing on Pile Axial Load. $q = 430 \text{ kN/m}^2$

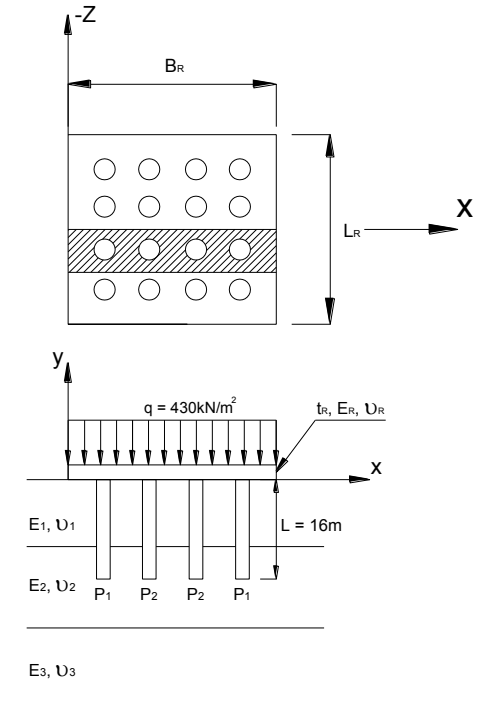
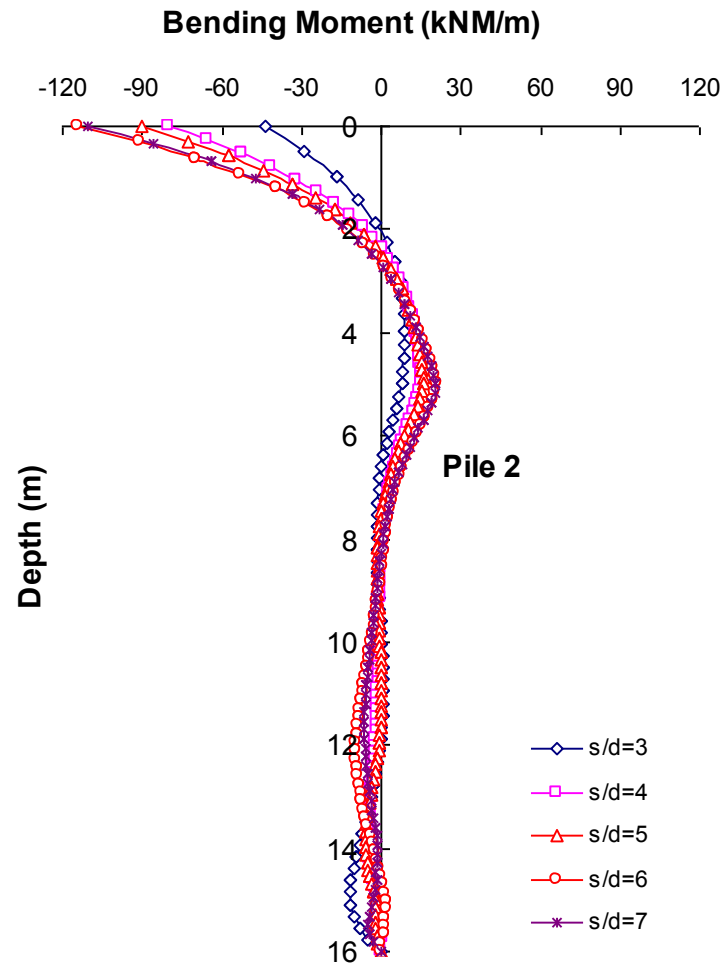
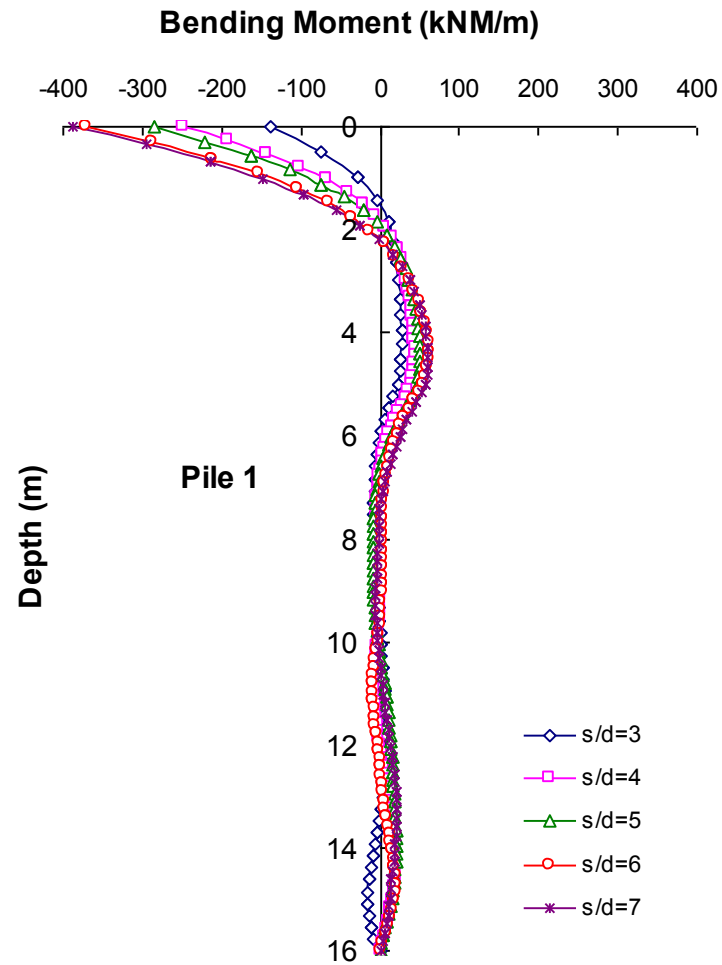


Figure 5.19 Effect of Pile Spacing on Pile Bending Moment. $q = 430 \text{ kN/m}^2$

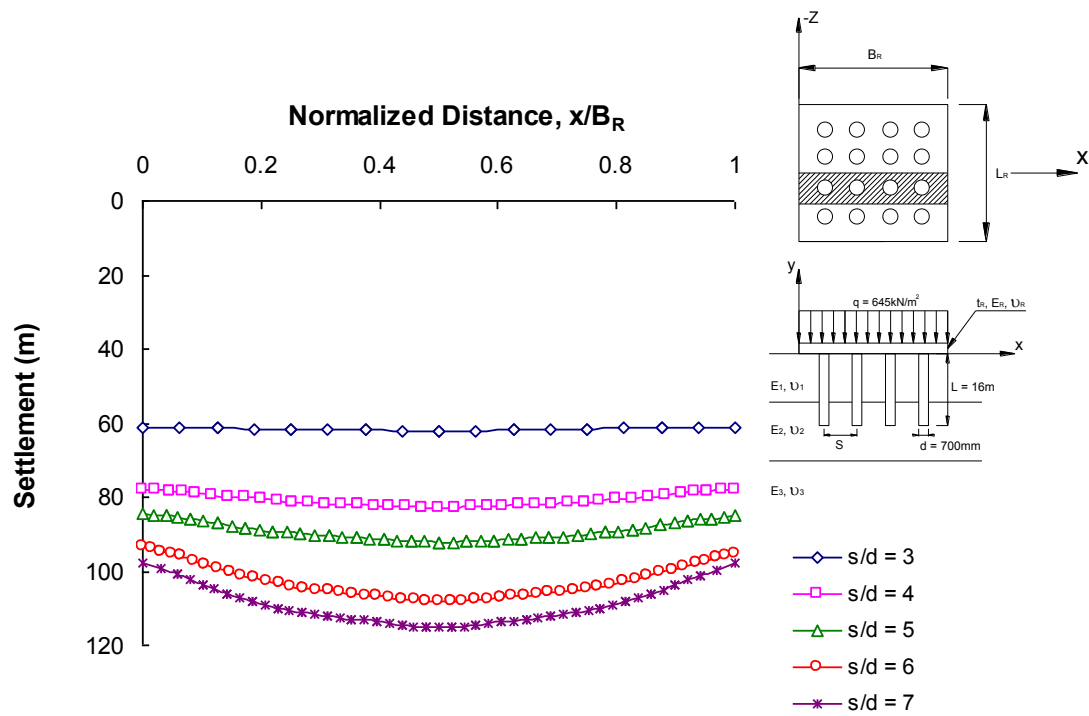


Figure 5.20 Comparison of Piled Raft Settlement Profile Response for Different Spacings of Piles. $Q = 645 \text{ kN/m}^2$

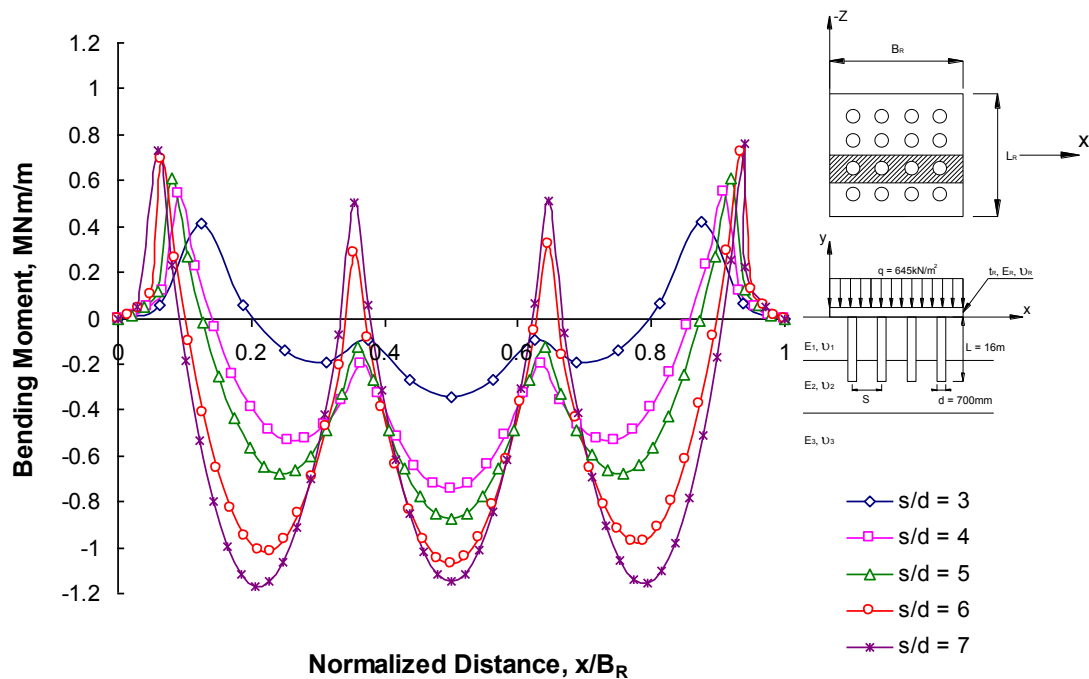


Figure 5.21 Comparison of Piled Raft Bending Moment Response for Different Spacings of Piles. $q = 645 \text{ kN/m}^2$

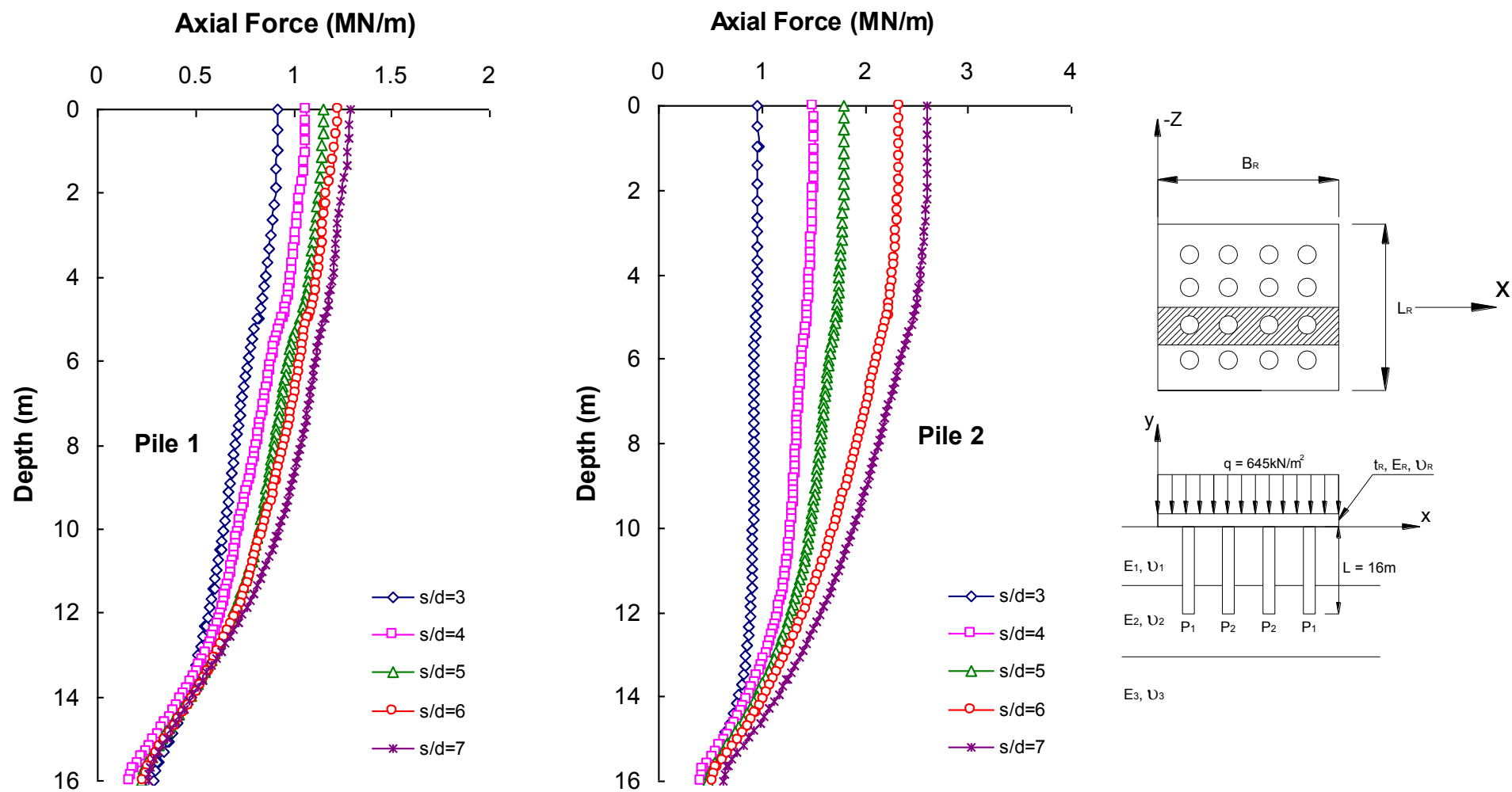


Figure 5.22 Effect of Pile Spacing on Pile Axial Load. $q = 645 \text{ kN/m}^2$

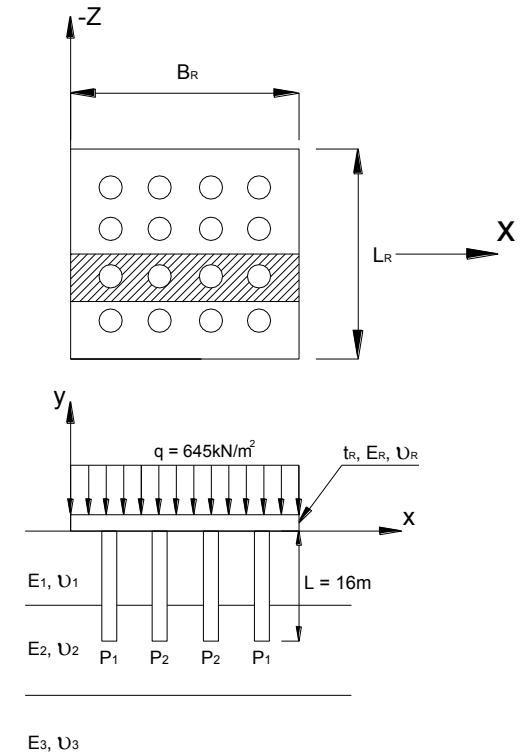
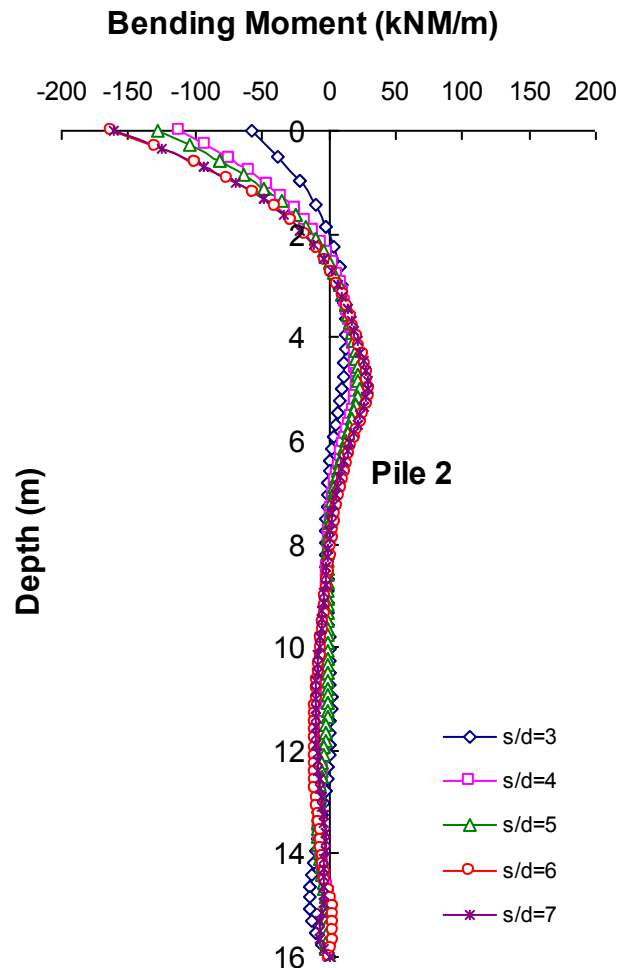
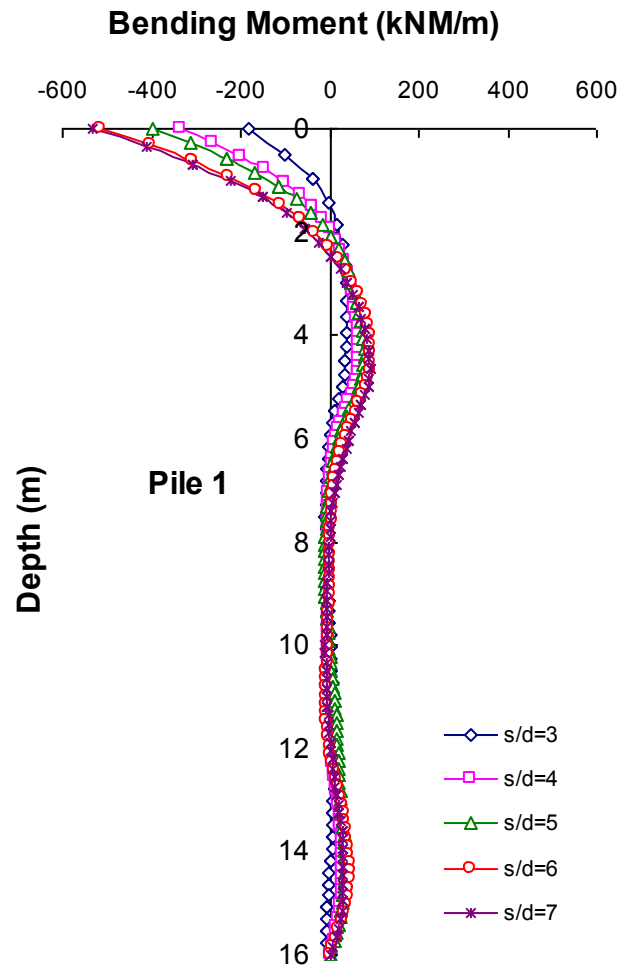


Figure 5.23 Effect of Pile Spacing on Pile Bending Moment. $q = 645 \text{ kN/m}^2$

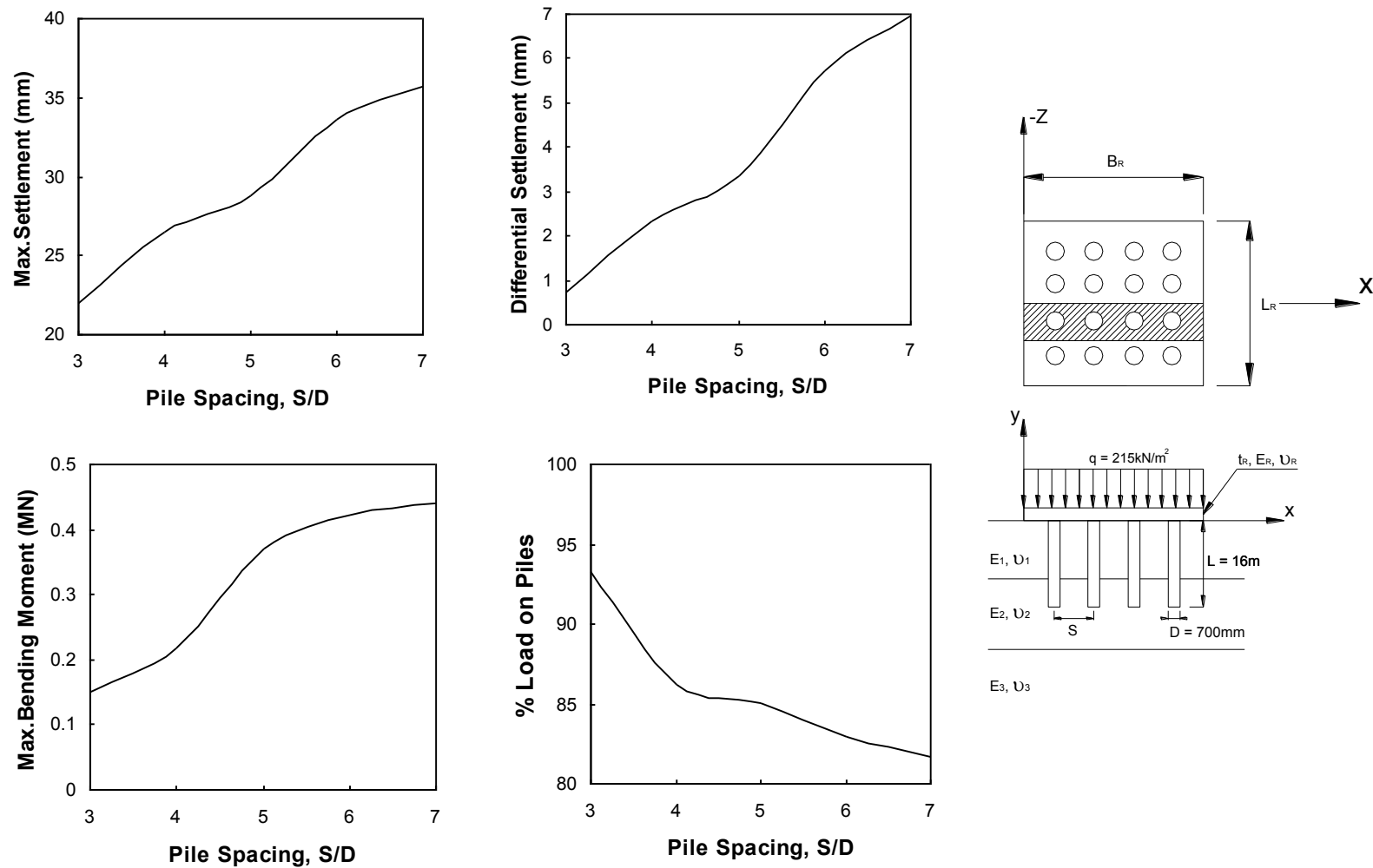


Figure 5.24 (a) Summarized Effect of Pile Spacing on Piled Raft Performance. Raft with 16 Piles, 16m long. Load = 215 kN/m²

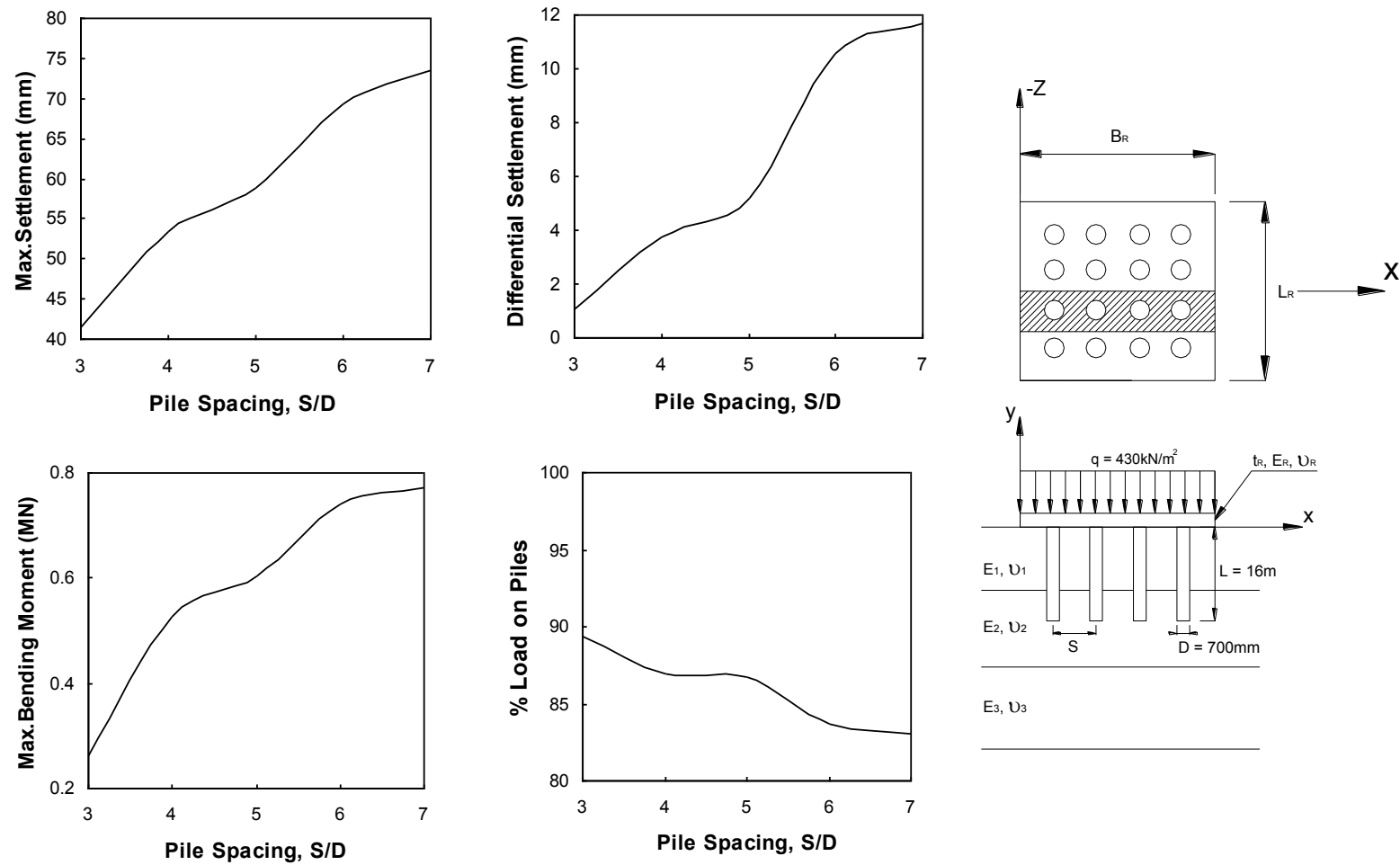


Figure 5.24 (b) Summarized Effect of Pile Spacing on Piled Raft Performance. Raft with 16 Piles, 16m long. Load = 430 kN/m²

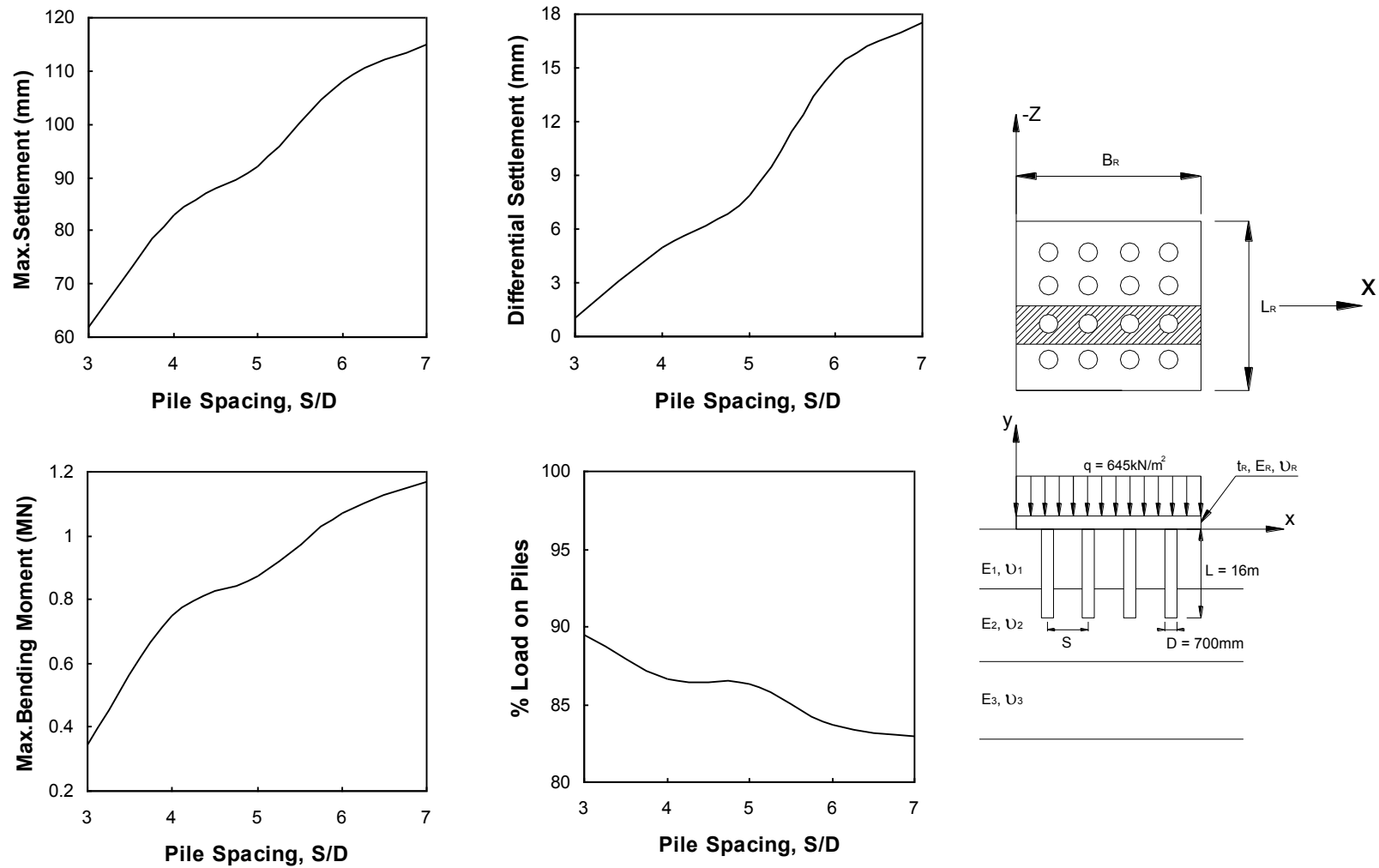


Figure 5.24 (c) Summarized Effect of Pile Spacing on Piled Raft Performance. Raft with 16 Piles, 16m long. Load = 645 kN/m^2

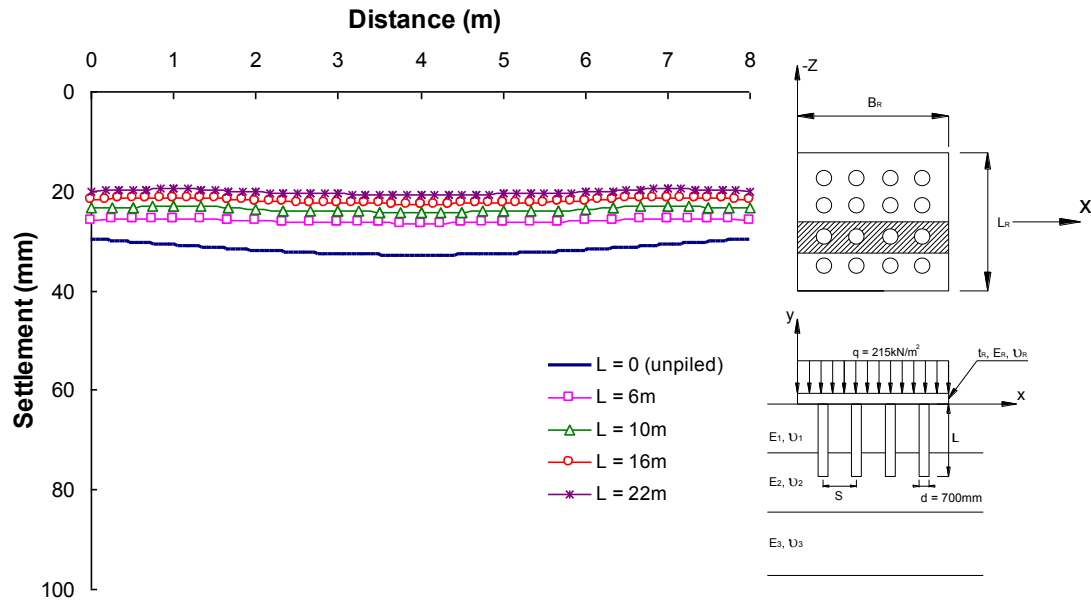


Figure 5.25 Comparison of the Piled Raft Response on Settlement Profile for Different Length of Piles. Raft Thickness = 0.25m. $q = 215\text{ kN/m}^2$

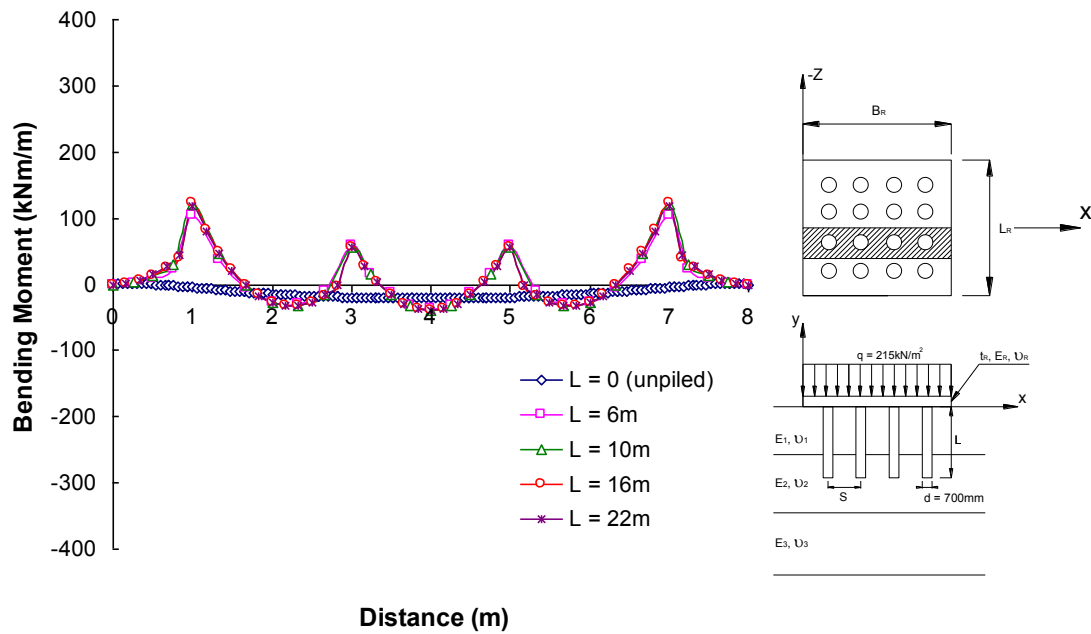


Figure 5.26 Comparison of the Piled Raft Response on Bending Moment Profile for Different Length of Piles. Raft Thickness = 0.25m. $q = 215\text{ kN/m}^2$

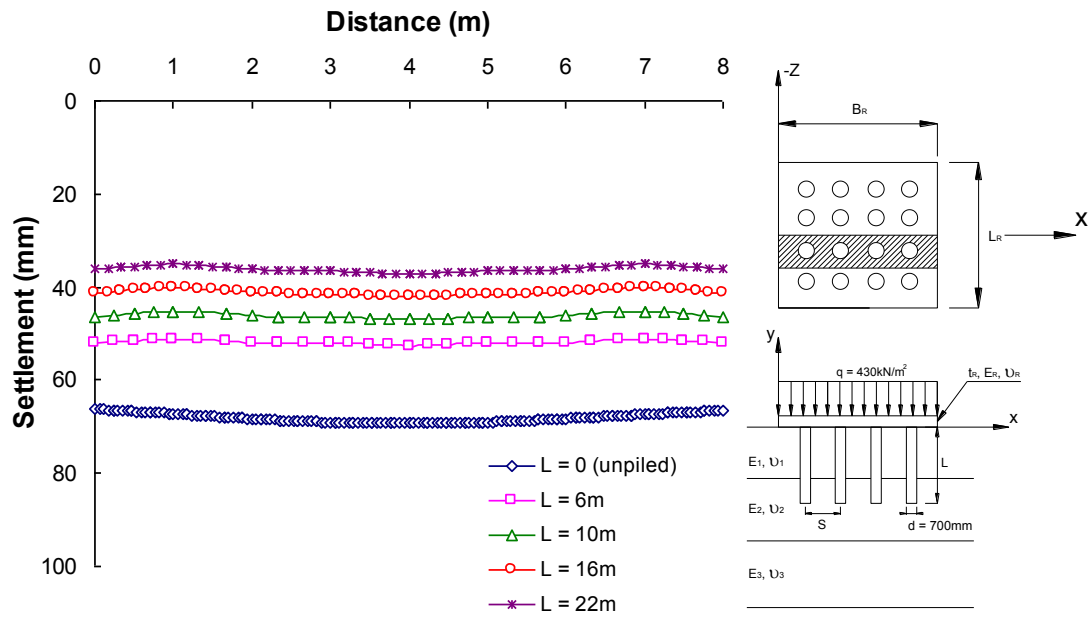


Figure 5.27 Comparison of the Piled Raft Response on Settlement Profile for Different Length of Piles. Raft Thickness = 0.25m. $q = 430 \text{ kN/m}^2$

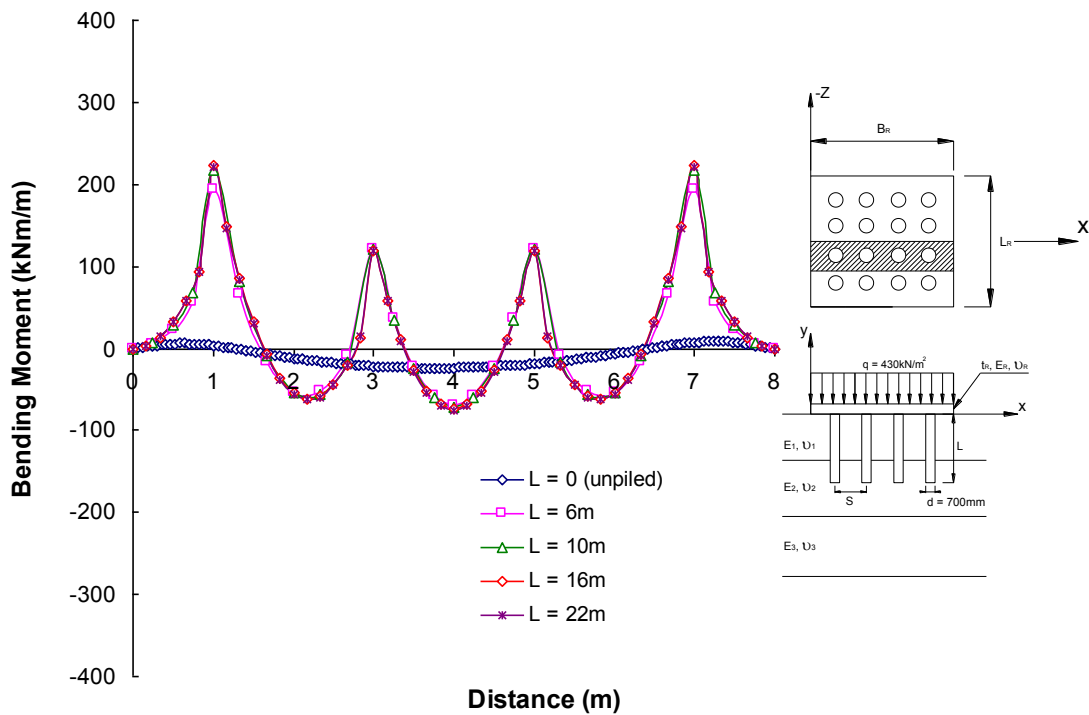


Figure 5.28 Comparison of the Piled Raft Response on Bending Moment Profile for Different Length of Piles. Raft Thickness = 0.25m. $q = 430 \text{ kN/m}^2$

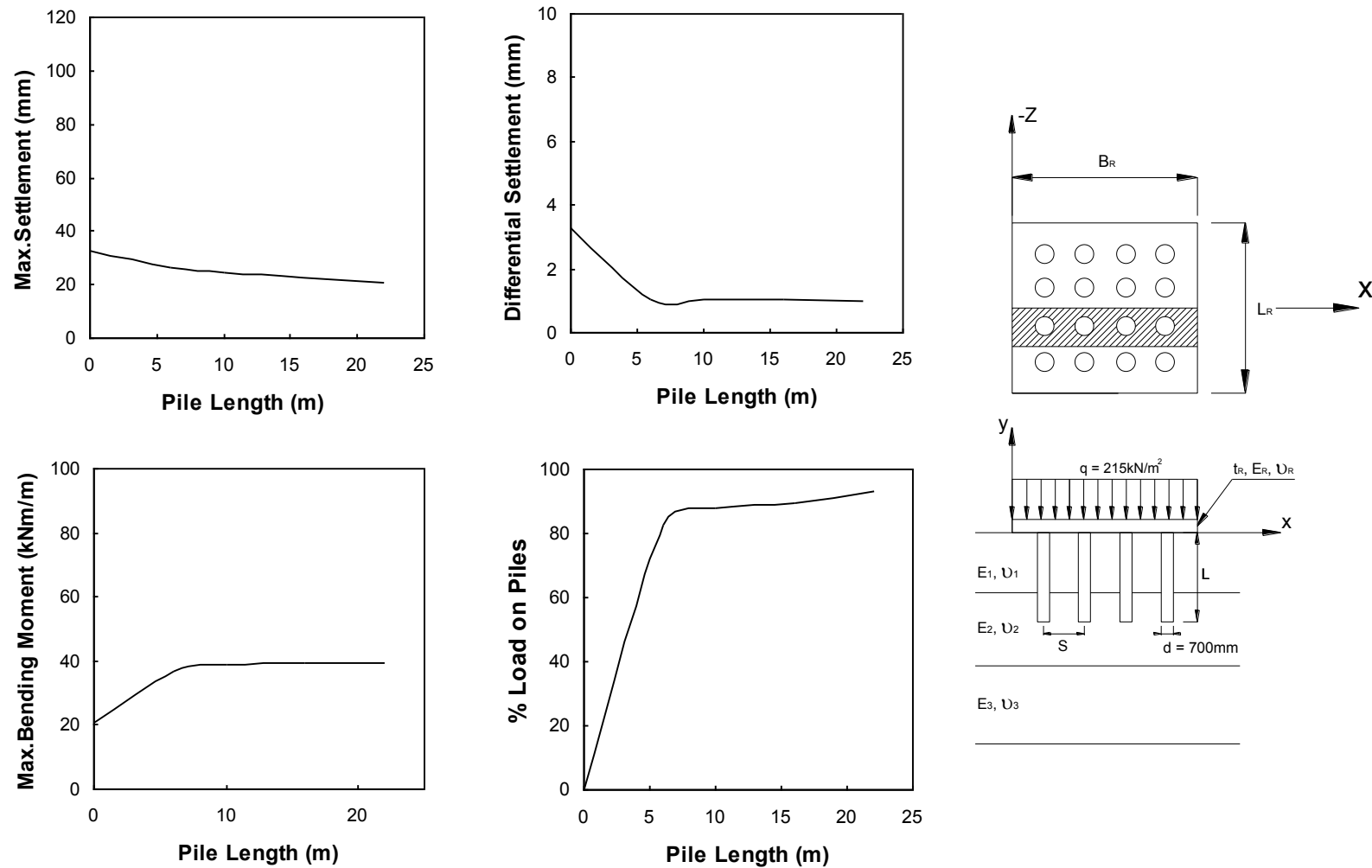


Figure 5.29 (a) Summarized Effect of Pile Length on Piled Raft Performance. Load = 215 kN/m^2

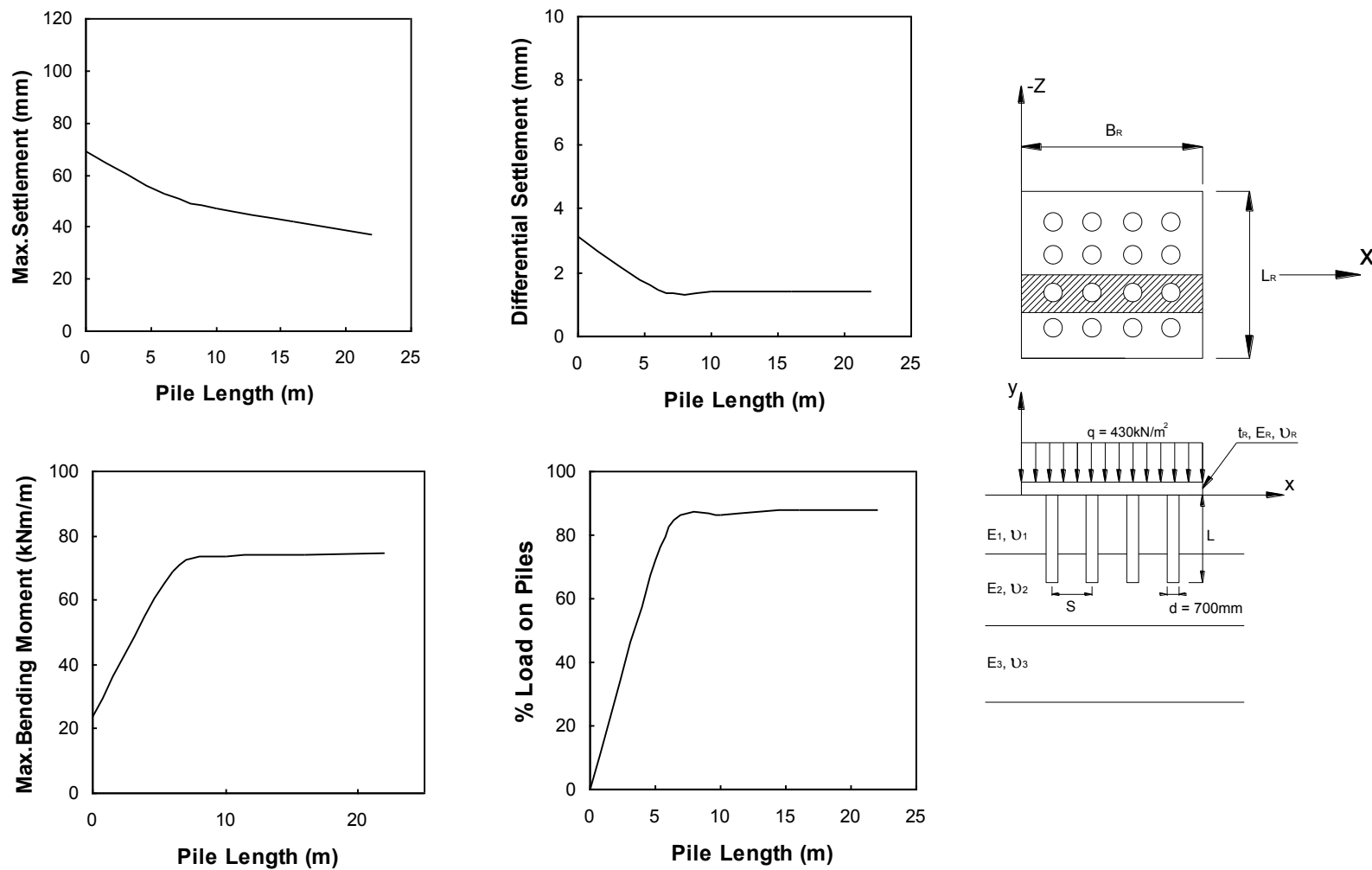
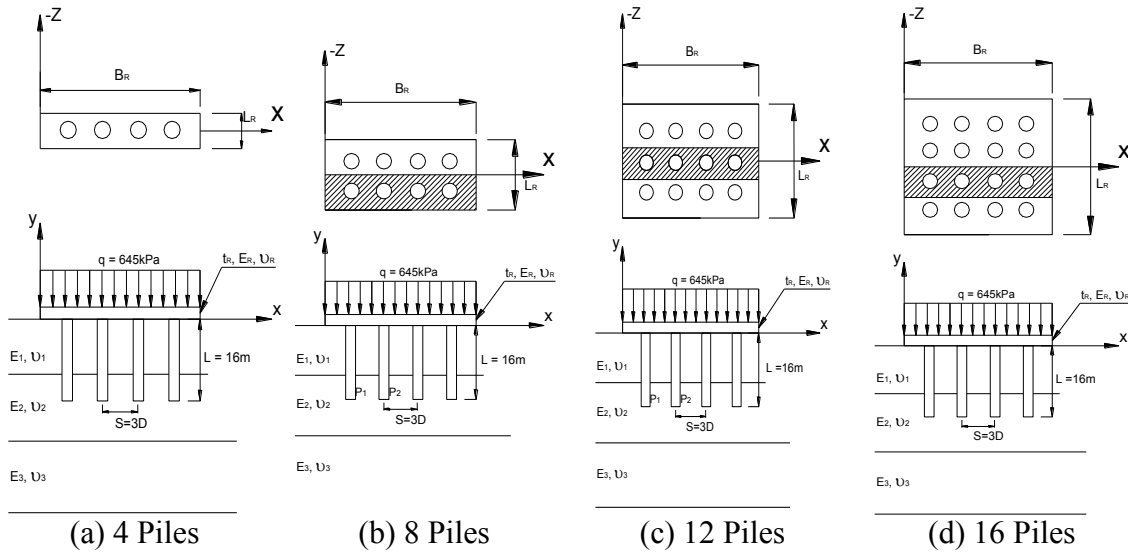
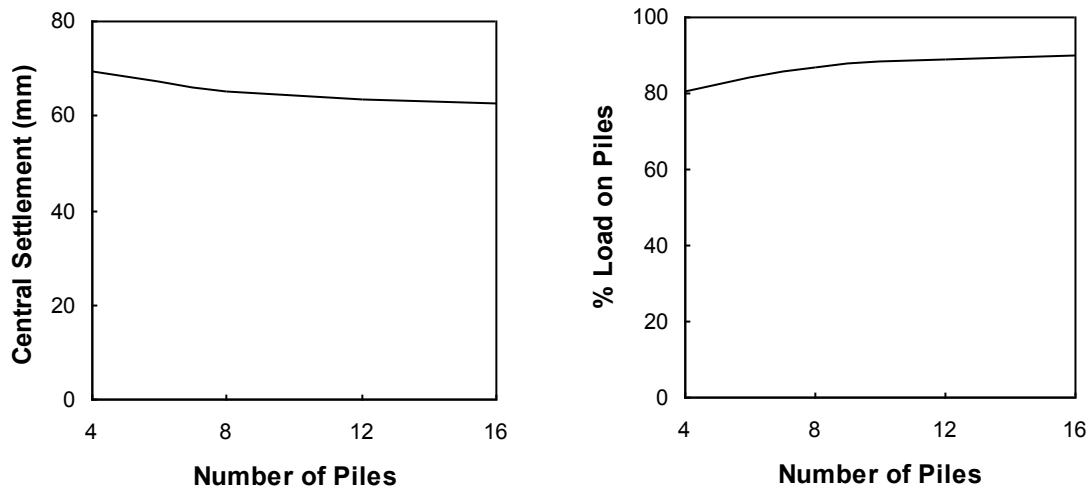


Figure 5.29 (b) Summarized Effect of Pile Length on Piled Raft Performance. Load = 430 kN/m^2



(i) Piled Raft lay-out



(ii) Central Settlement and Percentage Load on Piles

Figure 5.30 Effect of Number of piles on Piled Raft Performance. Load = 645 kN/m²